RBM24 IS ESSENTIAL FOR NORMAL EARLY EMBRYONIC DEVELOPENT

By

Samantha D. Maragh

A dissertation submitted to Johns Hopkins University in conformity with the requirements for the degree of Doctor of Philosophy

Baltimore, MD

February, 2014

Abstract

Rbm24 was recently identified as a gene expressed during early mouse cardiac development (Miller et al., 2008). Due to its tightly restricted and persistent expression from formation of the cardiac crescent onwards and later in forming somites we posited it to be a key player in cardiovascular development and somitogenesis.

To determine the role of this gene in cardiac development, we have identified its zebrafish orthologs (*rbm24*a and *rbm24b*), and functionally evaluated them during zebrafish embryogenesis. Consistent with our underlying hypothesis, reduction in expression of either homolog through injection of morpholino antisense oligonucleotides results in cardiogenic defects including cardiac looping and reduced circulation, leading to increasing pericardial edema over time. Additionally, morphant embryos for either ortholog display incompletely overlapping defects in the forming vasculature of the dorsal aorta (DA), posterior caudal vein (PCV) and caudal vein (CV) which are the first blood vessels to form in the embryo, with additional apparent impairment to angiogenesis.

This work goes on to demonstrate that both Rbm24a and Rbm24b are also required for proper somite and craniofacial development. Investigations into early developmental pathways revealed diminution of *rbm24a* or *rbm24b* gene products by morpholino knockdown resulted in significant reduction of Notch-mediated signaling. Subsequent characterization of Notch-pathway components revealed reduced expression of the cyclic muscle pattering genes *dlc* and *dld* encoding Notch-ligands, and their respective target genes *her1*, *her7* in *rbm24a* or *rbm24b* morpholino-injected

embryos. Analysis of affected Notch-pathway mRNA populations in *rbm24a* and *rbm24b* morpholino injected embryos revealed aberrant splice fragments of *dlc* and *dld*, but not *her1* or *her7*. The integrity of Notch-receptor mRNA was similarly unaffected, suggesting the origins of the observed Notch-signaling deficit is derived from aberrant splicing of its ligands.

Taken together these data imply a previously unknown requirement for Rbm24a and Rbm24b in normal cardiovascular somite and craniofacial development. Further they suggest these protiens may play a crucial role in modulating Notch-mediated signaling through RNA post-transcriptional processing of *dlc* and *dld*.

Advisor: Andrew S. McCallion, Ph.D.

Preface

I can't even begin to express the thoughts and emotions I have at this conclusion of my graduate studies. I can't image what this journey would have been like without the many that have enhanced my experience. To my lab family the McCallion lab I say thank you for your generosity of time, and knowledge and your gift of friendship. To my first family members, Ron Miller, Megana Prasad, David McGaughey and Zach Stine and Colin Huck, thank you for the warm environment you provided and the knowledge you shared. To my current lab family, Maggie Baker, Paul Hook, Courtney Woods and Frazer Matthews, I say you rock and I wouldn't trade you for the world. Then there are my constant companions whom I spend the majority of my journey with, Dave Gorkin, Seneca Bessling and Xylena Reed. These three have been my lab family nucleus my friends and often times my sanity. Life would have been more difficult and less enjoyable without you. All families have a head of household and that for me was Dr. Andy McCallion. Andy is as wonderful of a boss, mentor, advisor and friend as I had prayed for. Thank you Andy for giving me some water to float in, teaching and guiding me to building a ship of knowledge, experience and good scientific practice and then helping to steer me in the calm and stormy waters to being a successful contributor and good citizen of the scientific and general community. I will miss you all, as we will be separated by space, but you are always in my heart.

A special thank you goes to Dr. Mike Parsons and his lab, without whom I would have a lesser knowledge and appreciation of early developmental pathways and the value of a chocolate covered blackberry. To Sandy Muscelli, Dr. David Valle and

Dr. Kirby Smith thank you for the opportunity to receive training and support in the Human Genetics Program. It was a fantastic educational experience. Thank you to Dr. Laurie Locascio and Dr. Willie May at NIST pushing me towards a Ph.D. and giving me the support and opportunity to reach for the stars.

Friends truly make the journey. To my Taras, Tara Dutka and Tara Doucet you two keep me laughing and smiling all day. To Tejas Niranjan we have journeyed a long way together my friend and I'm looking forward to the next adventures. To my constant and my best Eric Stevens, thank you for being my rock and my never ending source of love and acceptance literally from day one. Forever and always in LD, even if only in spirit & heart. To Tanya Curtis and the Curtis family I love you all!

I'd like to thank my family for the largest contribution to my successful completion of this degree. To my sister Lesia and brother-in-law DePorres, it's been wonderful having you back in town. Thank you for provided me a hiding place at your home both physically and emotionally. To my brother Marlon you have been my buddy all through life. Without the smiles and laughs and good times we always have I wouldn't know how enjoyable life can be even when everything isn't going the way I'd like. To my mom and dad, there are no words for how much I love, appreciate and admire you. You left your island paradise in Jamaica so that I could have a better life and opportunity at education and you supported me 100% through ups and downs whatever I needed with no sacrifice to great. I love you to my core. May God bless and keep you for all you have done.

Finally I thank God the father and Jesus for being the source of my life, strength, joy and hope. You are my all and I adore you.

Table of Contents

List of Tables

List of Figures

CHAPTER 1

INTRODUCTION

1.1 RNA Recognition Motifs

RNA Recognition Motifs (RRMs) are the most common and best characterized protein domains (Finn et al., 2006). Classically in the literature this protein domain is known by several additional names, including RNA binding domain (RBD) or ribonucleoprotein domain (RNP) (Maris et al., 2005; Whittock et al.). The general primary structure of the RRM domain was first identified in the late 1980's as consisting of approximately 90 amino acids with two internal highly conserved sub-domains. These sub-domains are termed RNP1 consisting of 8 amino acids and RNP2 consisting of 6 amino acids, and are spaced approximately 20-40 amino acids apart, with RNP2 at the N-terminus of the RRM domain. The consensus sequences have been identified as (Lys/Arg)-Gly-(Phe/Tyr)-(Gly/Ala)-(Phe/Tyr)-(Val/Ile/Leu)-X-(Phe/Tyr) for RNP1 and (Ile/Val/Leu)-(Phe/Tyr)-(Ile/Val/Leu)-X-Asn-Leu for RNP2 where X represents any amino acid (Adam et al., 1986; Dreyfuss et al., 1988; Swanson et al., 1987). Mutagenesis studies on the properties of the RNP1 and RNP2 sub-domains indicate these consensus sequences are necessary for RRM motif binding as well as sufficient to confer RNA binding capacity (Bandziulis et al., 1989; Birney et al., 1993; Kenan et al., 1991)

The RRM secondary structure is composed of four-stranded anti-parallel β-sheets with two helices packed against it such that the domain has the split αβ ($\beta_4\alpha_2\beta_1\beta_3\alpha_2\beta_2$) topology. The RNP1 sub-domain is located in the β_3 β-sheet while

RNP2 is located in the β_1 β-sheet (Oubridge et al., 1994; Swanson et al., 1987). Often, RRMs function in concert to increase binding specificity possibly because the number of nucleotides recognized by a single RRM is generally too small (4-6 nucleotides) to define a unique binding sequence (Auweter et al., 2006). RRMs are found in a variety of RNA binding proteins throughout eukaryotic cells which encompass virtually all post-transcriptional processes including (for example), pre-mRNA processing (La protein), splicing (U2AF or hnRNPA1) alternative splicing (SR proteins or hnRNPA1), mRNA stability (CBP20), mRNA export (TLS), RNA editing (ACF), pre-rRNA complex formation (nucleolin) and translation regulation (PABP) (Birney et al., 1993). The diverse roles of proteins with RRM domains suggest these motifs are important for cellular development and function.

1.2 RBM proteins

RNA Binding Motif (*RBM)* genes encode a diverse protein family defined by the shared presence of RNA-binding motifs (RBMs) which are defined as containing one or more RRM. Genes encoding RBM proteins are found throughout eukaryotes with at least 38 human *RBM* genes identified to date (Chen and Varani, 2005; Chen and Varani, 2013).

Little is known about the functions of the majority of RBM proteins. Recent reports on RBM3 (Jayasena and Bronner, 2012), RBM4 (Lin et al., 2013), RBM8A (Albers et al., 2012) and RBM38 (Miyamoto et al., 2009), however, reveal potentially important developmental roles for these genes in such processes as craniofacial, pancreas, skeleton and muscle development. Thus far, dysfunctional *RBM* gene

products have been causally implicated in four human developmental disorders. Null or hypomorphic *RBM8A* alleles cause thrombocytopenia with absent radii (TAR syndrome) (Albers et al., 2012). X-linked syndrome talipes equinovarus, atrial septal defect, Robin sequence, persistence of the left superior vena cava (TARP syndrome) is caused by mutations in *RBM10* (Johnston et al., 2010), whereas a heritable dilated cardiomyopathy in which the pre-mRNA of the cardiac splice variant of *TITIN* is incorrectly processed results from mutations in *RBM20* (Guo et al., 2012; Li et al., 2013). Lastly, alopecia, progressive neurological defects and endocrinopathy (ANE syndrome) are caused by loss-of-function mutations in *RBM28* (Nousbeck et al., 2008).

2.2.1 RBM24

RBM24 has emerged as a gene of interest in early cardiac development (Maragh et al.; Miller et al., 2008). This gene was first associated with cardiac development as a result of a transcriptional profiling study by Miller *et. al.*, 2008 where transgenic mouse embryonic stem cells possessing a GFP labeled early cardiac marker (Nkx2.5) were differentiated towards cardiac cell fates. Transcript populations from GFP positive mouse embryonic stem cells were compared to those of the GFP negative mouse embryonic stem cells in an effort to uncover novel critical cardiac genes. A total of 176 transcripts unique to the GFP positive cell population were identified with 43/176 having known roles in early cardiac development. A significant fraction (31/133) of the remaining transcripts not previously reported to be expressed in cardiac progenitors or during cardiogenesis was selected for validation via mouse whole embryo RNA *in situ* hybridization at stages E7.5 (cardiac crescent), E8.5 (heart tube) and E9.5 (looping

heart). The resulting spatial and temporal expression patterns confirmed all 31 transcripts evaluated were expressed in cardiac populations during cardiac development. Furthermore, 9 of these transcripts were expressed in the forming cardiac crescent at E7.5 of the mouse embryo, consistent with roles in the earliest stages of heart development. Based on the early cardiac expression of these genes we predicted they likely play significant roles in heart development. Of the 9 transcripts with expression in the cardiac crescent at E7.5, *Rbm24* had the strongest expression in the cardiac crescent and showed strong primarily cardiac restricted expression at E8.5 and E9.5 (Figure 1-1). Of note by E9.5 *Rbm24* was also expressed in skeletal muscle precursors. The study from Miller *et. al.* 2008 presents *Rbm24* as a gene of interest in early cardiac development and potentially of interest in skeletal muscle development. Human *RBM24* codes for proteins of unknown but likely important function, as its homologs are conserved though mammals and vertebrates down to worms. This thesis will present functional studies using a zebrafish animal model system to study *RBM24* in an attempt to uncover any functional or biological requirement for *RBM24* in cardiac or skeletal muscle development.

1.3 Cardiovascular development

During vertebrate embryogenesis the heart is the first organ to develop and achieve functionality. Model organism studies have uncovered a number of genes such as Nkx2.5, which have important functions in early vertebrate myocardial development and differentiation (Lints et al., 1993; Stainier et al., 1996). Despite an increasing body

of data illuminating the roles played by several key genes during cardiac development, there is still much to learn about what other factors may be critical.

The general stages of cardiac development are invariable throughout vertebrate model organisms where heart development has been examined, with zebrafish progressing through these stages at a particularly rapid rate (Bakkers, 2011) (Table 1-1). Following the completion of gastrulation, the heart filed is the first cardiac structure to form consisting of linearly oriented atrial and ventricular precursor cells. This is followed by the development of the cardiac crescent (heart cone in zebrafish) by the movement and expansion of atrial and ventricular cell precursors and the development of endocardium. This structure expands and elongates into a heart tube, at which point the nascent ventricular and atrial chambers can be distinguished and myocardial contraction begins. The heart tube undergoes a multiple specification events, including early chamber formation, atrio-ventricuar septation, and turning of the heart tube. Primordial cardiac formation completes with the looping of the heart tube to form a functional chambered heart. Heart looping is completed in humans by embryo day 25-28, in mouse by embryo day 9-10 and in zebrafish by 48 hours post fertilization (hpf) or the equivalent of embryo day 2 (Evans et al., 2010); (Bruneau, 2008).

Zebrafish have been shown to be a powerful and relevant model system to study cardiac development (Bakkers, 2011; de Pater et al., 2009; Poon et al., 2010; Stainier, 2001). Zebrafish progress through early heart development, to the stage of a looped heart with circulation, approximately 5 times faster than mouse and 12 times faster than humans. For zebrafish the heart field forms by 13 hpf, with a heart cone between 19-20 hpf, followed by the formation of a short cardiac tube lacking discrete chambers by 24

hpf. Subsequent cardiac tube lengthening and distinct chambers are discernable by 30 hpf with heart tube turning occurring around 36 hpf. A looped functional two chambered zebrafish heart is visible by 48 hpf (Stainier, 2001) (Figure 1-2).

Cardiac development occurs in concert with vascular development. Vascular development consists of vasculogenesis which is the *de novo* formation of the first vascular vessels and subsequently angiogenesis which is the formation of additional vasculature as extensions of existing vasculature. Zebrafish vasculogenesis results in the formation of the main trunk vessels with the DA first to form (24 – 26 hpf) followed by the CV (Albers et al.) and the PCV (28 – 30 hpf) and several heart vessels generating the first single circulation loop. Angiogenesis can be observed in the trunk by 24 hpf as intersegmental vessels (Se) begin to form as paired dorsally extending branches off the DA and subsequently off the PCV (~32 hpf). As the Se reach the dorsal line of the embryo the ends of the vessels form connections resulting in two dorsal longitudinal anastomotic vessels (DLAVs) running along the anterior-posterior (Goodrich et al.) axis of the embryo at the dorsal line. By 48 hpf these trunk vessels are fully formed with circulation (Ellertsdottir et al., 2010; Isogai et al., 2001). Zebrafish transgenic lines and whole embryo staining techniques have been developed and used successfully to study vascular development and circulation (Cross et al.; Drake et al., 1997; Hogan et al., 2009).

1.4 Somite development

Somites are developmental tissue blocks derived from the paraxial mesoderm. Structurally somites are paired tissue segments (one either side of the midline) along the

trunk of the developing embryo (Gridley, 2006; Pourquie, 2011) (Figure 1-3). Somites give rise to skeletal muscle (myotome), cartilage of vertebrae (sclerotome), dermis (dermatome) and endothelial cells (Maroto et al., 2012; Stickney et al., 2000). After the completion of gastrulation, a niche within the tailbud of the embryo containing multipotent mesodermal progenitor cells (MPCs), provides the precursors that ultimately differentiate and organize into somite blocks (Kimelman, 2006; Szeto and Kimelman, 2006). As an embryo continues to develop, the tailbud extends posteriorly and MPCs being to populate a zone called the pre-somitic mesoderm (PSM) just anterior to the tailbud and differentiate into myotome, dermatome and sclerotome precursors. Myotome precursors form both the myotome progenitor population of the somite and the embryonic precursor cells to slow muscle fibers called adaxial cells. Myogenic regulatory factors (MRFs) Myf5, Myod, Myog and Myf6 are pivotal components of myogenesis, and their genes are expressed sequentially in myotome precursors beginning with *myf5* in the PSM, adaxial cells and nascent segmenting somites. This is followed by *myod* expression in adaxial cells, nascent segmenting somites and mature segmented somites, contributing to somite patterning and maturation of myoblasts. Myoblast fusion to form myofibers then terminally differentiated myotubes requires *myog* and *myf6* expression (Coutelle et al., 2001; Osborn et al., 2011).

Maintenance of the MPC niche and continuous somite segmenting with the appropriate periodicity (~every 30 minuets) is critical for normal skeletal muscle, cartilage, dermis and vascular development (Maroto et al., 2012; Stickney et al., 2000). Normal development requires coordinated regulation of signaling for both the

segmentation of new somites and the patterning of formed somites. Components of the Wnt, FGF, Shh, BMP and Notch developmental pathways have been shown in model organisms to be required for normal somitogenesis (Bryson-Richardson and Currie, 2008; Jiang et al., 2000; Marcelle et al., 1997; Niwa et al., 2011; Sawada et al., 2001; Tiedemann et al., 2012). Zebrafish mutants for *gli2a*, *ntla*, *smad5*, *bmp7a*, *tbx6*, *tbx16*, *dlc*, *dld* or *notch1a* have dysregulated somitogenesis and aberrantly formed somites (van Eeden et al., 1996). It is plausible that dysregulation of these critical developmental pathways underlies developmental disorders of as yet unknown etiology.

1.5 The Notch-signaling pathway and somitogenesis

Notch-mediated signaling is among several pathways that play key roles in segmentation and somite patterning (Bray, 2006; High and Epstein, 2008; Oates and Ho, 2002). The Notch pathway acts via a complex multi-component path to achieve paracrine signaling. A simplified model of this pathway can be stated as cell surface ligands interacting with cell surface receptors on a neighboring cell to activate the expression of a target gene within that cell (Bray, 2006). Specifically, ligands Dlc and Dld and target genes Her1 and Her7 have been shown in zebrafish to be critical components of somitogenesis and the segmentation clock, signaling within MPCs, the PSM and nascent segmenting somites (Giudicelli et al., 2007; Julich et al., 2005; Oates et al., 2005; Schroter et al., 2012; Trofka et al., 2012) (Figure 1-4). The genes encoding these four proteins are commonly referred to as the somite clock genes. Dlc and Dld ligands function to activate transcription of *her1* and *her7* target genes in neighboring cells by signaling through Notch1a and Notch3 receptors (Giudicelli et al., 2007; Oates

et al., 2005). The normal functions of Her1 and Her7, include negative regulation of *dlc* and *dld* transcription which contributes to both perpetuation of the somite clock and maintenance of unsegmented cells within the PSM (Tiedemann et al., 2012). The cycling expression of these ligands and target genes persists through to the completion of somitogenesis and is partially maintained by negative feedback of target gene proteins on transcription of *dlc* and *dld* (Giudicelli et al., 2007; Holley et al., 2000).

Thus far Notch pathway dysregulation has been implicated as causal for two human disorders involving tissues of somite origin. These are Alagille Syndrome and spondylocostal dysostosis (Shifley and Cole, 2007). In Alagille Syndrome somitogenesis is believed to be impaired due to patients presenting with skeletal deformities and facial abnormalities with cardiac disease also prevalent. Several studies have linked loss of activity of the Notch ligand Jagged1 to the pathogenicity of Alagille Syndrome (Li et al., 1997; McCright et al., 2002; Oda et al., 1997; Spinner et al., 2001). Spondylocostal dysostosis represents a family of disorders all sharing the feature of short trunk dwarfism accompanied by vertebral segmentation defects along the length of the spinal column, with studies identifying mutations in Notch Ligand DLL3 as causal for the disorder (Penton et al., 2012; Shifley and Cole, 2007; Whittock et al., 2004).

1.6 Functional studies in a zebrafish model

Danio rerio commonly known as zebrafish is a powerful model system to observe and functionally evaluate processes of early development due to their natural characteristics as well as their easy manipulation with molecular-genetic techniques.

Zebrafish fertilization and development occur externally with a single male and female mating yielding up to hundreds of embryos. These embryos are initially transparent allowing for *in vivo* visualization and imaging of early developing tissues. Chemicals such as 1-phenyl 2-thiourea (PTU) can be used to inhibit melanocyte development allowing for continued *in vivo* visualization of development through the embryonic stage. These characteristics coupled with a generation time of 3 months present zebrafish as an attractive system in which to investigate early development (Kimmel et al., 1995; Westerfield, 1995).

A variety of molecular genetic tools have been developed for studying development in zebrafish both *in vivo* and *in vitro*. Among the most common tools used are microinjection, microscopy and whole embryo staining. Through microinjection, exogenous plasmids, RNAs or morpholinos (MOs) are directly introduced into the zebrafish embryo between 1-4 cell stages. The purposes of such manipulation include generation of tagged transgenic zebrafish lines, over expression models and knockdown models (Pickart and Klee, 2014). MOs are short oligos (~ 25 bp) with a morpholine backbone designed to result in knockdown of protein levels through targeted complementary binding to RNA. MOs can act via splice-blocking (causing mis-processing of pre-mRNAs by binding to and occluding splice junctions) or translation blocking (preventing translation by binding to mRNAs at or near the translation start size) mechanisms to confer short term knockdown lasting up to several days (Nasevicius and Ekker, 2000; Pickart and Klee, 2014; Vacaru et al., 2014). Zebrafish embryos can be visualized and recorded *in vivo* via microscopy tools. Transgenic zebrafish lines are often tagged with a fluorophore allowing for *in vivo* observation and

recording of cell population housing the protein of interest. Whole embryo staining is an *in vitro* tool used to observe spatial and temporal localization of molecular targets. Zebrafish whole mount *in situ* hybridization (*ISH*) is widely used to visualize spatial and temporal expression of RNA populations in fixed staged whole embryos (Thisse and Thisse, 2008). Cartilage and bone development can also be assessed and visualized using in vitro staining techniques (Walker and Kimmel, 2007). This thesis details the investigation of the functional requirement for RBM24 in cardiovascular and somite development through *in vivo* and *in vitro* analysis techniques in zebrafish model system.

1.7 Tables: Chapter 1

Table 1-1. Cardiac developmental staging times

	Zebrafish (hpf)	Mouse (dpf)	Human (days)
Gastrulation	5.5	7	15-16
Heart fields	13	7	18
Heart trough	19 (cone)	8	21-23
Heart tube	22	8.5	24
Looping	24-48	8.5-10.25	24-25
Myocardial contraction	22	8.5	24

hpf, Hours post fertilization; dpf, days post fertilization. Adapted from (Evans et al., 2010).

1.8 Figures: Chapter 1

Figure 1-1. *Rbm24* is expressed in the heart early in cardiogenesis

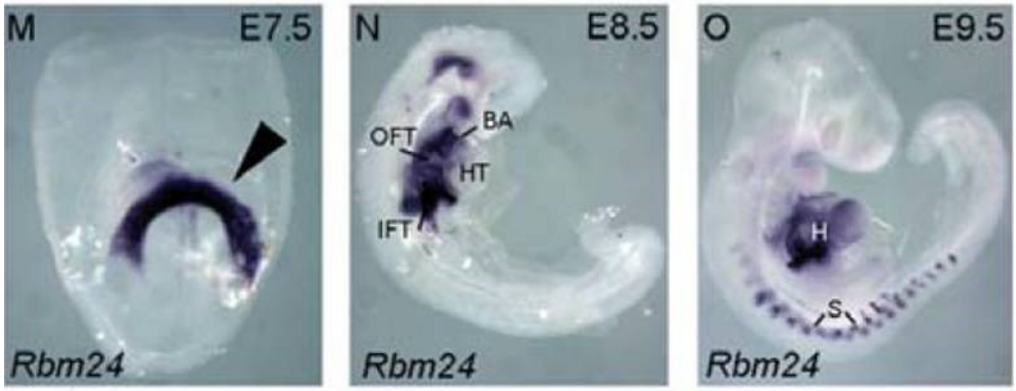

Rbm24 is expressed in the cardiac crescent of E7.5 embryos (arrowhead). At E.8.5 expression is in the HT, OFT, BA, and IFT. AT E9.5 expression persists in the heart and is additionally detected in the somites. HT, heart tube; H, heart; OFT, out flow tract; IFT, inflow tract; BA, branchial arches; S, somites; E7.5-9.5; embryonic days 7.5-9.5. Adapted from (Miller et al., 2008).

Figure 1-2. Schematic of zebrafish cardiac development

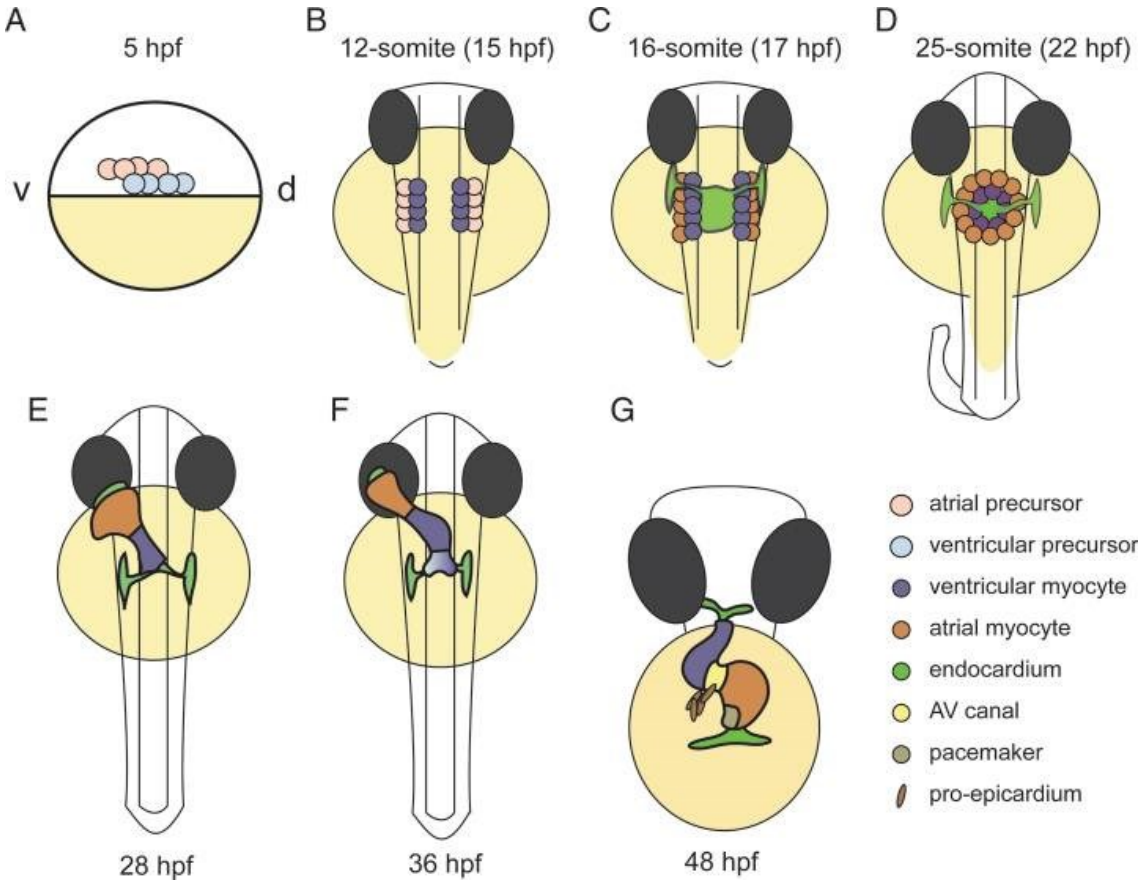

At 5 hpf atrial and ventricular cardiac progenitor cells become visible and organized (A). Cardiogenic differentiation is initiated in the future ventricle myocardial cells by the expression of cardiac myosins (purple) at the 12-somite stage (B). During mid- and late-somite stages, the myocardial tissue expands by continuous cardiogenic differentiation of future atrial myocytes (orange), while endocardial cells (light green) begin populating (C). When the bilateral heart fields fuse at the mid-line, they form a cardiac disc structure with the endocardial cells within the hole at the centre, ventricular myocytes at the circumference and atrial myocytes at the periphery of the disc (*D*). Cardiac morphogenesis transforms the cardiac disc into a cardiac tube. The

endocardium forms the inner lining of the myocardial tube. At 28 hpf, the linear heart tube has formed (E). At 36 hpf, the AV canal is first visible and cardiac looping has started with cardiogenic differentiation continuing by adding new cardiomyocytes to this region (purple gradient) (F). At 48 hpf loopint is completed and the heart tube has formed an S-shaped loop (*G*). Ellipsoid extra-cardiac pro-epicardial cells (brown), AV canal (yellow), pacemaker cells (dark green). Adapted from (Bakkers, 2011).

Figure 1-3. Somite development in zebrafish

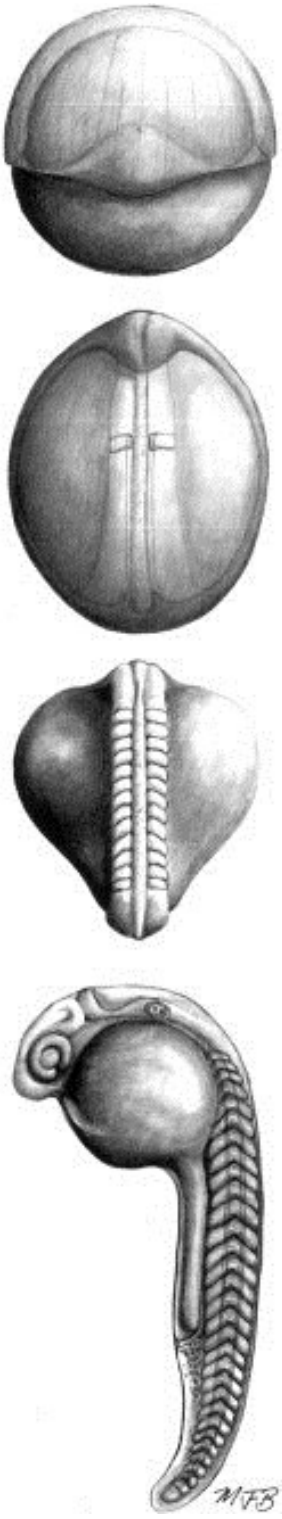

Adapted from (Stickney et al., 2000).

Figure 1-4. Notch segmentation clock

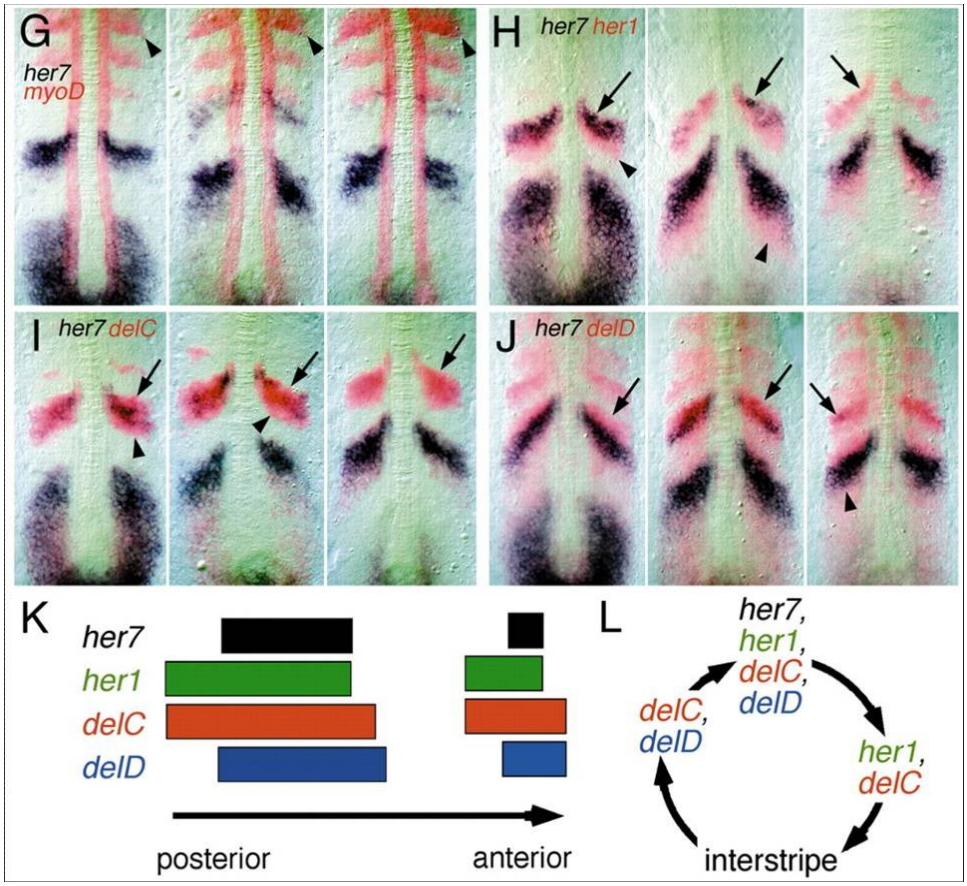

Comparison by two-color in situ hybridization of segmental and cyclic genes in the presomitic mesoderm in embryos at 14 hpf (10 somites) is shown in dorsal view after flat mounting with anterior upwards (G-J). In all panels, her7 has been developed in blue/black. Domains of cyclic gene expression at stages III, I+ and II, according to the nomenclature of Jiang et al. (Jiang et al., 2000); in G-J. The co-expression of myod (G), her1 (H), dlc (I) and dld (J) are shown in red. (K) Diagram of the relative positions of the domains of cyclic gene expression (her7, black; her1, green; dlc, red; dld, blue) to each other within a combined domain moving anteriorly (arrow) in the PSM. (L) The gene expression cycle experienced multiple times by individual cells in the PSM, inferred from the spatial relationships (K). Adapted from (Oates and Ho, 2002)

CHAPTER 2

rbm24a & *rbm24b* ARE EXPRESSED DURING EMBRYOGENESIS AND ESSENTIAL FOR NORMAL CARDIOVASCULAR DEVELOPMENT

2.1 Preface

In this chapter we investigate the putative role of RBM24 in cardiac development. The following study details the identification of two RBM24 zebrafish homologs (termed *rbm24a* and *rbm24b*), and demonstration that their spatial expression is consistent with what was previously observations in mouse (Miller et al., 2008). We use *rbm24a* and *rbm24b* translation blocking morpholino antisense oligonucleotides in the early embryo and demonstrate that each zebrafish *rbm24* homolog has a key but unequal role to play in cardiac development. Additionally, we demonstrate a role for *rbm24a* and *rbm24b* in normal vascular development. Our findings show the requirement for *rbm24a* and *rbm24b* in cardiac development and vasculogenesis with a more pronounced role for *rbm24a*, and an additional putative role for *rbm24a* in angiogenesis.

2.2 Results

2.2.1 Phylogenetic comparative analysis establishes two rbm24 homologs in zebrafish

We recently reported the identification of *Rbm24* as one of a number of novel transcripts discretely expressed in the earliest stages of cardiac development in the mouse embryo (Miller et al., 2008). To facilitate determination of the biological requirement for this gene during vertebrate embryonic development, we first set out to identify the homologs gene/s in zebrafish. In the transition between assembly Zv8 and Zv9 of the zebrafish genome, first one and then a second putative *rbm24* homolog was identified. The current assembly (Zv9) identifies a protein coding gene as *rbm24a* residing on chromosome 19 and also a novel annotation of a putative *rbm24b* protein coding gene residing on chromosome 16. To confirm the validity of these most recent changes to the genome annotation we compared these findings to our own comparative genomic analyses.

The first annotated *rbm24a* gene encodes a protein that displays strong similarity to the mouse Rbm24 (E-value = 3e-90; 188/237 (79%) amino acids). Using the mouse Rbm24 as a blastp query to search the NCBI RefSeq database of *D. rerio* proteins we detected strong similarity (E-value = 5e-61; 103/116 (88%)) to a hypothetical protein LOC562236 encoded by a gene (*zgc:136803*) on chromosome 16 (Zv8). This protein is now termed *rbm24b* in Zv9. The identification of these genes as *rbm24* homologs is further supported by the identification of a pair of annotated *rbm24* paralogs in both the medaka (*Oryzias latipes*; chr. 11, 16) and pufferfish

(*Tetraodon nigroviridis;* chr. 21 and 8) genomes. Zebrafish chromosome 19, where *rbm24a* resides, shares a common evolutionary origin with *O. latipes* chromosome 11 and *T. nigroviridis* chromosome 21 (Kasahara et al., 2007). Similarly, chromosomes 16 and 8 in *O. latipes* and *T. nigroviridis*, respectively, map to the *rbm24b* region of chromosome 16 in *D. rerio*.

2.2.2 rbm24a and rbm24b display cardiovascular expression during embryogenesis

The spatial and temporal expression of both *rbm24* homologs was determined using RNA *in situ* hybridization (*ISH*) (Figure 2-1). Both *rbm24* homologs show cardiac expression early in development. At 15.5 hpf we detected *rbm24a* but not *rbm24b* expression in myocardial precursor cells (Figure 2-1 B and C). By 24 hpf both *rbm24a* and *rbm24b* expression was detected in the forming heart (Figure 2-1 E and F). Expression of *rbm24a* was also detected in the lens of the eye. By 48 hpf, and continuing through 72 hpf, *rbm24a* and *rbm24b* exhibit broad expression throughout the heart, although expression of *rbm24a* was higher in the atrium than the ventricle. By contrast expression of *rbm24b* appeared uniformly expressed in both heart chambers (Figure 2-1 I and L). These data are consistent with cardiac expression of the mouse *Rbm24* homolog, and suggest incompletely overlapping requirements for *rbm24a* and *rbm24b* during zebrafish cardiac development.

By 72 hpf both *rbm24a* and *rbm24b* show incompletely overlapping vascular expression in addition to cardiac expression. *rbm24a* is expressed in the DA and intestinal vasculature (Albers et al.) while *rbm24b* is expressed in the PCV as well as the IV (Figure 2-1 N and O). The early expression of both *rbm24a* and *rbm24b* in both

the heart and vasculature suggests potentially important roles in cardiogenesis and vasculogenesis.

2.2.3 rbm24a and rbm24b are required for normal cardiac development

To determine the functional role of the *rbm24* homologs in cardiac and vascular development, translation blocking MOs were designed against the 5' UTR of each transcript. The effects of gene knockdown was assessed for each homolog individually post microinjection of either MO into zebrafish embryos at the 1-2 cell stage. Titration experiments were conducted to determine MO quantities sufficient to induce a consistent phenotype in a majority of embryos injected (Figure 2-2). Injection of 5 ng of *rbm24a*MO or 8 ng *rbm24b*MO resulted in a robust cardiac phenotype for a significant number of injected embryos at 48 hpf (64/67 and 59/62 respectively) (Table 2-1), compared to uninjected embryos (Figure 2-3 A, B and D). During cardiogenesis the heart tubes of all affected morphant embryos failed to correctly loop, remaining linear but with distinct ventricular and atrial chambers (Figure 2-3). Affected embryos also exhibited reduced blood circulation, which led to cardiac edema in all cases by 48 hpf and continually worsened as development progressed (Figure 2-3). A subset of *rbm24a*MO treated embryos (6/64) displayed an even more severe phenotype, lacking a distinct heart tube and exhibiting a beating focus of periodically contracting cells. This poorly organized cardiac structure was located ventral to the embryo between the embryo and the yolk suggesting a defect in the migration and organization of the cardiac fated cells. Similarly reduction of *rbm24a* or *rbm24b* expression using splice blocking morpholinos, designed against the second intron/exon boundary, also resulted

in cardiac looping defects and cardiac edema in a majority of embryos (92.7% and 54.4% respectively) (Figure 2-4). Knockdown efficiency was evaluated by RT-PCR for embryos displaying cardiac looping defects and cardiac edema after injection with splice blocking morpholino. Both rbm24a and rbm24b transcript levels were significantly reduced to 42.80% +/- 3.35, $P < 6.5 \times 10^{-4}$ and 40.27% +/- 3.19, $P < 4.4 \times 10^{-5}$ of transcript levels in respective uninjected controls (Table 2-2). We used translation blocking MO in all subsequent MO-based experiments due to their greater efficacy.

To confirm the phenotype observed in the *rbm24* morphants was not due to non-specific morpholino toxicity, embryos were co-injected with *p53* morpholino and *rbm24a*MO or *rbm24b*MO (Methods). The cardiac phenotypes remained unchanged in the presence of the *p53* morpholino (Figure 2-5). We then performed phenotype rescue for both *rbm24* morphants to determine the sequence specificity of the observed morphant phenotypes. We generated full length capped poly-A RNA transcripts for each homolog and co-injected each along with the respective *rbm24*MO, directed against the 5'UTR not present in the *in vitro* transcribed RNA. Rescue for *rbm24a*MO was achieved with 800 pg of RNA (36/45) while 50 pg of RNA was sufficient for *rbm24b*MO rescue (35/47). For both homologs rescue resulted in properly looped hearts, normal systemic circulation and an absence of cardiac edema and by 72 hpf and continuing to 96 hpf (Figure 2-3 F, H, J, K, M and P). Taken collectively, these data suggest the phenotype seen with each *rbm24*MO is a specific result of reduction in gene expression and support the inference from ISH expression data that both *rbm24* homologs are required for normal cardiac development.

2.2.4 Depletion of **Rbm24a** *and* **Rbm24b** *compromise cardiac myocardium development*

To better evaluate the impact to the heart of reducing *rbm24a* or *rbm24b* we assayed the expression of several key myocardial transcripts by ISH, including myosin light polypeptide 7, *myl7* (heart), myosin heavy polypeptide 6, *myh6* (atrium) and ventricular myosin heavy chain, *vmhc* (ventricle). Expression of each marker was evaluated in control (uninjected), *rbm24a*MO and *rbm24b*MO injected embryos fixed at 72 hpf at which point the zebrafish heart is normally, looped, fully developed and functioning, allowing us to comment in greater detail on the structural deficits contributing to the gross morphological morphant phenotypes. When examining the entire heart, both *rbm24a* and *rbm24b* morphant embryos exhibit strong *myl7* expression levels comparable to that of controls albeit within an unlooped heart tube. The hearts of controls by contrast are appropriately looped (Figure 2-6 A – F). Additionally in *rbm24a* morphants defects of the presumptive atrium of the forming heart tube appear more severe than in the ventricular portion (Figure 2-6 C and D). By contrast organization of the developing ventricle and atrium in *rbm24b*MO embryos appears equally compromised (Figure 2-6 E and F). Expression of the atrial marker *myh6* for both *rbm24* morphants appears qualitatively similar to levels in uninjected controls. Presumptive atria of *rbm24a* morphant heart tubes appear linear and truncated, while to *rbm24b* morphants also have linear longer heart tubes, both contrasting with the looped atrium observed in uninjected controls (Figure 2-6 G – L). These data are consistent with the observations that *rbm24a* expression was higher in

the atrium than the ventricle by 72 hpf, contrasting with the more uniform expression observed for *rbm24b* across both heart chambers (Figure 2-1).

Both *rbm24* morphant conditions exhibited a near abrogation of the levels of the ventricular marker *vmhc* compared to strong expression in uninjected controls (Figure 2-6 M – R). In *rbm24a*MO morphants expression of *vmhc* was faint but with expression clearly bounded to the heart tube with a clear ventricular portion; however, the expression uncharacteristically extended beyond the ventricular portion into the presumptive atrium of the heart tube (Figure 2-6 O and P). For *rbm24b* morphants *vmhc* expression was very diffuse and failed to clearly mark a ventricular boundary. These findings for *vmhc* expression were unexpected; both in the reduction of total expression seen for both *rbm24* morphants and the apparent stronger severity of the ventricular phenotype compared to the atrial phenotype for both *rbm24* morphants. Taken together the expression of these markers highlight the differential spatial impact of each *rbm24* homolog in heart structure development of the myocardium, and is consistent with our previous gross morphological observations. These data indicate an incompletely overlapping role for *rbm24a* and *rbm24b* in heart tube formation and subsequent heart looping.

2.2.5 Edema in rbm24 morphant embryos may have multiple origins

The observed cardiac edema may result from reduced circulation as a consequence of defects in heart structure, heart rate, aberrant vasculature or combinations of these factors. Given the observed structural defects, we additionally assayed heart rate as a potential contributor to cardiac edema in the *rbm24a*MO and

*rbm24b*MO injected embryos (Baker et al., 1997). Heart rate counts were determined for uninjected, *rbm24a*MO and *rbm24b*MO injected embryos (n = 50) at 48, 72 and 96 hpf. At 48 hpf both *rbm24a* and *rbm24b* morphants displayed significantly lower heart rate compared to uninjected controls ($P < 0.0002$) (Figure 2-7). Heart rates in *rbm24a*MO injected embryos remain significantly lower than uninjected controls at 72 hpf and 96 hpf. By contrast the heart rate of *rbm24b*MO injected embryos recovered such that it did not differ significantly from uninjected controls at 72 hpf and 96 hpf ($P > 0.12$) despite their continued structural anomalies. These data demonstrate cardiac edema is not ameliorated in *rbm24b* morphants despite heart rates increasing to normal levels, suggesting the role of other factors must be considered as contributing to compromised circulation. Although defects in structure and rates of contraction may contribute to compromised circulatory function, we posit that vascular disruption likely also plays a role in the resulting edema.

2.2.6 rbm24a and rbm24b are required for normal vasculogenesis with a potential role in early angiogenesis

To determine the functional role of *rbm24a* and *rbm24b* in vascular development we also undertook MO-based analyses of each homolog in the TG(*kdrl*:G-RCFP) transgenic zebrafish reporter line which fluorescently marks all endothelial cells highlighting the forming cardiovascular structures (Cross et al., 2003). Embryos were examined for vascular expression, after injection of *rbm24a*MO or *rbm24b*MO as described above, after heart formation and completion of vasculogenesis at 48 and 72 hpf (Figure 2-8). As per our earlier experiments, morphant embryos for both genes

exhibit endocardial cardiac edema and a lack of heart looping displaying little to no circulation with 30/31 and 45/50 embryos displaying cardiac defects for *rbm24a* and *rbm24b* morphants respectively (Figure 2-8 D – F and M – O). Additionally, all *rbm24a* and *rbm24b* morphant embryos display a reduction in total trunk vasculature and vascular organization in 100% of the embryos (Figure 2-8 G – I and P – R); however vasculogenic and angiogenic vessels are disrupted to differing degrees. At 48 hpf *rbm24a* morphants posses a clearly present PCV appearing thicker than normal with no detectable DA or CV (Figure 2-8 H). Angiogenesis is severely disrupted in these embryos with unpaired stunted dysmorphic Se also appearing thicker extending only to the midline of the embryo and thus a complete lack of DLAVs. By contrast the *rbm24b* morphant at 48 hpf shows little to no disruption of the DA, a visible but malformed CV and no detectable PCV (Figure 2-8 I). Unlike *rbm24a* morphants, *rbm24b* morphants have less disruption of angiogenesis. Se in *rbm24b* morphants display pairing at the posterior end of the embryo and extend dorsally the length of the embryo forming one DLAV; however, all these vessels are structurally dysmorphic. Both *rbm24a* and *rbm24b* vascular morphant phenotypes become progressively more severe between 48 hpf and 72 hpf. Vessels are less well organized and the number of vessels present is reduced, with no evidence of IV (Figure 2-8 J – L and P – R). Of the morphant embryos displaying cardiac defects *rbm24a* and *rbm24b* morphants segregated into different classes of vascular defects, with 31/31 *rbm24a* morphants analyzed possessing disorganized trunk vasculature where Se do not extend the entire dorsal length of the embryo and the DA and CV are undetectable; and 50/50 *rbm24b* morphants had disorganized trunk vasculature where the Se formed DLAV and yet the PV was

undetectable (Figure 2-8 S and T). These data correlate with respective primary vascular expression locations of *rbm24a* of DA and *rbm24b* of PCV and both displaying expression in the IV (Figure 2-1 G and H). When expression of *rbm24a* or *rbm24b* is compromised formation of the vessels required for the initial circulation loop is similarly compromised, likely contributing significantly to the observed cardiac edema in morphant embryos. These findings indicate the endocardium is also compromised as a result of *rbm24* knockdown and also suggests that both *rbm24a* and *rbm24b* are independently necessary for normal early vascular development and support a putative role for *rbm24a* in angiogenesis.

2.2.7 rbm24a and rbm24b exhibit incompletely overlapping functions in zebrafish development

To determine whether *rbm24a* and *rbm24b* interact genetically in the developing zebrafish embryo, we injected low doses of both *rbm24a* and *rbm24b* MOs into the same embryo. Although each MO dosage amount was too low (2.5 ng and 4 ng respectively) to elicit a strong consistent phenotype alone as evidenced by titration experiments (Figure 2-2), a much more severe phenotype resulted in the morphants receiving both MOs in concert (Figure 2-9). The double morphants displayed greater cardiac edema at 24 hpf than either morphant alone (Figure 2-9 A – D). By 48 hpf, the double morphants also displayed very little cardiac organization, with most (73/93) failing to form any heart tube structure. No double morphants displayed any circulation (Figure 2-9 E– H). This severe and distinctive phenotype exceeds that observed for either MO when assayed independently, even at the higher concentrations that yield

consistent cardiac defects (5 ng of *rbm24a*MO or 8 ng *rbm24b*MO). These data support the possibility that roles for *rbm24* homologs may overlap during cardiovascular development.

2.3 Conclusions

We previously identified *Rbm24* as a novel gene expressed during mouse cardiac development (Miller et al., 2008). Due to its tightly restricted and persistent expression from formation of the cardiac crescent onwards and later in forming vasculature we posited it to be a key player in cardiogenesis with additional roles in vasculogenesis and angiogenesis.

To investigate the role of *RBM24* in cardiac development, we identified its zebrafish homologs, *rbm24a* and *rbm24b*, and functionally evaluated them during zebrafish embryogenesis. Consistent with our underlying hypothesis, reduction in expression of either homolog through injection of morpholino antisense oligonucleotides resulted in cardiogenic defects including cardiac looping and reduced circulation, leading to increasing pericardial edema over time. Additionally, morphant embryos for either homolog displayed incompletely overlapping defects in the forming vasculature of the DA, PCV and CV (Albers et al.). Vasculogenesis and early angiogenesis in the trunk were similarly compromised in *rbm24* morphant embryos. Subsequent vascular maintenance was impaired in both *rbm24* morphants with substantial vessel degradation noted at 72 hpf.

Taken collectively, our functional data support the hypothesis that *rbm24a* and *rbm24b* are key developmental cardiac genes with unequal roles in cardiovascular formation, with each essential for normal cardiovascular development. The results of these investigations present *rbm24a* and *rbm24b* as developmental genes of interest for further functional and mechanistic evaluation.

2.4 Methods

2.4.1 Zebrafish maintenance

Adult AB zebrafish were maintained in system water according to standard methods (Westerfield, 1995). Embryos were obtained from natural mating of adult fish. All experiments were in accordance with ethical permits by Johns Hopkins Animal Care and Use Committee under protocol number FI10M369.

2.4.2 Bioinformatic identification of zebrafish rbm24 homologs

We used the amino acid sequence of the protein encoded by the mouse *Rbm24* gene to perform a blastp query searching the NCBI RefSeq database of *D. rerio* proteins from the Zv8 2008 genome assembly. Two genes were identified (*rbm24* and *zgc:136803*) which encode proteins displaying strong similarity to the mouse Rbm24 protein (E-value = 5e-61; 103/116 (88%) and E-value = 3e-90; 188/237 (79%), respectively). As of the Zv9 2010 *D. rerio* genome assembly NCBI RefSeq now annotates the two genes we previously identified as two *rbm24* paralogs with protein coding transcripts: *rbm24a* on chromosome 19 (RefSeq ID: NM_212865) and *rbm24b* on chromosome 16 (RefSeq ID: NM_001039925).

2.4.3 Nucleic Acid in situ hybridization

Total RNA was isolated from whole zebrafish embryos at 24 hpf using **TRIzol** Reagent and total cDNA was generated with oligo-dT using the SuperScript III First-Strand Synthesis Kit (Invitrogen). Riboprobes for *rbm24a, rbm24b, myl7*, *myh6*, and *vmhc* were generated by PCR amplification of embryo cDNA. PCR fragments were TOPO

cloned into PCRII vector (TA Cloning Kit Dual Promoter with pCRII vector, Invitrogen) and transformed into TOP 10 Cells (Invitrogen). Colonies were mini cultured and plasmid DNA was harvested using the QIAprep Spin Miniprep Kit (Qiagen) Digoxygenin-labeled riboprobes were synthesized from 1 μg plasmid DNA using Sp6 and T7 RNA Polymerase (DIG RNA Labeling Kit SP6/T7, Roche), and purified (SigmaSpin Colums, Sigma). Embryos for *in situ* hybridization at 48 hpf and older were treated with 0.003% PTU beginning at 48 hpf to reduce pigmentation. Embryos were fixed in 4% paraformaldehyde in PBS overnight at 4°C at 15.5 hpf, 24 hpf, 48 hpf, and 72 hpf; and *in situ* hybridization was performed as previously described (Miller-Bertoglio et al., 1997).

2.4.4 Morpholino design and injection

Antisense morpholinos for *rbm24a* and *rbm24b* were designed and provided by Gene Tools, LLC. The *rbm24a* translation blocking morpholino (5'-TGCATCCTCACGAAACGCTCAAGTG-3') and the *rbm24b* translation blocking morpholino (5'-AAATAAACTCCTTGCTCCTTGAAGG-3') were designed to hybridize to the 5' UTR immediately upstream of the translational start site. Morpholinos were diluted with dH_2O to 20 ng / nL and titration experiments were conducted at 1, 2, 5 and 10 ng *rbm24a*MO and 1, 2.5, 5, 7 and 9 ng *rbm24b*MO to determine an effective dose (n = 100 embryos per concentration). Experimental concentrations of 5 ng *rbm24a*MO or 8 ng *rbm24b*MO were selected and injected into the yolks of 1-2 cell fertilized embryos (n = 75). Double knockdown experiments were conducted with co-injection of 2.5 ng *rbm24a* and 4 ng *rbm24b* translation blocking

MO into embryos and compared to embryos injected with these amounts of either MO alone. The *rbm24a* splice blocking MO (5' CGTTATTTGAGATGCCTGACTGTT 3') and the *rbm24b* splice blocking MO (5' TATTTTGACGTTATTTACCTGGCTG 3') were designed to hybridize to the boundary of the second exon and second intron of the transcript and injected at 7.5 ng and 9 ng respectively. Antisense *p53* MO (5'-GCGCCATTGCTTTGCAAGAATTG-3') previously published (Langheinrich et al., 2002) was purchased from Gene Tools, LLC and 1 ng was injected into 1-2 cell stage fertilized embryos both with and without each *rbm24* translation blocking MO (n = 50) (Robu et al., 2007). Embryos were analyzed for cardiac and vascular phenotypes at 48, 72 and 96 hpf.

2.4.5 RT-PCR to determine transcript knock down efficiency

Total RNA was isolated using **TRIzol** Reagent (Invitrogen) from whole morphant zebrafish embryos at 24 hpf after injection of either 7.5 ng *rbm24a* or 9 ng *rbm24b* splice blocking MO. Total cDNA was generated with oligo-dT using SuperScript III First-Strand Synthesis (Invitrogen). RT-PCR was carried out via the standard curve method on a Bio-Rad DNA Engine Opticon 2 Real-Time Detection System with primers specific to the correctly spliced transcripts at 100 ng input cDNA. Uninjected 24 hpf embryo cDNA was used to generate a standard curve and cDNA from uninjected experimental control embryos was assayed at 100 ng cDNA as the standard for 100% expression. All reactions were run in triplicate at 25μL volumes using Power Sybr Green PCR Master Mix (1x final) (Applied Biosystems), primers at final concentration 0.08 μM each. Significance of expression reduction was determined using the students

t-test statistic comparing transcript levels of *rbm24a* or *rbm24b* in uninjected controls to that measured cDNA from their respective morphants.

2.4.6 rbm24 MO phenotype rescue

Total RNA was isolated from whole zebrafish embryos 24 hpf using **TRIzol** Reagent (Invitrogen) and total cDNA was generated with oligo-dT using SuperScript III First-Strand Synthesis (Invitrogen). Full length *rbm24a* and *rbm24b* cDNA were PCR amplified and cloned into the pCR8 gateway vector (pCR8⁄GW⁄TOPO TA Cloning Kit, Invitrogen) before being cloned into the pCSDEST destination vector (kindly provided by the lab of Nathan Lawson, UMass Med School). Full length sense capped Poly-A RNA was generated for *rbm24a* and *rbm24b* with the **mMESSAGE** mMACHINE kit (Ambion) and quantified with a NanoDrop 1000. Full length RNA was co-injected into 1-2 cell embryos with *rbm24a*MO or *rbm24b*MO at titrating levels and evaluated for phenotype rescue at 48, 72 and 96 hpf. Rescue was confirmed with 800 pg *rbm24a* RNA and 50 pg *rbm24b* RNA.

2.4.7 Sequence analysis

Genomic DNA from two patients and an unaffected family member were included (Wessels et al., 2008). Direct sequencing of part of the promoter region (1031 bp), all exons plus exon-intron boundaries and a putative regulatory element in intron 3 (1164 bp) of the *RBM24* gene was undertaken. Primers were designed to cover all four exons representing the "canonical" sequence (ENST00000379052, transcript length 2,458 bp and 236 aa, www.ensembl.org). PCR primers were designed by Primer3 software

(http://frodo.wi.mit.edu/cgi-bin/primer3/primer3.cgi) and are available on request. Amplified PCR products were purified and sequenced using BigDye Terminator chemistry v3.1 on an ABI Prism 3130*xl* genetic analyzer (Applied Biosystems). Biomedical research involving human subjects has been performed according to the principles of the Helsinki's Declaration. Written informed consents were obtained from the patients and relatives involved in the research. Genomic DNA was taken from patients as per standard care and therefore ethical approval was not required.

2.4.8 Heart Rate counts

Heart rates (beats per minute) were counted for uninjected, *rbm24a*MO and *rbm24b*MO injected embryos displaying the morphant phenotype at 48, 72 and 96 hpf. 50 embryos were analyzed per condition per time point. Average heart rates with standard error were plotted and significant heart rate deviation of morphants compared to uninjected controls was determined using the students t-test.

2.4.9 Fluorescent vascular imaging

The transgenic zebrafish line TG(*kdrl*:G-RCFP) generated by Cross and colleagues (Cross et al., 2003) was used for vascular expression. Adult fish and embryos were maintained as described (Westerfield, 1995). Embryos were injected with either 5 ng *rbm24a*MO or 8 ng *rbm24b*MO at the 1-2 cell stage and analyzed at 48 and 72 hpf for G-RCFP expression via fluorescence microscopy.

2.5 Tables: Chapter 2

Table 2-1. Number of embryos with cardiac defects in *rbm24* morphant and rescue conditions.

Morpholino	Dosage	Embryos Studied	Looping Defects	Cardiac Edema	No Cardiac Organization
*rbm24a*MO	5 ng	67	58 (86.6 %)	64 (95.5 %)	6 (9 %)
rbm24a rescue	+ 800 pg RNA	45	9 (20 %)	9 (20 %)	0
*rbm24b*MO	8 ng	62	59 (95.2 %)	59 (95.2 %)	0
rbm24b rescue	+ 50 pg RNA	47	12 (25.5 %)	12 (25.5%)	0

Table 2-2. Cardiac phenotypes displayed upon knockdown of *rbm24a* or *rbm24b* expression via splice blocking morpholino.

Morpholino	Dosage	Embryos Studied	Looping Defects	Cardiac Edema	No Cardiac Organization
*rbm24a*MO sb	7.5 ng	96	89 (92.7 %)	89 (92.7 %)	0
*rbm24b*MO sb	9 ng	79	43 (54.4 %)	43 (54.4 %)	0

2.6 Figures: Chapter 2

Figure 2-1. *rbm24a* and *rbm24b* display cardiovascular expression during embryogenesis.

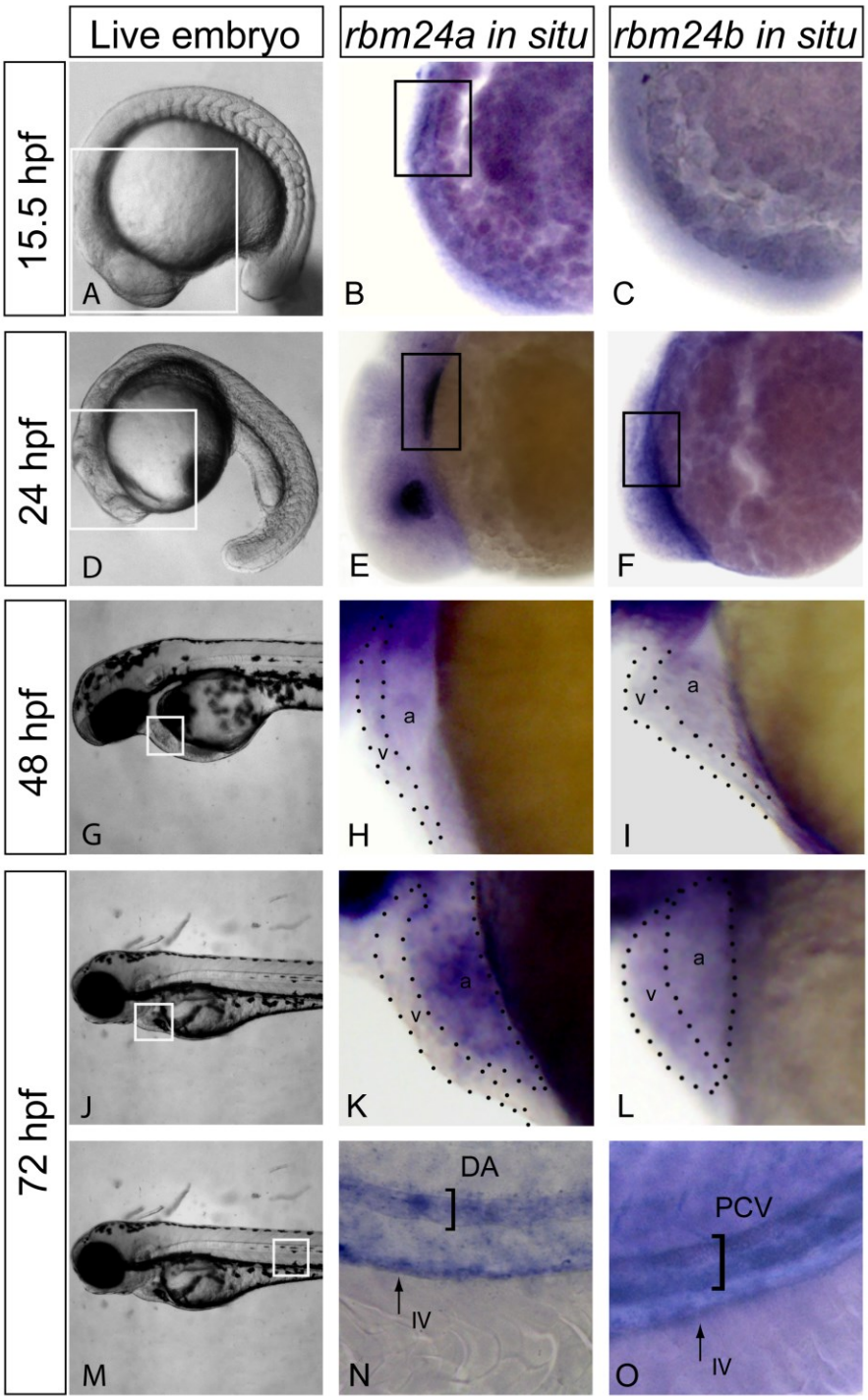

Expression of *rbm24* transcripts was evaluated in uninjected embryos fixed at 15.5, 24, 48 and 72 hpf. Live embryos 15.5 hpf with area of interest for rbm24 *in situ* boxed in white (A). Lateral heart views of *rbm24a* and *rbm24b in situs* on uninjected 15.5 hpf embryos showed expression linearly organized myocardial precursor cells for *rbm24a* (black box, B) but not *rbm24b* (C). Live embryos 24 hpf with area of interest for rbm24 *in situ* boxed in white (D). Lateral heart views of *rbm24a* and *rbm24b in situs* showed expression in the developing heart tube at 24 hpf (black box, E, F) with lens expression for *rbm24a* alone. 48 hpf live embryo showing the heart boxed in white (G). Lateral zoom of the heart showed *rbm24a* and *rbm24b* were expressed in the ventricle (v) and atrium (a) of the looped heart at 48 hpf (H, I). Live 72 hpf embryos with the heart boxed in white (J). Expression of both *rbm24* transcripts was detected in the heart at 72 hpf (K, L). Live image of a 72 hpf embryo with the area of interest for vascular expression boxed in white (M). Expression of both *rbm24* transcripts was detected in the trunk vasculature with differing expression patterns. *rbm24a* shows arterial expression in the DA (N) while *rbm24b* shows venous expression in the PCV (O) with both being expressed in the IV. DA, dorsal aorta; PCV, posterior caudal vein; IV, intestinal vasculature.

Figure 2-2. Translation Blocking MO titrations.

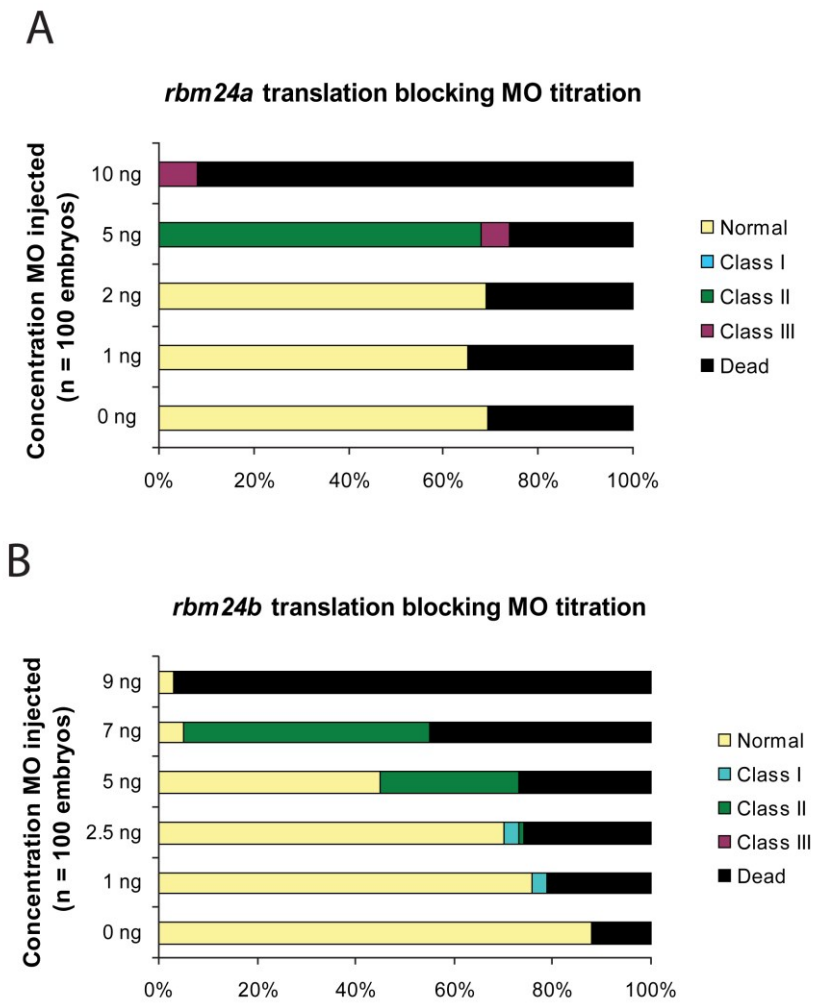

Quantitative representation of percentage of embryos displaying cardiac phenotypes achieved from MO titrations. *rbm24a*MO 1, 2, 5 and 10 ng injected (A). *rbm24b*MO 1, 2.5, 5, 7 and 9 ng (B). Normal, looped beating heart with no cardiac edema; Class I, looped beating heart with cardiac edema; Class II, unlooped beating heart tube with cardiac edema; Class III, beating heart cell mass with cardiac edema; Dead, extreme cell death and degradation of embryo. n = 100 embryos per concentration.

Figure 2-3. *rbm24a* and *rbm24b* are required for normal cardiac development.

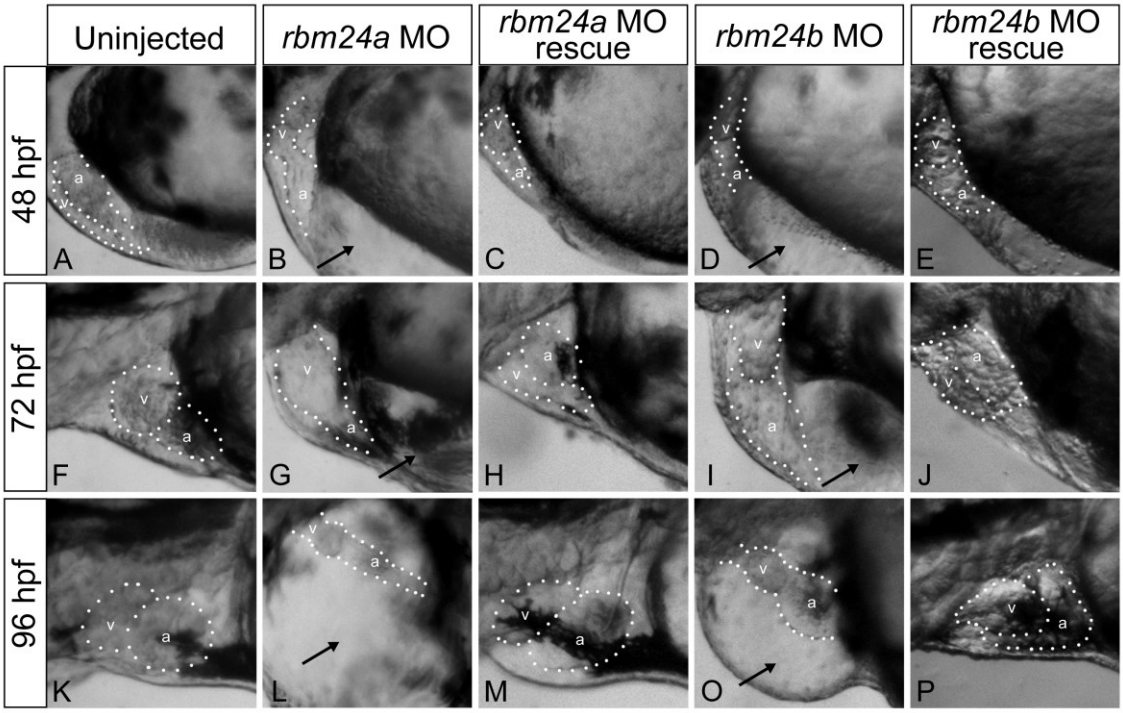

Translation blocking morpholinos complementary to *rbm24a* (5 ng) *or rbm24b* (8 ng) were injected into 1-2 cell stage zebrafish embryos and the resulting phenotypes were evaluated compared to uninjected controls at 48 hpf (A, B, D), 72 hpf (F,G,I), and 96 hpf (K, L, O). Lateral heart views are shown with a dotted outline around the heart chambers. Both morphant embryo conditions exhibited cardiac looping defects and edema at all stages. Heart chambers are shown with a dotted outline with chambers denoted: v, ventricle; a, atrium; black arrows, cardiac edema. Phenotype rescue was achieved for each *rbm24* via co-injection of each respective full length capped poly-A RNA transcript (*rbm24a* 800 pg , *rbm24b* 50 pg) along with the respective complementary translation blocking morpholino into 1-2 cell stage embryos where 800 pg *rbm24a* (C, H, M) or 50 pg *rbm24b* (E, J, P) achieved rescue. Rescued embryos posses looped hearts absent of edema.

Figure 2-4. *rbm24a* and *rbm24b* splice blocked morphants display cardiac defects.

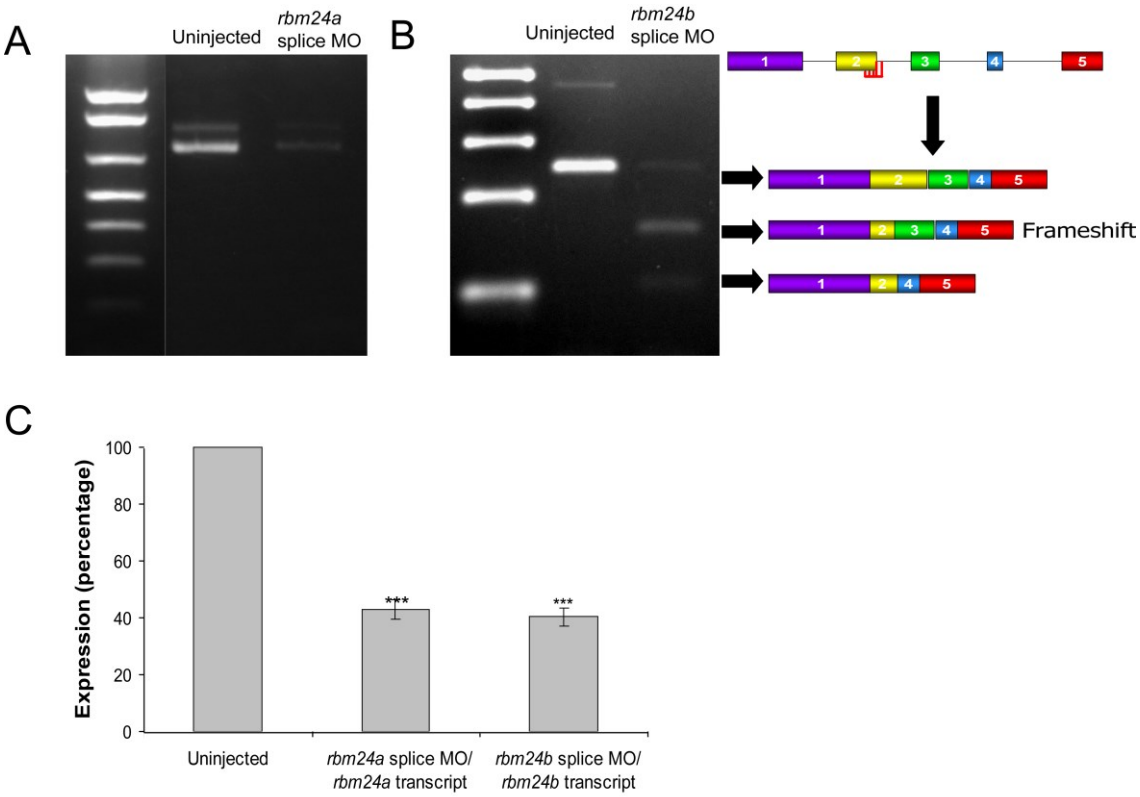

Injection of 7.5 ng of *rbm24a* splice blocking morpholino results in a substantial reduction of full-length transcript (A). Injection of 9 ng of *rbm24b* splice blocking morpholino results in aberrant splicing of the transcript. There is a reduction of full-length transcript 250 bp fragment and appearance of trace amounts of the shortened frameshift fragment 164 bp and shortened in-frame transcript 109 bp (B). RT-PCR measurement of transcript levels show both *rbm24a* (42.80% +/- 3.35, $P < 6.5 \times 10^{-4}$) and *rbm24b* (40.27 +/- 3.19, $P < 4.4 \times 10^{-5}$) morphants have significant reduction of transcript levels compared to uninjected controls (C) Error bars are standard deviation, *** $P < 0.001$.

Figure 2-5. *p53 MO* co-injection does not alter *rbm24a* and *rbm24* morphant phenotypes.

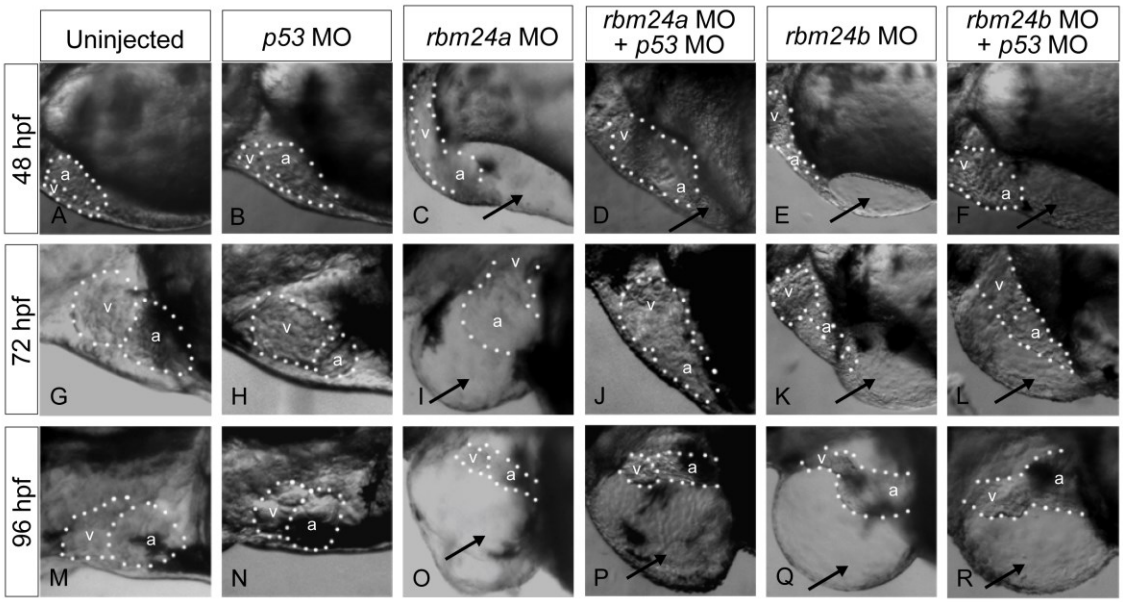

Phenotypes were evaluated for embryos post injection *rbm24a* MO (5 ng) *or rbm24b* MO (8 ng) alone or in conjunction with *p53* MO (1 ng) phenotypes were compared at 48, 72 & 96 hpf. Lateral heart views are shown with a dotted outline around embryo heart chambers. No cardiac phenotype is detected for *p53* MO embryos compared to uninjected controls at any time point (A-B, G, H, M, N). At all time points *rbm24a* morphants maintain unlooped hearts and display cardiac edema in the presence of *p53* MO (C, D, I, J, O, P). Morphant phenotype was also maintained between *rbm24b* morphants in the presence of *p53* MO (E, F, K, L, Q, R). v, ventricle; a, atrium; black arrows, cardiac edema.

Figure 2-6. Depletion of *rbm24a* and *rbm24b* compromise cardiac myocardial development.

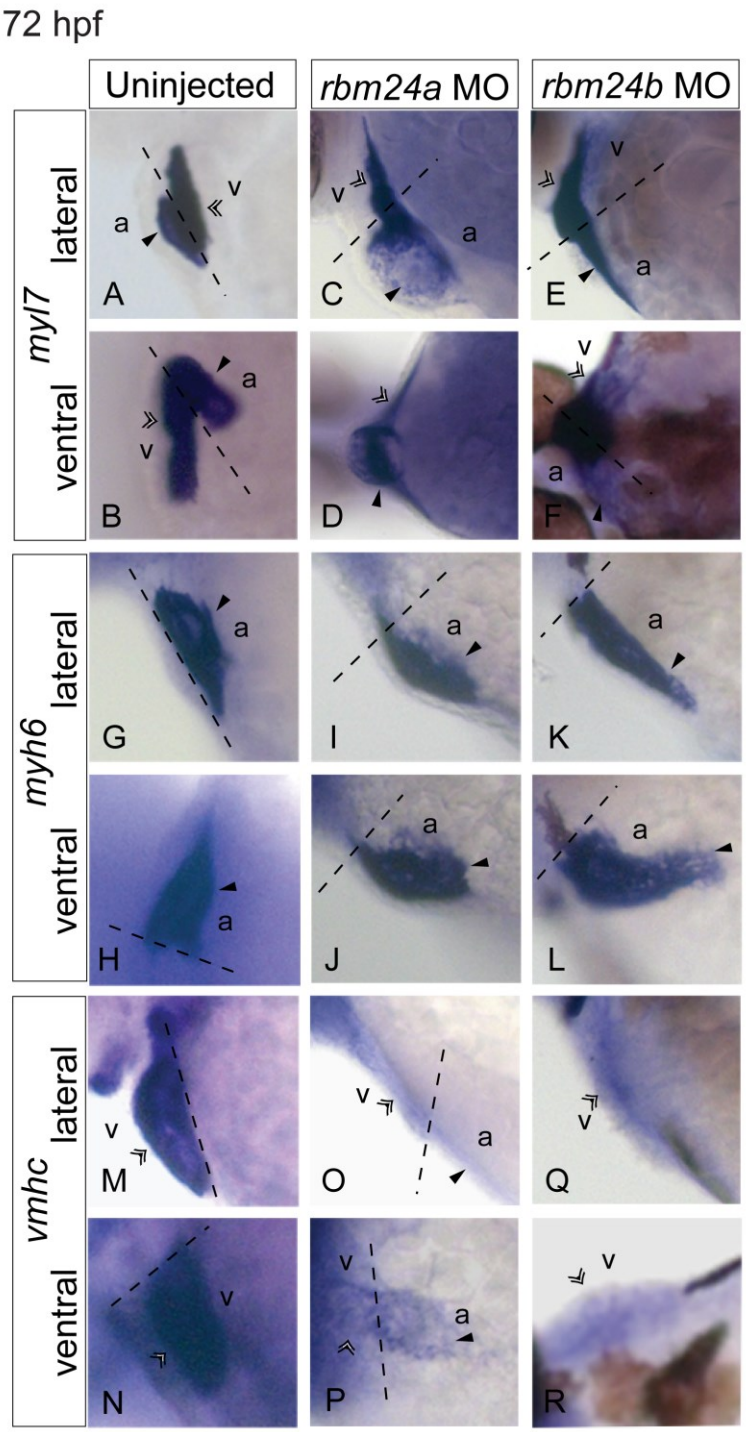

The expression patterns of cardiac markers were analyzed in *rbm24* morphants and uninjected controls at 72 hpf. Ventral and lateral images of the heart are shown with a dotted line marking the boundary between heart chambers. By *myl7* expression of the entire heart, uninjected controls possess looped hearts with defined ventricle and atrium chambers (A, B) in contrast to unlooped hearts for both *rbm24* morphants. *rbm24a* morphants displayed linear presumptive ventricle and an incompletely formed presumptive atrium (C, D). *rbm24b* morphants displayed a linear presumptive atria and ventricle (E, F). *myh6* marking the atrium displayed a looped atrium in controls (G, H) with linear atrium in *rbm24*a (I, J), and *rbm24b* morphants (K, L). *vmhc* expression demarks looped ventricles in controls (M, N). *rbm24a* morphants displayed little expression bound to an unlooped heart tube where expression extends to the presumptive atrium (O, P). Almost no *vmhc* expression is detectable in *rbm24b* morphants (Q, R). v, ventricle region; double arrow, ventricular expression a, atrium region; solid black arrow, atrial expression.

Figure 2-7. Slow heart rate may contribute to cardiac edema in *rbm24* morphants.

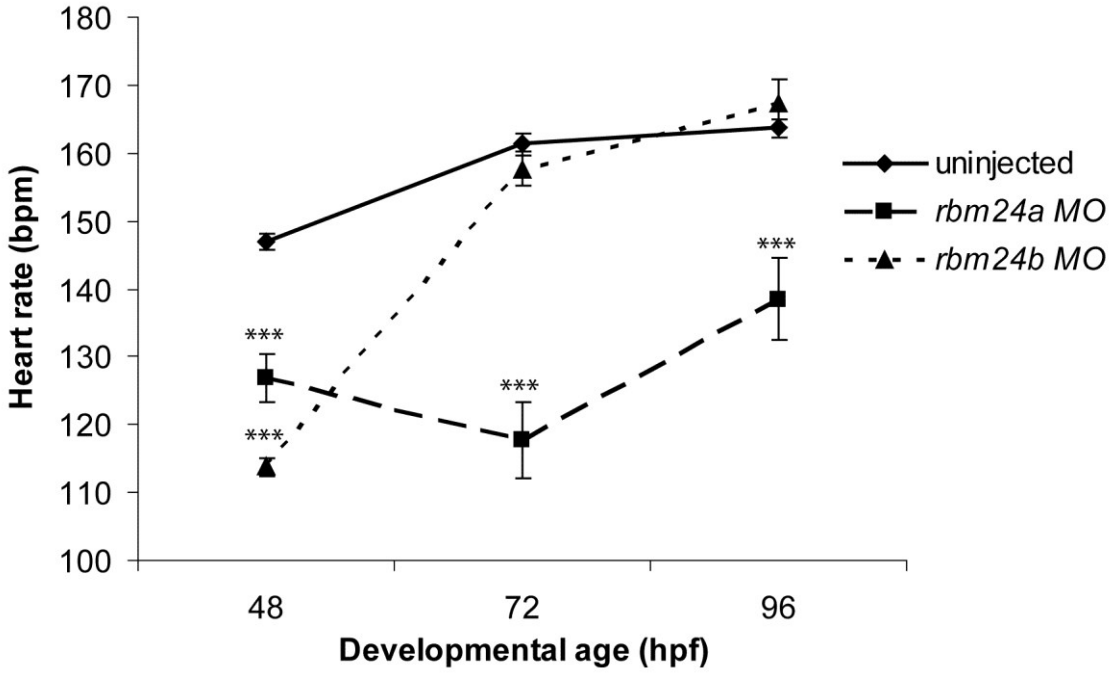

Heart rates were determined for uninjected control, *rbm24a* and *rbm24b* morphant embryos at 48, 72 & 96 hpf and significance was ascribed from a t-test statistic. 50 embryos were examined for each condition at each time point. At all time-points the heart rate of *rbm24a* morphants was significantly lower than controls where $P < 2x10^{-5}$. At 48 hpf *rbm24b* morphants had significantly lower heart rates than controls ($P = 1x10^{-32}$). The heart rates for *rbm24b* morphants then rose to rates not different from controls by 72 hpf and 96 hpf ($P > 0.12$) while maintaining the features of the morphant phenotype. Error bars here are standard error. *** $P < 0.001$.

Figure 2-8. Reduction of *rbm24a* or *rbm24b* results in aberrant vasculature and a lack of vascular maintenance.

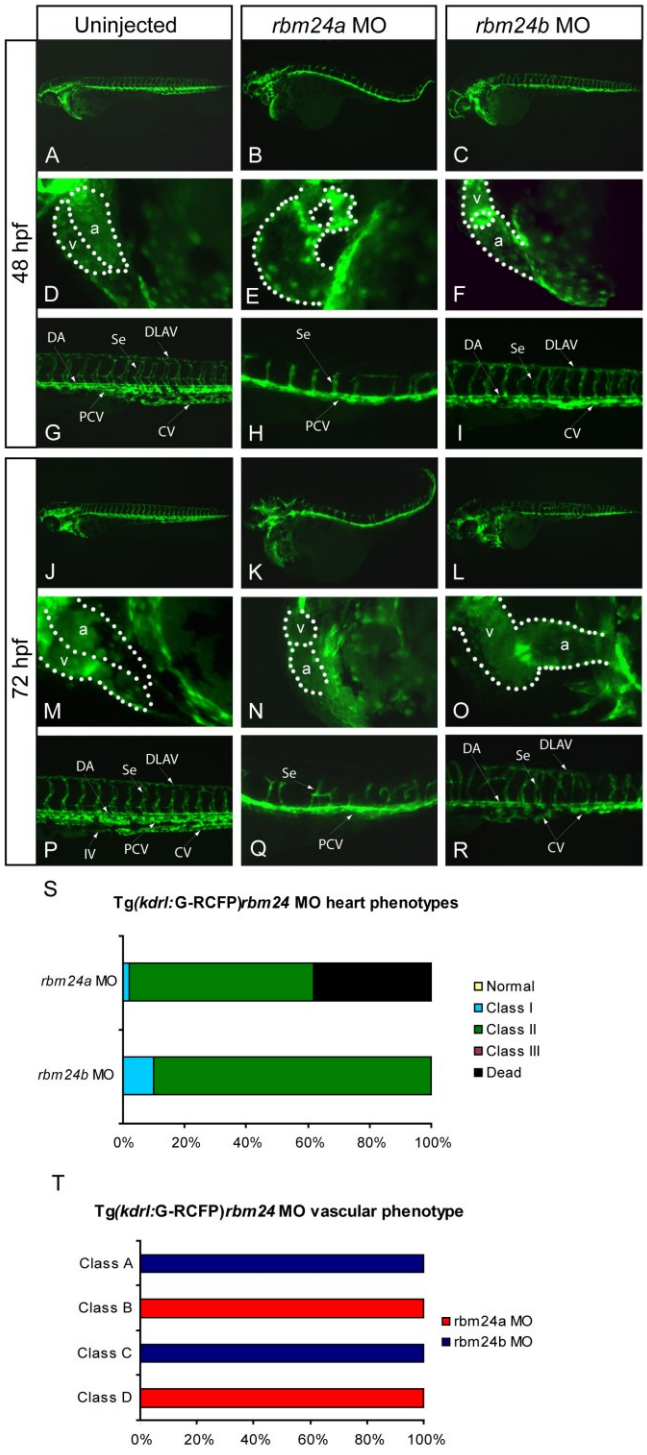

TG(*kdrl*:G-RCFP) zebrafish line was used to asses the impact of *rbm24* depletion on vasculature at 48 hpf and 72 hpf. Lateral views are shown for whole embryo, heart and trunk with a dotted outline indicating heart chamber boundaries. Uninjected controls at all time-points display looped hearts and properly developed vasculature. (A, D, G, J, M, P). 48 hpf *rbm24a* morphants possess unlooped hearts but display only the PCV and stunted disorganized Se (B, E, H). 48 hpf *rbm24b* morphants possess unlooped hearts, and only the DA and CV are visible with disorganized Se (C, F, I). By 72 hpf there was increased vascular disorganization and degeneration and a lack of heart looping and in both *rbm24* morphants (K, N, L, O, Q, R). Cardiac morphant phenotypes are displayed quantitatively as percentages; Normal, looped beating heart with no cardiac edema; Class I, looped beating heart with cardiac edema. Class II, unlooped beating heart tube with cardiac edema, Class III, beating heart cell mass with cardiac edema; Dead, extreme cell death and degradation of embryo (S). Morphant vascular phenotype classes; Class A, disorganized trunk vasculature with formed DLAV; Class B, disorganized trunk vasculature with truncated Se and no DLAV; Class C, no discernable PCV; Class D, no discernable DA or CV (T). v, ventricle; a, atrium; DA, dorsal aorta; CV, caudal vein; PCV, posterior caudal vein; Se, intersegmental vessels, DLAV, dorsal longitudinal anastomotic vessels; IV, intestinal vasculature.

Figure 2-9. Double *rbm24a* and *rbm24b* morphants display more severe cardiac defects.

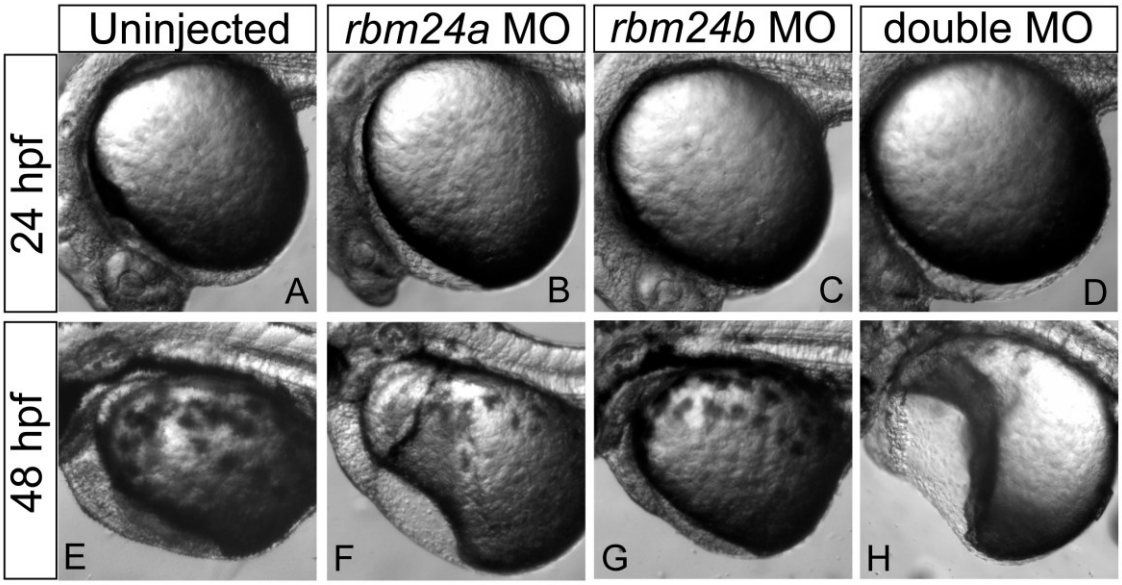

Morpholinos directed to each *rbm24* homolog were injected individually and in tandem into zebrafish embryos and assessed at 24 hpf and 48 hpf compared to uninjected embryo hearts (A and E). Individual morpholino injections were titrated to a low dose for both *rbm24a,* 2.5 ng (B and F) and *rbm24b*, 4ng (C and G). Embryos receiving low doses of both *rbm24a* and *rbm24b* morpholinos resulted in more severe phenotype than either low dose MO alone, exhibiting severe cardiac defects and increased edema (D and H).

CHAPTER 3

Rbm24a & Rbm24b ARE ESSENTIAL FOR SOMITE AND CRANIOFACIAL DEVELOPMENT

3.1 Preface

We initially identified *Rbm24* in a screen for early cardiac genes and demonstrated it to be expressed at multiple time points during mouse cardiogenesis as well as in the somites (9.5 dpc) (Miller et al., 2008). Our subsequent cardiovascular-focused studies in zebrafish determined a pivotal role for both zebrafish homologs (*rbm24a* and *rbm24b*) in the genesis of the cardiovascular system (Maragh et al., 2011). In addition to the reported cardiovascular defects, there was an apparent impairment to the development of other embryonic systems. In this chapter we more generally investigate the expression and functional requirement for *RBM24* in normal early embryonic development using the zebrafish model system. The results of this study present the zebrafish RBM24 homologs as important players in the regulation of somite and craniofacial development.

3.2 Results

3.2.1 rbm24a and rbm24b are expressed in somites and presumptive skeletal muscle populations

We initially identified *Rbm24* in a screen for early cardiac genes and demonstrated it to be expressed at multiple time points during mouse cardiogenesis as well as in the somites (9.5 dpc) (Miller et al., 2008). Our subsequent cardiovascular-focused studies in zebrafish determined a pivotal role for both zebrafish homologs (*rbm24a* and *rbm24b*) in the genesis of the cardiovascular system (Maragh et al., 2011). In addition to the reported cardiovascular defects, there was an apparent impairment to the development of other embryonic systems. Taking these data collectively we postulate that *rbm24a* and *rbm24b* may similarly contribute to the development of other systems in which they are expressed. To address this question we assayed the embryonic expression of *rbm24a* and *rbm24b* in the embryo throughout development. We detected transcripts corresponding to both *rbm24a* and *rbm24b* in the tailbud at the bud stage and in forming somites during somitogenesis via *ISH* (Figure 3-1). By 8 somites both *rbm24a and rbm24b* are expressed in patterned somites and somite progenitors (Figure 3-1 C, D). Somitic expression of both *rbm24a* and *rbm24b* persists through 24 hpf (Figure 3-1 E, F), at which time *rbm24a* transcripts are predominately localized in the most posterior somites and somites progenitors. By 48 hpf, however, *rbm24a* expression is undetectable in the somites by *ISH* (Figure 3-1 G). By contrast, *rbm24b* is expressed uniformly throughout all somites at 24 hpf, and remains readily detected in the somites at 48 hpf (Figure 3-1 F, H).

In addition to their somitic expression, both *rbm24a* and *rbm24b* were also detected in developing craniofacial structures (Figure 3-2 A). The spatial expression pattern observed for each is consistent with multiple craniofacial muscle populations including those in the forming mandible, pharyngeal arches, otic vesicle and in optic muscles. Taken collectively these data are consistent with potential roles in development for both Rbm24a and Rbm24b beyond those previously described in cardiovascular development (Maragh et al., 2011).

3.2.2 **Rbm24a** ***and*** **Rbm24b** ***are required for normal somite and craniofacial development***

We evaluated the requirement for Rbm24a and Rbm24b during somite development, using MO technology to elicit knock down of each protein product independently. We previously assayed the efficacy of both translation-blocking and splice-blocking MOs designed against *rbm24a* and *rbm24b* transcripts (Maragh et al., 2011). The translation-blocking MOs consistently displayed higher efficiency although both classes of MO resulted in the same phenotype (Maragh et al., 2011). We, therefore, used translation blocking antisense MO to evaluate the independent impacts of Rbm24a or Rbm24b knockdown on somite integrity and directly compared *rbm24a*MO and *rbm24b*MO injected embryos to embryos injected using a control non-targeting morpholino (ctrlMO). Reduction of either Rbm24a (*rbm24a*MO) or Rbm24b (*rbm24b*MO) disrupted normal somite patterning (Figure 3-3). At the 8 and 13 somite stages, *rbm24a*MO embryos frequently lacked distinct inter-somitic boundaries among multiple somites. By contrast although somitic boundaries remained in *rbm24b*MO

embryos their somites were laterally distended and demonstrated compression along the A-P axis (Figure 3-3 A-F). As further evidence of impaired somitogenesis in *rbm24a*MO and *rbm24b*MO embryos, the internal angle of somitic chevrons were measured in 13 somite stage embryos. The internal chevron angle was measured for somites 6-10 individually as representative for each embryo. We observed the internal angle of somitic chevrons to be significantly more obtuse among *rbm24a*MO ($p \leq 0.037$) and *rbm24b*MO ($p \leq 0.0029$) embryos when compared to ctrlMO embryos (n= 3-5 per treatment; Figure 3-3 V). There was no significant difference in chevron angle, however, between uninjected and ctrlMO injected embryos.

Dysmorphic somites persisted in *rbm24a*MO and *rbm24b*MO embryos at 24 hpf, and showed no sign of recovery after the completion of somite pattering (48 hpf), rather both showed an additional curving tail phenotype (Figure 3-3 G-U). We then assayed the phenotypes of *rbm24a*MO and *rbm24b*MO embryos based upon the expression of *myod* and *dystrophin* (*dyst*) (Parsons et al., 2002) established markers of somites and inter-somitic boundaries, respectively. *ISH* for *myod* and *dyst* clearly reveal the persistence of the somite patterning disruption in *rbm24a*MO and *rbm24b*MO embryos throughout patterning (24 hpf) and beyond (48 hpf). Although the effect of Rbm24a reduction on somite organization remained most marked in the posterior somites, consistent with localization of its expression, the structure of more rostral somites was also perturbed (Figure 3-3 K). *rbm24a*MO embryos also showed marked reduction of *dyst* at 24 hpf, indicating that the integrity of somitic boundaries was compromised (Figure 3-3 N). These defects persisted at 48 hpf with dramatic defects in somitic structure remaining among *rbm24a*MO embryos (Figure 3-3 T). Similarly, the

effects of Rbm24b reduction were obvious at 24 hpf (Figure 3-3 L). The integrity of truncal somites was severely compromised and *dyst* signal was completely ablated (Figure 3-3 O). By contrast with *rbm24a*MO embryos, somite structure of *rbm24b*MO embryos recovered significantly by 48 hpf as seen by *myod* expression (Figure 3-3 U). This may reflect recovery enabled by the persistent expression of Rbm24b beyond the effective window of the corresponding MO.

In addition to these somite phenotypes, abnormalities in craniofacial development were also detected in *rbm24a*MO and *rbm24b*MO embryos consistent with their observed spatial and temporal expression (Figure 3-2 B). Independent MO-based knockdown of either Rbm24a or Rbm24b resulted in shortened mandible, reduction in the size of the otic vessicle, micropthalmia and microcephaly. Effects on the development of these structures, however, appeared more pronounced in *rbm24a*MO embryos (Figure 3-2 B). Craniofacial muscle patterning at 72 hpf in mandibular, pharangeal arch, optic and fin bud muscle was reduced in both *rbm24a*MO and *rbm24b*MO embryos. Alcian blue cartilage staining at 96 hpf revealed a dramatic reduction of the craniofacial cartilage in *rbm24a*MO and *rbm24b*MO embryos yielding little to no signal corresponding to the ethmoid plate, palatoquadrate, hyomandibular and Meckel's cartilage (Figure 3-2 B). By 48 hpf and continuing through 96 hpf, concurrent with somite and craniofacial defects, we also observed our previously described cardiovascular defects in *rbm24a*MO and *rbm24b*MO embryos (Maragh et al., 2011).

RNA rescue experiments were performed to confirm the specificity of MO phenotypes. As with previously described cardiac phenotypes, all observed *rbm24a*MO

and *rbm24b*MO somite and craniofacial phenotypes were appropriately alleviated in at least 74% of embryos via mRNA rescue (Figure 3-2 C, Figure 3-3 W-Z).

These results suggest both Rbm24a and Rbm24b function early in somite/skeletal and craniofacial muscle patterning and are required for normal development.

3.2.3 Knockdown of **Rbm24a** *or* **Rbm24b** *does not deplete myogenic regulatory factors or MPCs*

MRFs Myf5, Myod, Myog and Myf6 are pivotal components of myogenesis, and their genes are expressed sequentially in myotome precursors beginning with *myf5* in the PSM and somite progenitors. This is followed by *myod* expression in somite progenitors and somites, contributing to maturation of myoblasts. Myoblast fusion to form myofibers then terminally differentiated myotubes requires *myog* and *myf6* expression (Coutelle et al., 2001; Osborn et al., 2011). To characterize the Rbm24 knockdown phenotype during somitogenesis in greater depth we performed *ISH* with probes to the MRFs at the 13 somite stage of development. We previously used *ISH* against *myod* as a somite marker and found no qualitative loss of *myod* while observing aberrant somite morphology (Figure 3-2 D-E). Likewise, we did not observe quantitatively reduced expression of any MRF in *rbm24a*MO or *rbm24b*MO embryos compared to ctrlMO embryos (13 somite stage, Figure 3-5). However, at the same stage, spatial distribution of *myf5, myog and myf6* was consistent with brightfield observations of *rbm24a*MO and *rbm24b*MO embryo somite phenotypes. In the PSM *myf5* expression was more markedly expanded in *rbm24b*MO embryos compared to

*rbm24a*MO and ctrlMO embryos. Spatial expression of *myf5*, *myog* and *myf6* were similarly distorted in segmented somites of *rbm24a*MO and *rbm24b*MO embryos highlighting once again the observation of compressed somites along the A-P axis of *rbm24b*MO embryos with additional severe lateral distention.

3.2.4 Double knockdown of rbm24a and rbm24b effects somites with greater severity

Knockdown experiments evaluating the impact of *rbm24a* or *rbm24b* depletion on cardiovascular experiments revealed a more severe cardiac phenotype was achieved upon double knockdown of *rbm24a* and *rbm24b* in the same embryo (Maragh et al., 2011). This was investigated here in relation to the observed somite phenotype. Half the effective dose of both *rbm24a* and *rbm24b* MOs (2.5 ng and 4 ng respectively) were injected in the same embryo and compared embryos injected with to full doses of only one *rbm24* MO (5 ng and 8 ng respectively). A much more severe phenotype resulted in the morphants receiving both MOs in concert (Figure 3-4). The double morphants displayed more indistinct somite boundaries at 8 somites than either morphant alone. By 30 hpf, the double morphants also displayed increased somite compression along the A-P axis and considerable tail kinking. These data support and confirm the previous observation in the heart that the roles for *rbm24* homologs may overlap during somite development.

3.3 Conclusions

We previously demonstrated that the gene encoding Rbm24 is expressed during mouse cardiogenesis, and determined its zebrafish homologs, Rbm24a and Rbm24b, are essential for cardiac and vascular development. We undertook in this set of studies to more completely evaluate requirement of Rbm24a and Rbm24b in early embryonic development.

We demonstrate here by whole embryo *ISH* that both *rbm24a* and *rbm24b* are expressed by the bud stage of development and are subsequently expressed in the PSM and somites during segmentation. During segmentation, spatial detection of *rbm24a* was more concentrated in the posterior trunk in the most nascent somites, while *rbm24b* expression appeared equally present in all somites. After the completion of segmentation *rbm24a* expression was no longer detectable in the somites, while *rbm24b* expression was continually detected. After segmentation both *rbm24a* and *rbm24b* were detected in developing craniofacial structures spatially and temporally consistent with craniofacial muscle populations.

Functional evaluation of the requirement of Rbm24a and Rbm24b using translation blocking antisense MO revealed both Rbm24a and Rbm24b are required for normal somite and craniofacial development. *rbm24a*MO and *rbm24b*MO embryos exhibited somite patterning defects and malformation of craniofacial structures. These MO induced phenotypes were not consistent with simply developmental delay and were rescued upon microinjection of either respective mRNA. Characterization of the somite phenotype using MRF markers suggests somite patterning defects do not result upon a loss of MRF expression.

These studies uncover a previously unreported requirement for Rbm24a and Rbm24b in somite and craniofacial development. Further they highlight the value of investigating a mechanism of action for Rbm24a and Rbm24b in early embryonic development.

3.4 Methods

3.4.1 Zebrafish Maintenance

Adult AB,zebrafish lines were maintained in system water according to standard methods (Westerfield, 1995). Embryos were obtained from natural mating of adult fish.

3.4.2 Morpholino injection & mRNA rescue

*rbm24a*MO and *rbm24b*MO embryos were generated by injection of previously published *rbm24a* and *rbm24b* translation blocking antisense morpholinos into 1-2 cell stage embryos at 5 ng and 8 ng respectively (Maragh et al., 2011). The standard Gene Tools negative control morpholino oligo (CCTCTTACCTCAGTTACAATTTATA) was injected into 1-2 cell stage embryos at 8 ng to generate ctrlMO embryos. Double MO embryos were generated by co-injecting 2.5 ng *rbm24a*MO with 5 ng *rbm24b*MO in a single injection solution. mRNA rescue experiments were performed as previously described (Maragh et al., 2011).

3.4.3 Microscopy

Brightfield images were acquired on a Zeiss Luminar.V12 Stereoscope and a Nikon AZ100 dissecting microscope with white light. Zeiss Stereoscope images were analyzed with Zeiss AxioVision 4.8 software for embryo lateral somite angle measurements.

3.4.4 Whole embryo in situ hybridization & Alcian Blue cartilage staining

Beginning at 24 hpf AB embryos were treated with 0.003% PTU to reduce pigmentation. Embryos were fixed in 4% paraformaldehyde in PBS overnight at 4°C. Antisense RNA *in situ* hybridization was performed on bud, 8 somite, 13 somite, 24 hpf, 48 hpf and 72 hpf zebrafish embryos with methods previously reported (Maragh et al., 2011). Alcian blue cartilage staining was performed on 96 hpf embryos using published methodology (Walker and Kimmel, 2007).

3.5 Figures: Chapter 3

Figure 3-1. *rbm24a* and *rbm24b* are expressed throughout somitogenesis.

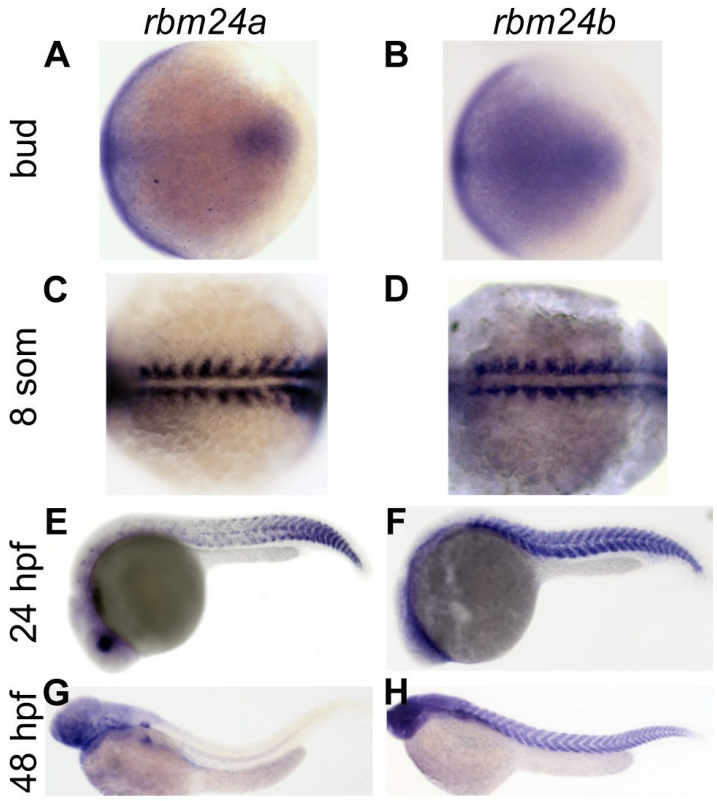

ISH images of uninjected AB embryos using *rbm24a* or *rbm24b* riboprobes individually marking spatial and temporal RNA expression. Tailbud expression of bud stage embryos (Raya et al.). 8 somite embryos in dorsal facing orientations show all patterned somites marked by *rbm24a* and *rbm24b* riboprobes (C-D). Trunk images of embryos at 24 hpf show spatial expression of *rbm24a* in the somites concentrated at the posterior, while *rbm24b* is uniformly expressed in somites along the A-P axis (E-F). Embryos at 48 hpf show no somite *rbm24a* expression, while somite expression of *rbm24b* remains uniform thought the somites (G-H). som, somites; hpf, hours post fertilization.

Figure 3-2. Rbm24a and Rbm24b are required for craniofacial development.

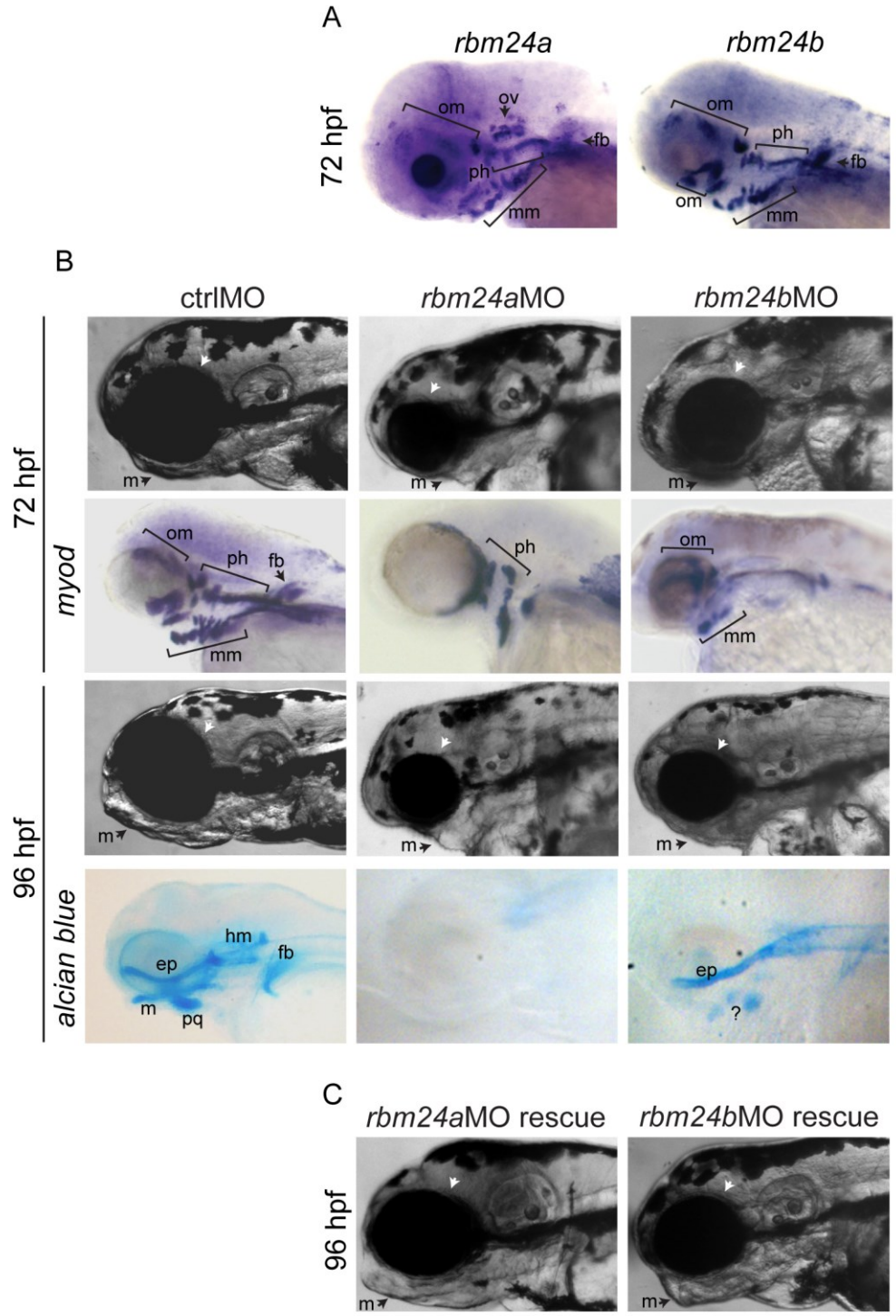

Brightfield, *ISH*, and alcian blue images of ctrlMO, *rbm24a*MO and *rbm24b*MO embryos. 72 hpf lateral oriented embryos show expression of *rbm24a* and *rbm24b* in

presumptive optic muscles, pharyngeal arch muscles, mandibular muscles, and fin bud. *rbm24a* shows additional expression in the otic vesicle (A). The anterior region of 72 hpf and 96 hpf embryos are shown oriented laterally for visualization of eye and mandible phenotypes (B). Brightfield and *ISH* images of *myod* expression in the anterior region of dorsally oriented 72 hpf ctrlMO, *rbm24a*MO and *rbm24b*MO embryos (B rows 1 and 2). *myod* expression is detected in the find bud, optic muscles, pharyngeal arch muscles and mandibular muscles of uninjected embryos. Normal *myod* expression is diminished in *rbm24a*MO and *rbm24b*MO embryos. Brightfield and alcian blue cartilage staining of ctrlMO, *rbm24a*MO and *rbm24b*MO embryos in lateral orientation at 96 hpf (B rows 2 and 3). Normal cartilage staining is observed in the fin buds, ethmoid plate, palatoquadrate, hyomandibularand Meckel's cartilage of uninjected embryos. Cartilage formation of these structures is ablated in *rbm24a*MO embryos and severely reduced in *rbm24b*MO embryos. Brightfield craniofacial images of RNA rescue *rbm24a*MO and *rbm24b*MO phenotypes at 96 hpf (C). *rbm24a*MO rescue, by co-injection of 5 ng*rbm24a*MO with 800 pg of capped poly-A *rbm24a* mRNA and *rbm24b*MO rescue, by co-injection of 8 ng*rbm24b*MO with 200 pg of capped poly-A *rbm24b* mRNA, show rescue of somite and craniofacial *rbm24a*MO and *rbm24b*MO phenotypes. fb, fin bud; om, optic muscles; ov, otic vesicle; ph, pharyngeal muscles; mm, mandibular muscles. white arrow, eye; black arrow, mandible; m, Meckel's cartilage; ep, ethmoid plate; pq, palatoquadrate; hm, hyomandibularcartilage.

Figure 3-3. Rbm24a and Rbm24b are required for normal somitogenesis.

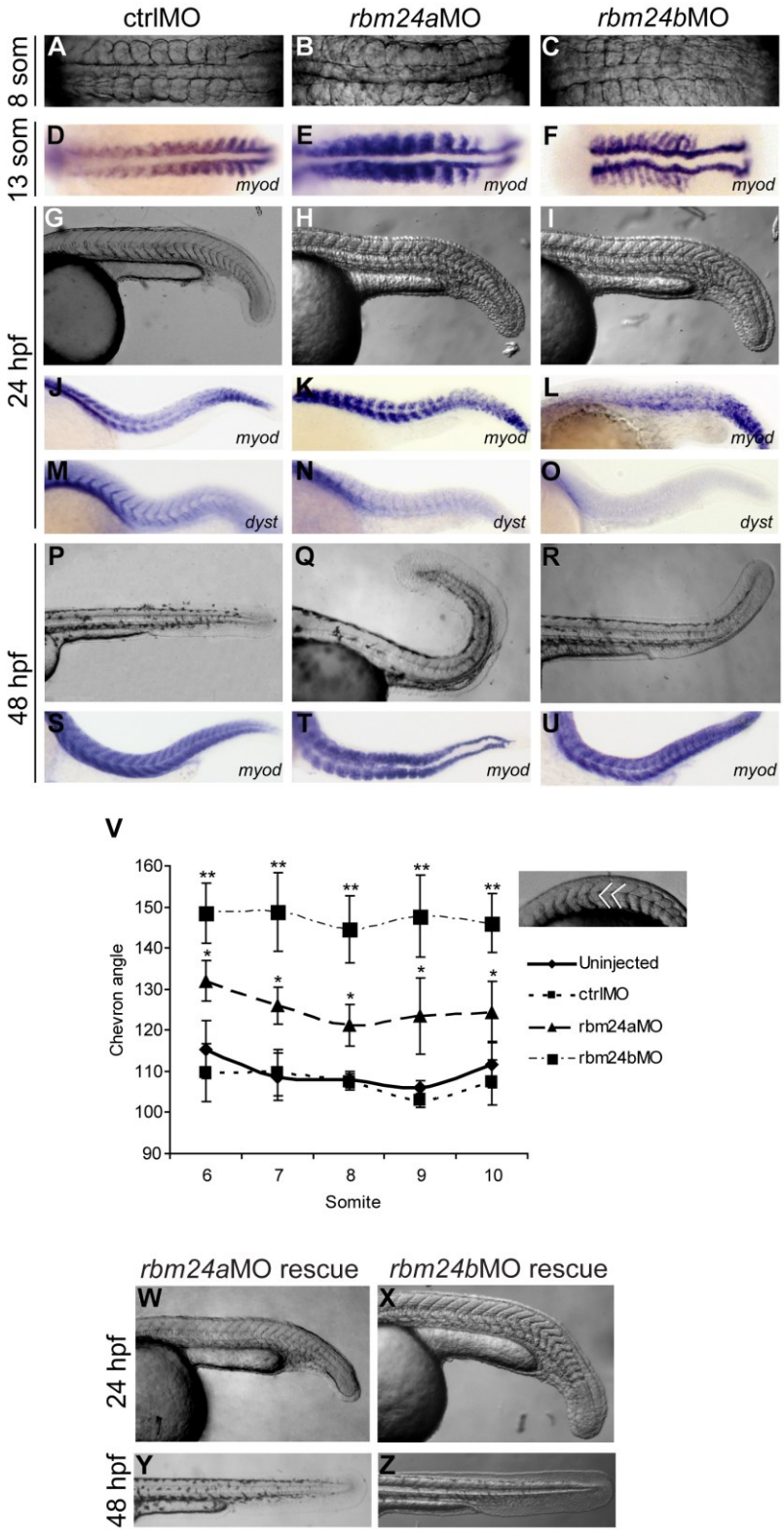

Brightfield and *ISH* images of ctrlMO, *rbm24a*MO and *rbm24b*MO embryos. Brightfield 8 somite embryos are shown in dorsal orientation (A-D). Spatial expression of *myod* in somites of 13 somite embryos was detected using antisense DIG labeled riboprobes (D-F). The trunks of 24 hpf embryos are shown in the lateral orientation via live imaging (G-I), *myod ISH* (J-L), and *dyst ISH* (M-O). 48 hpf embryos are shown in the lateral orientation via live imaging (P-R) and *myod ISH* (S-U). Measurements of individual chevron angle measurements of somites 6-10 of 13 somite embryos for uninjected, ctrlMO injected *rbm24a*MO and *rbm24b*MO embryos, n = 3-5 embryos each (V). Statistically significant differences in lateral length and somite angle as compared to ctrlMO is shown using an asterisk. mRNA phenotype rescue of *rbm24a*MO embryos with *rbm24a* mRNA and *rbm24b*MO embryos with *rbm24b* mRNA imaged at 24 hpf (W-X) and 48 hpf (Y-Z). *= $p<0.05$; **= $p<0.01$; hpf, hours post fertilization.

Figure 3-4. doubleMO embryos show a more severe somite phenotype than individual *rbm24a*MO and *rbm24b*MO embryos

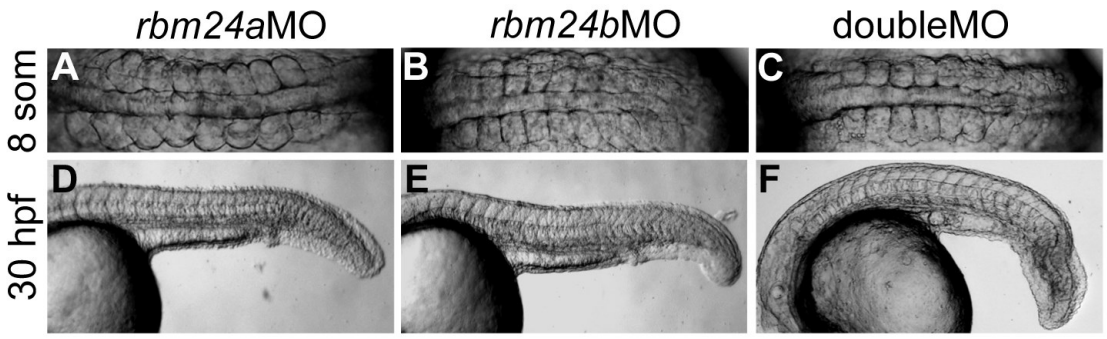

Brightfield imaging of 8 somite and 24 hpf embryos injected with *rbm24a*MO (5 ng) (A, D), *rbm24b*MO (8 ng) (B, E) or half doses of both *rbm24a* (2.5 ng) and *rbm24b* (4 ng) MOs (C, F).

Figure 3-5. MRF expression is not repressed in *rbm24a*MO and *rbm24b*MO embryos.

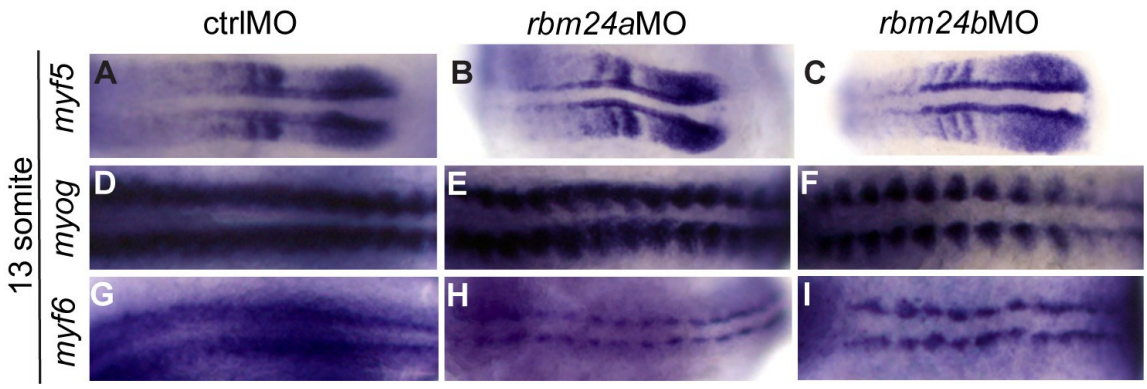

ISH images of 13 somite ctrlMO, *rbm24a*MO and *rbm24b*MO embryos. Spatial expression of *myf5* in somite precursors and PSM (A-C), *myog* (D-F) and *myf6* (G-I) in somites was detected using respective antisense DIG labeled riboprobes.

CHAPTER 4

COMPONENTS OF THE NOTCH-SIGNALING PATHWAY ARE DYSREGULATED UPON Rbm24a & Rbm24b KNOCKDOWN

4.1 Preface

We focus in this chapter on understanding the requirement of both Rbm24a and Rbm24b in somite development because it is the earliest developing muscle population in which we observed both expression and developmental malformation. Somite patterning originates within a niche of undetermined MPCs in the tailbud shortly after the conclusion of gastrulation. Multiple pathways contribute to the maintenance of MPCs and subsequent somite segmentation, patterning and specification (Kimelman, 2006; Niwa et al., 2011; Szeto and Kimelman, 2006; Tiedemann et al., 2012). Notch-mediated signaling is among several pathways that play key roles in segmentation and somite patterning (Bray, 2006; High and Epstein, 2008; Oates and Ho, 2002). Specifically, ligands genes *dlc* and *dld* and downstream target genes *her1* and *her7* are critical components of somitogenesis and the segmentation clock. The protein products of these genes act via cyclical cell-cell signaling within MPCs and somite progenitors (Giudicelli et al., 2007; Julich et al., 2005; Oates et al., 2005; Schroter et al., 2012; Trofka et al., 2012). The cycling expression of these ligands and target genes persists through to the completion of somitogenesis and is partially maintained by negative feedback of target gene proteins on transcription of *dlc* and *dld* (Giudicelli et al., 2007; Holley et al., 2000).

Our data reveal perturbations in Notch pathway components as one possible contributor to abnormal somite phenotypes resulting from Rbm24a or Rbm24b titration *in vivo*. We provide evidence that zebrafish RBM24 homologs may normally act to ensure appropriate pre-mRNA processing of the *dlc* and *dld* transcripts that encode Notch ligands in PSM cell populations. We propose that perturbation of Notch-mediated signaling may, in part, explain the somitic deficits observed upon disruption of Rbm24 levels.

4.2 Results

4.2.1 Notch-pathway genes are reduced in rbm24aMO and rbm24bMO embryos

Given the demonstrable somite deficits upon Rbm24 knockdown, we investigated whether the Notch clock genes (Figure 4-1) were perturbed in *rbm24* morphant embryos. At the 13 somite stage *dlc* expression was almost ablated in the PSM in both *rbm24a*MO and *rbm24b*MO embryos (Figure 4-1 A-C). Further, *dld* expression was diminished in *rbm24b*MO embryos (Figure 4-1 D -F). Expression of the target genes *her1* and *her7* in the PSM was also diminished in both *rbm24a*MO and *rbm24b*MO embryos (Figure 4-1 G-L).Notwithstanding the observed reduction in *dlc*, *dld*, *her1* and *her7* expression, *tbx16* expression marking MPCs was unchanged in *rbm24*MO embryos, indicating the reduced expression of Notch components does not a result from an absence of MPCs within the PSM (Figure 4-1 M-O). By 24 hpf, expression of *dlc*, *dld*, *her1* or *her7* failed to recover in either *rbm24a*MO or *rbm24b*MO embryos. In fact, their expression appeared to be further diminished compared with earlier time points, without the loss of *tbx16* expression (Figure 4-1 P-DD). The observed reduction of *her1* and *her7* expression suggests it is unlikely that the observed reduced *dlc* and *dld* levels results from negative feedback on ligand transcription levels caused by increased *her1* or *her7* transcripts. In the PSM and somite precursors, cell-cell signal transduction of Dlc and Dld ligands is mediated through cell surface receptors on neighboring cells (Bray, 2006; Cinquin, 2007), and receptors Notch1a and Notch3 are known components of the somite clock (Beres et al., 2011; Sieger et al., 2003). While we observed expression reduction of assayed ligands

and target genes, we did not observe altered expression of *notch1a* or *notch3* transcripts (Figure 4-2).

To determine whether the effects on Notch signaling were restricted to evaluated tissues, we then assayed in the impact of *rbm24a* and *rbm24b* depletion on *dla*, *dlb* and *dll4* transcripts. Dla, Dlb and Dll4 are Notch ligands that are not involved in somite patterning. Expression levels of *dla* or *dlb* (expressed neural cells), were not perturbed in *rbm24a*MO and *rbm24b*MO embryos at 24 hpf (Figure 4-3). Transcript corresponding to *dll4* and its cognate target gene *hey2*, however were disrupted in both *rbm24a*MO and *rbm24b*MO embryos (Figure 4-3). Spatial expression of *dll4* and *hey2* is largely depleted in *rbm24a*MO embryos and diminished *rbm24b*MO embryos compared with uninjected controls. *dll4* and *hey2* are known to be required for arterial vasculature formation (Scehnet et al., 2007), and this observation is consistent with our previously published finding that *rbm24a*MO embryos are unable to form the dorsal aorta (Maragh et al., 2011).

These studies indicate the transcripts for Notch ligands and their target genes, which are requisite for normal somitogenesis, are depleted as a consequence of knockdown of either *rbm24* homolog. Additionally the same may be postulated for Notch ligands in vascular development. These data implicate dysregulation of Notch signaling as a potential contributor to *rbm24a*MO and *rbm24b*MO phenotypes. Taking these findings together we further postulate disruption of Notch somite clock components is likely occurring at the level of ligand regulation.

4.2.2 The Notch-Signaling Pathway is dysregulated in the hearts of rbm24aMO and rbm24bMO embryos

Cardiac muscle is among the many embryonic tissues whose development is influenced by the Notch-signaling pathway. Defects in human NOTCH1 and associated proteins underlie malformations including cardiac septa and valve defects (Garg et al., 2005; McBride et al., 2008). We previously reported *rbm24a*MO or *rbm24b*MO embryos present with heart tube distention, cadiac looping and atrioventricular septation defects. To test the hypothesis that reduced Notch signaling, may also contribute to cardiac defects, we directly assayed Notch signaling in *rbm24a*MO and *rbm24b*MO embryos, using the zebrafish *Tg(Tp1bglob:hmgb1-mCherry)*^{jh11}, Notch-reporter line (Parsons et al., 2009). This transgenic line expresses a nuclear-localized mCherry fluorophore in cells undergoing Notch signaling. At 48 hpf Notch signaling was reduced around the atrioventricular septum in *rbm24a*MO or *rbm24b*MO embryos compared to uninjected controls (Figure 4-4).

We also wanted to determine whether reduction of *rbm24a* or *rbm24b* might also reduce signaling through another developmentally critical pathway. Thus we extended these analyses to include a zebrafish reporter lines for BMP *Tg(BRE:eGFP)* (Laux et al., 2011) signaling pathway, whose dysregulation might also contribute to the genesis of the observed cardiac or craniofacial phenotypes. While *rbm24a*MO and *rbm24b*MO embryos displayed the cardiac phenotypes associated with knockdown, BMP reporter activity was not reduced in cardiac or craniofacial structures as compared to uninjected controls at 48 hpf (Figure 4-4). Taken collectively these data support the hypothesis that Notch-signaling activity is reduced/altered in cardiac tissue of

*rbm24a*MO and *rbm24b*MO embryos. While this effect is stronger than any observed for other assayed pathways, we cannot exclude possible contributions from other developmental pathways to the resulting *rbm24a*MO or *rbm24b*MO phenotypes at this time.

4.2.3 **Rbm24a & Rbm24b** ***knockdown phenotypes do not appear to be due to gastrulation defects***

We evaluated whether observed *rbm24a*MOand *rbm24b*MO phenotypes were a consequence of gastrulation defects whose effects we were simply observing later in development. These phenotypes would include incomplete migration of cells during gastrulation, disorganized cellular organization at the tailbud, notochord distention or notochord kinking. (Yin and Solnica-Krezel, 2007). We performed live imaging and *ISH* for embryos evaluated at 75% epiboly and bud stages and found no observable deleterious phenotypes (Figure 4-5). These data suggest gastrulation occurs comparatively normally in *rbm24* morphants. Later in development one consequence of gastrulation defects can be observed as an increase in notochord width (Glickman et al., 2003). We observed no difference in notochord width between uninjected (38.37μm +/- 1.40), ctrlMO (37.72 μm +/- 2.48), *rbm24a*MO (38.73μm +/- 1.12), and *rbm24b*MO (38.83 μm +/- 1.23) embryos ($p > 0.3$) at the 13 somite stage. The findings from our gastrulation studies are consistent with the observed MO phenotypes arising post-gastrulation.

4.2.3 Aberrant dlc and dld transcripts are present in rbm24aMO and rbm24bMO embryos

Our findings thus far investigating somite development support a model in which reduction of either Rbm24a or Rbm24b results in both aberrant somitogenesis and reduced expression of the transcripts encoding Notch ligands, Dlc and Dld, along with those of their subsequent target genes, Her1 and Her7. We hypothesized that the reduction in Notch signaling is occurring at the ligand level. Recent reports suggest that the homolog for RBM24 in *C. elegans* (SUP-12) is a splicing factor active in muscle (Hamlett et al., 1992; Kuroyanagi et al., 2007; Ohno et al., 2012). Additionally several other RBM proteins are known to function as post transcriptional regulators and splicing factors (Gao et al., 2011; Guo et al., 2012; Jin et al., 2012; Kar et al., 2006; Li et al., 2013; Pedrotti et al., 2012; Suvorova et al., 2013; Yeo et al., 2009; Zhang et al., 2008; Zhou et al., 2008). While there have been no reports of RBM24 or other RBMs impacting the Notch pathway, based on the known role of RBMs in splicing we posited that a reduction of Rbm24a or Rbm24b would result in incorrect processing of pre-mRNA *dlc* and *dld* transcripts.

To test this hypothesis we designed primers within the 5' and 3' UTRs of *dlc*, *dld, her1* and *her7* to amplify across the coding region of each transcript. Using random hexamer-generated cDNA from 13 somite and 24 hpf uninjected, ctrlMO, *rbm24a*MO and *rbm24b*MO embryos, we performed RT-PCR and detected fragments of the expected size for full length *dlc*, *dld, her1* and *her7* mRNA from all cDNA samples. However, in cDNA generated from *rbm24a*MO and *rbm24b*MO embryos we also detected additional fragments shorter than the predicted sizes for *dlc* (*dlc* short_1) and

dld (*dld* short_1 & *dld* short 2) transcripts (Figure 4-6). All *dlc* and *dld* short fragments were detected solely in cDNA from both *rbm24a*MO and *rbm24b*MO embryos. No fragments in addition to wildtype were detected for *her1* or *her7* (data not shown). We then subcloned and sequenced the short *dlc* and *dld* amplicons, verifying them to be aberrant transcript variants of each respective pre-mRNA transcript. Sequence alignment of these fragments with the corresponding wildtype mRNA showed aberrant processing occurred in 3/3 instances such that between 5-7 exons were skipped and a unique junction formed by the joining of two truncated exons (Table 4-1). Wildtype *dlc* mRNA consists of exons 1-9 yielding 1,995 coding nucleotides (nt), while *dlc* short_1 consist of a truncated exon 1 (missing the last 11 nt) joined directly to a truncated exon 7 (missing the first 483 nt) with subsequent normal splicing to the inclusion of exons 8 and 9 for a coding length of 372 nt (Figure 4-6 A). Wildtype *dld* mRNA consists of exons 1-11 yielding 2,154 coding nt, while *dld* short_1 consist exons 1-4 where exon 4 is truncated (missing the last 4 nt) joined directly to the 3' UTR region of exon 11 such that the reading frame would include an additional 9 nt then a stop codon for a coding length of 612 nt; *dld* short 2 consists of a truncated exon 1 (missing last 8 nt) joined to a truncated exon 9 (missing the beginning 771 nt) followed by the retention of intron 9 (80 nt) and exon 10 with normal splicing and inclusion of exon 11 for a coding length of 256 nt (Figure 4-6 A). Mapping of all potential splice donor and acceptor sequences that could yield the identified short fragments revealed no cryptic splice sites around the break points of the truncated exons (Mount, 1982; Shapiro and Senapathy, 1987). These aberrant fragments therefore appear to have been generated via an alternate mechanism as oppose to canonical splice site recognition. Further sequence analysis

indicated none of the short fragments detected would be predicted to be functional. All short fragments lack motifs (delta-serrate domain or EGF-like domain repeats) required for the extracellular binding of Delta ligands to Notch receptors, and *dld* short 2 is also predicted to undergo nonsense-mediated decay. Using quantitative RT-PCR (qRT-PCR) on cDNA samples generated from 13 somite stage and 24 hpf embryos, wildtype *dlc* and *dld* mRNA levels were significantly decreased in cDNA generated from *rbm24a*MO and *rbm24b*MO embryos but not ctrlMO embryos, compared to uninjected controls (Figure 4-6). We then assayed the relative abundance of the two aberrant *dld* mRNA splice forms, and found these fragments detectable by qRT-PCR in cDNA from *rbm24a*MO and *rbm24b*MO embryos. However, neither short variant RNA fragment was detectable in cDNA from uninjected or ctrlMO embryos (data not shown).

These data support a model in which a reduction of either *rbm24a* or *rbm24b* results not only in a significant reduction of wildtype *dlc* and *dld* mRNA levels but also a molecular perturbation of the pre-mRNA transcripts of these genes by which there is production of aberrantly mRNA transcripts that are not readily detectable in uninjected or ctrlMO embryos. Our data suggest both *rbm24a* and*rbm24b* participate in post-transcriptional processing of *dlc* and *dld*.

4.3 Conclusions

In this section we uncover a link between the depletion of Rbm24a or Rbm24b and the Notch signaling pathway. We demonstrate here that transcript levels of *dlc*, *dld*, *her1* and *her7* encoding Notch-signaling pathway proteins critical for normal somitogenesis are depleted upon Rbm24a or Rbm24b knockdown. Further we demonstrate that this perturbation to Notch-signaling pathway transcripts is not largely general and does not impact transcripts encoding the neuronally expressed Notch ligands Dla and Dlb. However, investigations into Notch-signaling pathway components involved in cardiovascular development revealed a reduction of Notch signaling in the heart in a reporter assay and reduction of vascular ligand *dll4* and target gene *hey2* transcripts via *ISH*.

Our data reveal perturbations in Notch pathway components as one possible contributor to abnormal cardiovascular and somite phenotypes resulting from Rbm24a or Rbm24b titration *in vivo*. We provide evidence that zebrafish RBM24 homologs may normally act to ensure appropriate pre-mRNA processing of the *dlc* and *dld* transcripts that encode Notch ligands in PSM cell populations. We propose that perturbation of Notch-mediated signaling may, in part, explain the somitic deficits observed upon disruption of Rbm24 levels.

4.4 Methods

4.4.1 Zebrafish Maintenance

Adult AB, zebrafish lines were maintained in system water according to standard methods (Westerfield, 1995). Embryos were obtained from natural mating of adult fish.

4.4.2 Microscopy

Brightfield and images were acquired on a Zeiss Luminar.V12 Stereoscope and a Nikon AZ100 dissecting microscope with white light. Zeiss Stereoscope images were analyzed with Zeiss AxioVision 4.8 software for embryo lateral length and somite angle measurements.

4.4.3 Whole embryo in situ hybridization

Beginning at 24 hpf AB embryos were treated with 0.003% 1-phenyl-2-thiourea (PTU) to reduce pigmentation. Embryos were fixed in 4% paraformaldehyde in PBS overnight at 4°C. Antisense RNA *in situ* hybridization was performed on 75% epiboly, bud, 13 somite and 24 hpf zebrafish embryos with methods previously reported (Maragh et al., 2011). Riboprobe primer sequences are listed in Table 4-2.

4.4.4 Splice variant RT-PCR and qRT-PCR

Total RNA was isolated from AB uninjected, ctrlMO, *rbm24a*MO and *rbm24b*MO whole zebrafish embryos at 13 somite and 24 hpf stages (n = 50 embryos per stage) using TRIzol Reagent. cDNA was generated from 2 µg RNA with random hexamers

using the SuperScriptIII First-Strand Synthesis Kit (Invitrogen). RT-PCR was performed on embryo cDNA with primers designed to the 5' and 3' UTRs of *dlc*, *dld*, *her1* and *her7*. RT-PCR fragments were analyzed for size and Sanger sequencing was performed. qRT-PCR primers were designed to detect *elfalpha*, *dlc*, and *dld* wild-type transcripts as well as *dld* short_1 and *dld* short 2 transcripts. Primers for *dlc* and *dld* wild-type transcripts were designed in exons not present short *dlc* and *dld* transcripts. Primers to detect short *dld* fragments were designed across the unique splice junction present in these transcripts. qRT-PCR was performed in triplicate using Power SYBR Green (Applied Biosystems) on the Viia 7 Real-Time PCR System (Applied Biosystems). Fold amplification was determined via the delta-delta Ct method normalizing to endogenous control *elfalpha* and AB uninjected embryos. A students t-test was used to determine significance at $p < 0.05$ *, $p < 0.01$** and $p < 0.001$***. RT-PCR and qRT-PCR primers are listed in Table 4-2.

4.5 Tables: Chapter 4

Table 4-1. Splice junctions of detected *dlc* and *dld* fragments.

Exon	*dlc* wt mRNA coding nucleotides	*dlc* short 1 mRNA coding nucleotides
1	254 - 304	254 - 293 (-11 nt)
2	305 - 528	-
3	539 - 596	-
4	597 - 864	-
5	865 - 1216	-
6	1217 - 1433	-
7	1434 - 2127	(-438 nt) 1917 - 2127
8	2128 - 2242	2128 - 2242
9	2243 - 2248	2243 - 2248
Length	1,995 nt	372 nt

Exon	*dld* wt mRNA coding nucleotides	*dlc* short 1 mRNA coding nucleotides	*dlc* short 2 mRNA coding nucleotides
1	461 - 508	461 - 508	461 - 498 (-10 nt)
2	509 - 805	509 - 805	-
3	806 - 866	806 - 866	-
4	867 - 1124	867 - 1120 (-4 nt)	-
5	1125 - 1185	-	-
6	1186 - 1317	-	-
7	1318 - 1486	-	-
8	1487 - 1703	-	-
9	1704 - 2502	-	(-773 nt) 2477 - 2502 (+80 nt intron 9 whole)
10	2503 - 2608	-	2503 - 2608
11	2609 - 2614	-	2609 - 2614
		(+12 nt 3' UTR)	
Length	2154 nt	572 nt	253 nt

Exon boundaries are listed for each fragment detected and in Figure 4-6. Truncated exons are noted by numbers in parenthesis. Truncations on the 3' end are listed to the right of exon lengths and truncations on the 5' end are listed on the left of exon lengths.

Table 4-2. Primer sequences.

Riboprobe	Forward 5' - 3'	Reverse 5' - 3'
rbm24a	CCAGGGGTTATGGATTTGTG	TGCAGTTGTTGGGGTTGATA
rbm24b	CGGAGGTCTTCCCTATCACA	CCAAACGCACACAAGAGCTA
myod	ACCCTTGCTTCAACACCAAC	GCCCATAAAATCCATCATGC
tbx16	TCACCAAACCTGGCAGAAGG	AGAGCTTCACACGATGACGG
ntla	AGACGAATGTTTCCCGTGCT	GGTCTGGGACTTCCTTGTGG
dlc	GTGCACCTACGGCACCGGAA	CACTTGCACTCACCGGGGGC
dld	ATTCCTTTCGCGTTTGGGTTCACATGGCCA	TCCGTCTTGGCAAGTGCCGCC
notch1a	ACCCGTGTCTGAACCAGGGCT	TCCCGGCAAACACACGCAGG
notch3	AGCACCAAGGTATTCAGCAGC	TGGCGGCTCTTCAATAACAGC
her7	CATATCCTCATTGATATCAAC	AGAGATTACACAAGGCCCATCA
her1	TGATCCAAAACCTCCGCCTC	CACCAGGGTCTCCACAAAGG

Splice PCR	Forward 5' - 3'	Reverse 5' - 3'
dlc	TCGGACTACTCTCACAGTCTGCT	TGTGGTCAGGCCCACTGGTGT
dld	TGCCTGGCCCGTGGAAGTTT	CCGAGCCAGTATGGCCCAACG
her1	TCGTCTTCTTCCGATTTTCAGCC	ACAACGCTGGTTATTCTCATGCT
her7	CGATGAAAGACCTCCACCTGC	GGGGGAGAAGAAATCTGCGT

RT-PCR	Forward 5' - 3'	Reverse 5' - 3'
elfalpha	TCTGTTACCTGGCAAAGGGG	GGAGTCGACGTGGCCAATAA
dlc wt	TCGTGTCGTGTGCGATGAAT	ACAGCCAGACAAGCAGATGG
dld wt	GTCTTCCGGGGTGTGATGAA	GGCACGGTTTGTGATGTGTG
dld short 1	GAGCATTACTACGGCGAGGG	AGCTACAGCTCTGTTGTGCAG
dld short 2	TGGCTAGCGCAGATCCATTT	TGGCGTTACACCTCGGTTG

Primers used to generate antisense DIG labled riboprobes, conduct splice variant RT-PCR and conduct qRT-PCR are listed.

4.6 Figures: Chapter 4

Figure 4-1. Notch-signaling pathway transcripts are depleted in somites of *rbm24a*MO and *rbm24b*MO embryos

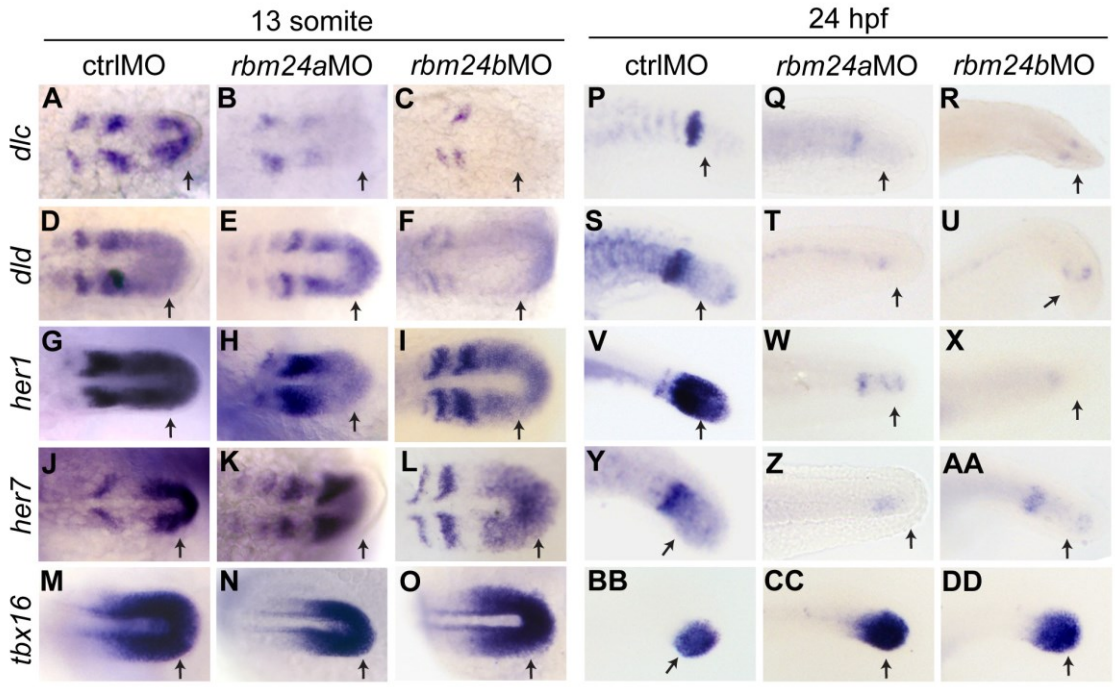

ISH images of the tailbud region of dorsally oriented 13 somite and laterally oriented 24 hpf ctrlMO, *rbm24a*MO and *rbm24b*MO embryos. 13 somite tailbud spatial expression of *dlc* (A-C), *dld* (D-F), *her1* (G-I) and *her7* (J-L) and *tbx16* (M-O) in the PSM and somite precursors using respective antisense DIG labeled riboprobes. 24 hpf tailbud spatial expression of *dlc* (P-R), *dld* (S-U), *her1* (V-X) and *her7* (Y-AA) and *tbx16* (BB-DD). black arrows, regions of interest for tailbud expression.

Figure 4-2. *notch1a* and *notch3* transcripts do not shown reduced tailbud expression in *rbm24a*MO and *rbm24b*MO embryos.

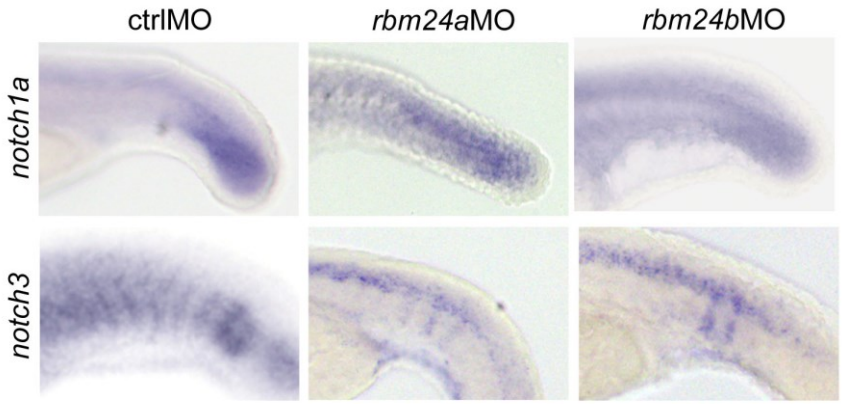

ISH of Notch pathway receptors transcripts *notch1a* (A-C) and *notch3* (D-F) in the somites of 24 hpfctrlMO, *rbm24a*MO and *rbm24b*MO embryos.

Figure 4-3. *ISH* of neutrally and vascularly expressed Notch-pathway transcripts in *rbm24a*MO and *rbm24b*MO embryos.

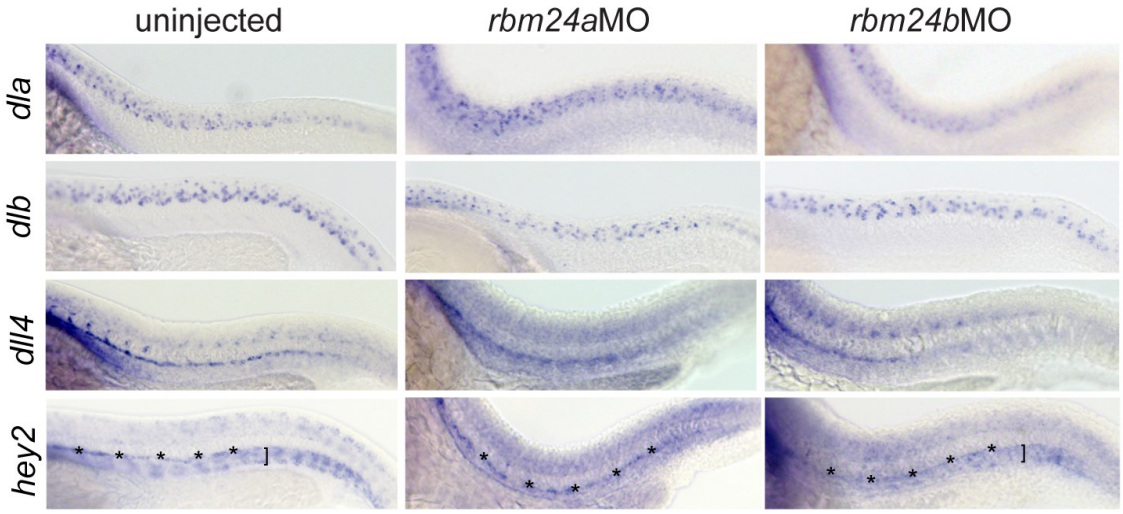

ISH images of the trunk region of laterally oriented 24 hpf uninjected, *rbm24a*MO and *rbm24b*MO embryos. Spatial expression of *dla* & *dlb* in cells of the central nervous system is not depleted; while *dll4* & *hey2* spatial expression in the vasculature is depleted. asterisk, dorsal aorta expression, black brackets, posterior cardinal vein expression.

Figure 4-4. Notch and BMP reporter activity in *rbm24a*MO and *rbm24b*MO embryos.

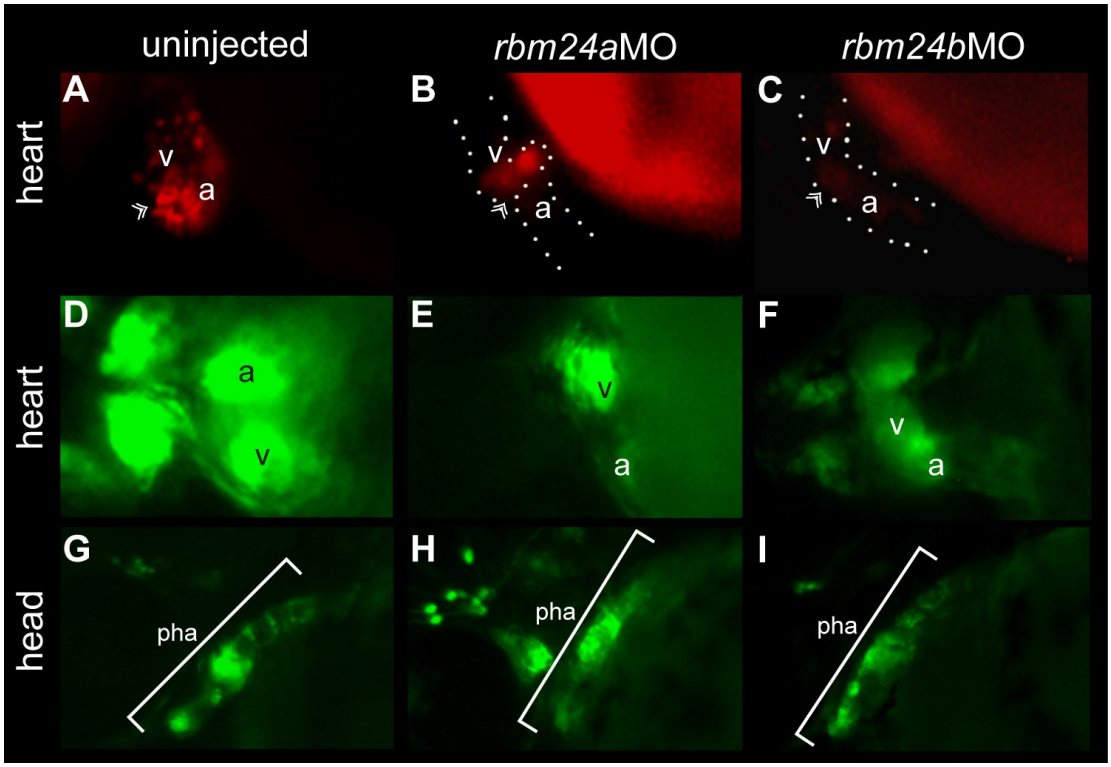

Fluorescent images of Notch-reporter activity using the*Tg(Tp1bglob:hmgb1-mCherry)*^{jh11}, reporter line and BMP reporter activity using the *Tg(BRE:eGFP)* reporter line at 48 hpf. Hearts of uninjected, *rbm24a*MO and *rbm24b*MO *Tg(Tp1bglob:hmgb1-mCherry)*^{jh11} embryos were imaged in the lateral orientation. Notch-reporter activity was recorded in the heart concentrated at the A-V boundary for all conditions at 48 hpf, however with limited detection in *rbm24a*MO and *rbm24b*MO embryos (A-C). Hearts of uninjected, *rbm24a*MO and *rbm24b*MO *Tg(BRE:eGFP)* embryos in the ventral orientation show strong detection of BMP activity in all conditions (D-F). Strong BMP expression is detected in the pharengeal arches of laterally oriented embryos for all

conditions. dotted outline, heart chamber boundaries; v, ventricle; a, atrium; double arrow, A-V boundary; white bracket, pharyngeal arches; pha, pharyngeal arches.

Figure 4-5. *rbm24a*MO and *rbm24b*MO embryos do not display gastrulation defects.

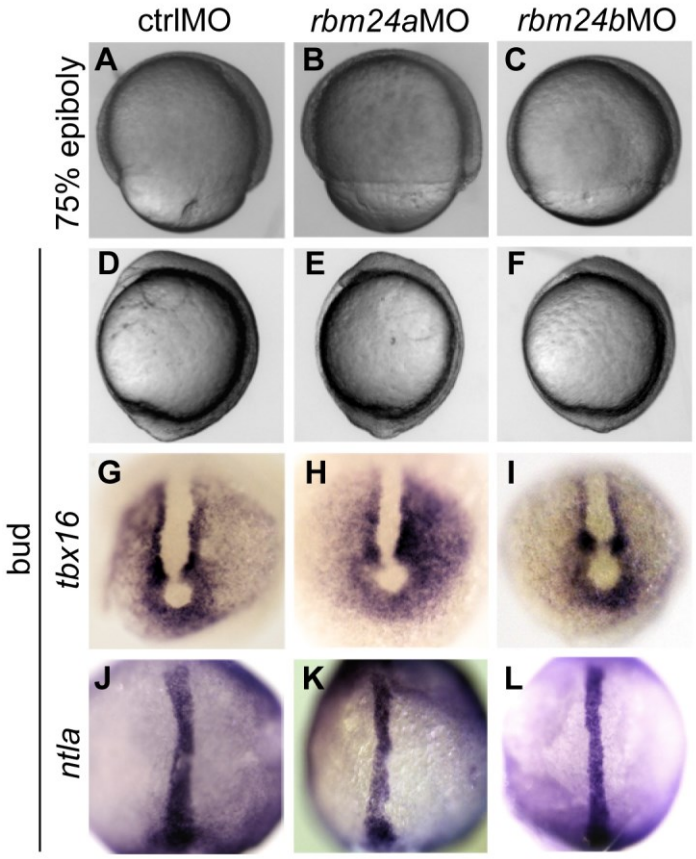

ctrlMO, *rbm24a*MO and *rbm24b*MO embryos during gastrulation. Brightfield imaging of 75% epiboly embryos (A-C). Brightfield imaging of bud stage (D-F). *ISH* of bud stage embryos with *tbx16* (G-I) and *ntla* (J-L) riboprobes.

Figure 4-6. Aberrant *dlc* and *dld* splice forms are detectable in cDNA from *rbm24a*MO and *rbm24b*MO embryos.

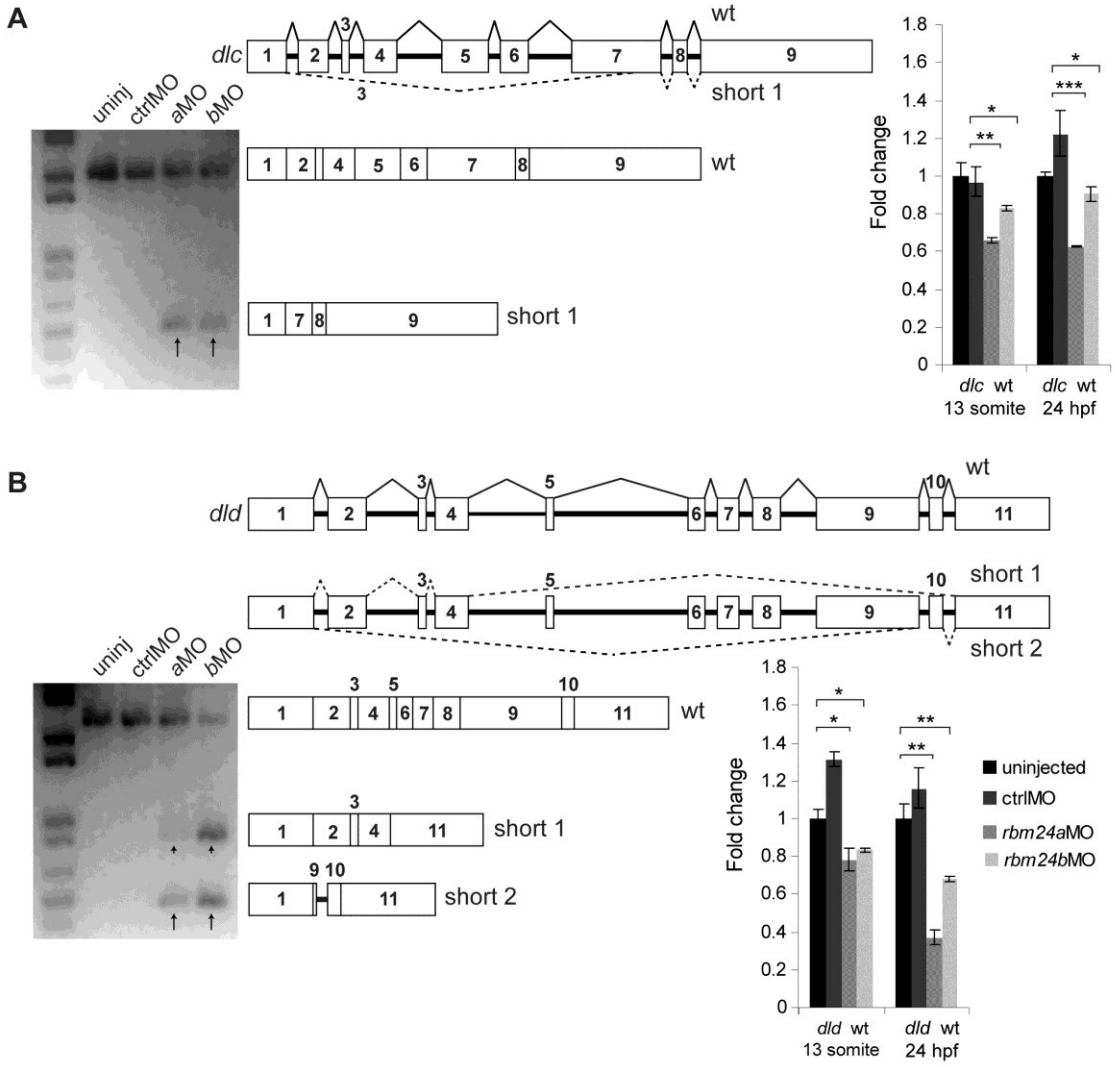

PCR experiments to amplify *dlc* and *dld* mRNA transcripts using total cDNA generated from 13 somite uninjected, ctrlMO, *rbm24a*MO and *rbm24b*MO embryos (n=50 embryos per condition). PCR for *dlc* transcript yielded a fragment of correct length for all conditions and an additional short fragment for *rbm24a*MO and *rbm24b*MO cDNA (A). *dlc* pre-mRNA, *dlc* mRNA and *dlc* short_1 fragment sequences are depicted graphically to scale. PCR for *dld* transcript yielded a fragment of correct length for all

conditions and two additional short fragments for *rbm24a*MO and *rbm24b*MO cDNA (B). *dld* pre-mRNA, *dld* mRNA and *dld* short_1 and *dld* short 2 fragments are depicted graphically to scale. 13 somite and 24 hpfuninjected, ctrlMO, *rbm24a*MO and *rbm24b*MO embryos were used to generate cDNA used for qRT-PCR. All transcripts were assayed in triplicate per cDNA sample. Transcript levels were normalized to *elfalpha* transcript levels and fold change for each transcript is shown as compared to uninjected embryos. Statistically significant fold changes compared to uninjected are denoted by an asterisk. *= $p<0.05$; **= $p<0.01$; ***=$p<0.001$. black arrows, short *dlc* and *dld* fragments; boxes, exons; thick black lines, introns; thin black lines, wildtype splicing, dashed lines, aberrant splicing.

CHAPTER 5

CONCLUSIONS

5.1 Preface

RBMs are a relatively poorly understood family of proteins, defined solely by the presence of RNA binding motifs (Nakano et al., 1992). To date, only a small subset of RBMs have been recognized to be functionally significant in humans and model organisms (Albers et al., 2012; Guo et al., 2012; Jayasena and Bronner, 2012; Johnston et al., 2010; Lin and Tarn, 2012; Lin et al., 2013; Miyamoto et al., 2009; Nousbeck et al., 2008). Recent work in a mouse model suggests that *RBM24*, encoding another family member, may similarly be developmentally critical (Miller et al., 2008).

Rbm24 is a cardiac gene candidate identified through transcript profiling of differentiating mESCs (Miller et al., 2008). It was initially selected for functional analysis due to its early cardiac expression during mouse development, first detected by *in situ* hybridization in the cardiac crescent of mice, and subsequently in the heart tube and looping heart with additional signal observed in the somites. This work set out to functionally investigate a role for RBM24 in cardiac and somite development using a zebrafish model system.

5.2 Rbm24 homologs are essential for normal cardiovascular development

Syntenic and sequence-based comparative genomic analyses were employed to identify two *Rbm24* homologs (*rbm24a* and *rbm24b*) in zebrafish. It was established through *ISH* that in the zebrafish *rbm24a* and *rbm24b* expression was concordant with

earlier observations in mice. In the zebrafish model, *rbm24a* and *rbm24b* expression were also clearly detected in the developing vasculature. Knockdown experiments using splice blocking and translation blocking morpholino technologies revealed in the zebrafish embryo, a reduction of either Rbm24 homolog results in cardiac edema, cardiac looping defects, heart tube distention, and reduced to non existent circulation. General toxicity or off target effects as the cause of the observed morphant phenotype were excluded by confirming they remain without amelioration in the presence of *p53* MO. Additionally RNA-based phenotype rescue successfully confirmed the morphant phenotypes are sequence-specific. It was unclear if the low to no circulation phenotype was a result of reduced cardiac contraction (Mitchell et al., 2010). Heart rate counts of *rbm24a*MO or *rbm24b*MO injected embryos did not support that a low heart rate could explain the reduced to no circulation. Observations of vasculature upon Rbm24a or Rbm24b knockdown in a GFP-endothelial reporter line (Cross et al., 2003) revealed Rbm24a and Rbm24b are required for normal vascular development. Additionally, reduction of either Rbm24a or Rbm24b independently yielded vascular defects of both myocardium and endocardium. It is therefore likely reduced circulation is due to a reduction in critical vasculature and not simply reduced heart rate.

Investigation of molecular markers for myocardial development further illuminated the impact of reducing *rbm24* expression. Both *rbm24* homologs are detected in the developing heart by *in situ* hybridization by 24 hpf and sustain expression at least through 72 hpf. In all cases a reduction of *rbm24a* or *rbm24b* was sufficient to prevent heart looping noted at 48 hpf and beyond, where normal heart looping occurs at approximately 36 hpf. Expression of *rbm24a* is unequal between the

ventricle and atrium with stronger expression in the atrium while *rbm24b* shows equivalent expression in both chambers. This skewed expression of *rbm24a* at higher levels in the atrium is illustrated by truncated and abnormal atrium formation of the developing heart in *rbm24a* MO injected embryos demonstrating its requirement for cardiogenesis, including atrial specification, at this early stage. A reduction in either *rbm24* homolog severely disrupts the expression level and localization of ventricular marker *vmhc* yielding little to no expression visible in either *rbm24* morphant condition. Reduced ventricular myocardial count disproportionate to the atrium has also been reported with deficient *nkx* and hedgehog signaling (Targoff et al., 2008; Thomas et al., 2008). Although reduction of each *rbm24* results in incompletely overlapping atrial and ventricular phenotypes, reduction of either is sufficient to compromise the looping of the heart tube. The looping of the heart tube is a result of both genetic and biophysical mechanisms, and perturbation of the mechanical force generated by the contraction of the heart chambers can affect proper heart formation (Taber, 2006). Zebrafish *wea* mutants (*myh6*), display distortions in cardiac looping, but still maintain a functional circulatory system due to the adaptation of the ventricle (Berdougo et al., 2003). This suggests that reduction in *rbm24a* expression impacts both the ventricle and atrium, likely in the organization or structure of the muscle filaments, in addition to cardiomyocyte count, in turn affecting the ability of the heart to circulate blood.

Although both *rbm24a* MO and *rbm24b* MO injected embryos display an additional phenotype of aberrant vascular morphology, with defects in vasculogenesis and angiogenesis the defect in *rbm24a* morphants appears more severe. The observed phenotypes, however, are also consistent with the exhibited localization of each *rbm24*

homolog, wherein *rbm24a* is expressed in the DA and *rbm24b* is expressed in the PCV by 72 hpf. The expression difference likely reflects the acquisition of independent roles since duplication of the ancestral gene (Ekker et al., 1992; Kleinjan et al., 2008), resulting in incompletely overlapping functions for these homologs in vasculogenesis. Angiogenesis is impaired when expression of either *rbm24* homolog is reduced. The integrity of these first vessesls of angiogenesis (Se and two DLAVs) deteriorates over time. In *rbm24a* morphants Se are more severely affected not reaching the dorsal line to form DLAVs at 48 hpf and continue to deteriorate by 72 hpf. This may result form the lack of any discernable DA. *rbm24b* morphants still possessed a visible DA but no PCV, Se and one DLAV were present and only displayed mild morphology alterations at 48 hpf with subsequent severe deterioration by 72 hpf. In the case of all *rbm24* morphants there is an inability to maintain the new vessels formed during angiogenesis and a wasting of any vessels resulting from vasculogenesis. It is unclear the molecular basis of this blood vessel deterioration. Normal *rbm24* expression may be playing a direct role in the vascular maintenance or the angiogenesis pathway. Also to be considered is that a lack of sufficient concentrations of growth factors and mitogens due to insufficient circulation may be preventing maintenance of initiated vasculature, since it has been shown Se sprouting and extension involves several rounds of cell division (Blum et al., 2008) and *vegfA* is required for vascular maintenance (Bahary et al., 2007).

The incompletely overlapping role of *rbm24a* and *rbm24b* in the developing heart and vasculature is underscored by the extreme phenotype observed in the double morpholino injections. *rbm24a* and *rbm24b* appear to act in parallel in cardiac development, converging on a common phenotype for which they are both overtly

required. By contrast in vasculogenesis, *rbm24a* and *rbm24b* appear to function in parallel but differentially in artery and vein formation, resulting in different vascular phenotypes which are individually sufficient to disrupt formation of the initial embryonic circulation loop. Further analyses will be required to determine the mechanistic role played by *rbm24a/b* and whether their roles involve one or all of the above-discussed mechanisms.

Our data provide significant insight into the role of *rbm24* in formation of cardiac and vascular systems, however much remains to be learned about the exact mechanism by which it functions and the role *RBM24* may play in human disease. Other RRM containing proteins have also been shown to serve important roles in embryonic development (Anyanful et al., 2004; Markus and Morris, 2006) and post-transcriptional regulation is a frequent theme. With this in mind, we hypothesize that the protein plays a role in the post-transcriptional regulation of gene expression important for cardiac and vascular development. In the case of *rbm24a and rbm24b* depletion for instance, we found that expression of the ventricular marker *vmhc* is nearly abolished in the heart at 72 hpf, suggesting they both may contribute to specific regulation of *vmhc* mRNA. This study demonstrates the power of the screen that uncovered *Rbm24* as a candidate cardiac gene, adding significant value to the original data set for which this work represents just the first of many such analyses awaiting completion.

5.3 Rbm24 homologs are essential for normal somitogenesis

Rbm24 has been shown to be expressed in somites early in development (Miller et al., 2008). In this second part of this work we expanded upon our developmental analysis of *rbm24a* and *rbm24b*, focusing on the skeleto-muscular system. We demonstrated that *rbm24a* and *rbm24b* are prominently expressed in the tailbud and forming somites throughout segmentation, consistent with recent reports that RBM24 plays a role in myogenic differentiation (Jin et al., 2010; Li et al., 2010; Miyamoto et al., 2009). Furthermore, we showed both genes to be expressed in developing craniofacial structures. Spatial expression localization of *rbm24a* and *rbm24b* was consistent with that of the skeletal muscle marker *myod,* suggesting *rbm24a* and *rbm24b* may be expressed in developing skeletal muscle tissue throughout the embryo.

Subsequent depletion of either Rbm24a or Rbm24b resulted in somite and craniofacial malformation, while also recapitulating our previous report of cardiovascular defects. Somite dysmorphologies included somite boundary defects, somite compression along the A-P axis and tail curving. Gross craniofacial malformations of a shortened mandible, reduction in the size of the otic vessicle, micropthalmia and microcephaly were detected upon knockdown of either Rbm24 homolog. All observed somitic and craniofacial phenotypes were appropriately ameliorated in RNA-based rescue experiments.

Our findings suggest Rbm24a and Rbm24b are essential for skeletal muscle development in addition to their established roles in cardiac and vascular development. All of these tissues share origins in the mesoderm germ layer. It is, therefore, possible that mesoderm-derived populations are particularly sensitive to depletion of Rbm24a or Rbm24b.

5.4 Depletion of Rbm24 homologs impacts the Notch-signaling pathway

Notch signaling is critical for the patterning of many embryonic tissues including the heart, hematopoeitic system and somites (Bigas et al., 2010; High and Epstein, 2008; McBride et al., 2008; Oates and Ho, 2002; Oates et al., 2005; Scehnet et al., 2007). During somite patterning the Dlc and Dld ligands function to activate Notch via of *her1* and *her7* target genes in neighboring cells in the PSM and somite precursors (Giudicelli et al., 2007; Oates et al., 2005).The normal functions of Her1 and Her7, include negative regulation of *dlc* and *dld* transcription which contributes to both perpetuation of the somite clock and maintenance of unsegmented cells within the PSM (Tiedemann et al., 2012). Mutants for *dlc*, *dld*, *her1* or *her7* exhibit a loss of somite boundaries and de-synchronization of the somite clock (Choorapoikayil et al., 2012; Holley et al., 2000; Tiedemann et al., 2012; van Eeden et al., 1996). The reported somite phenotypes of *dlc*, *dld*, *her1* and *her7* mutants appear more severe than, and incompletely overlap with, those we observed for *rbm24a*MO and *rbm24b*MO embryos. We observed dorsal-ventral somite distortion, most notably in *rbm24b*MO embryos, which is not a documented phenotype of *dlc*, *dld*, *her1* or *her7* mutants. Although we cannot restrict the impact of Rbm24 reduction to only one pathway, we did observe a diminution of *dlc*, *dld*, *her1* and *her7* transcript levels normally localized in MPCs in both *rbm24a*MO and *rbm24b*MO embryos. Taken together these observations indicate dysregulation of these components of the Notch pathway is likely incomplete and may only partially account for *rbm24a*MO and *rbm24b*MO somite phenotypes suggesting additional components critical for normal somitogenesis may also be compromised. In

addition to the Notch pathway, the Wnt, FGF, Shh, and BMP developmental pathways are key participants in MPC regulation and somitogenesis (Niwa et al., 2011; Tiedemann et al., 2012). We postulate that Rbm24a and Rbm24b may similarly act upon targets within these pathways as a normal component of somitogenesis but also recognize that their effects may not be restricted to these pathways.

Of those RBM members for whom functional data exists, several have been shown to be necessary for normal post-transcriptional processing. Indeed depletion of RBM4, RBM5, RBM11, RBM20 and RBM25are known to be involved in aberrant post-transcriptional processing, and have been identified as splicing factors for known targets (Gao et al., 2011; Guo et al., 2012; Jin et al., 2012; Li et al., 2013; Lin and Tarn, 2011; Pedrotti et al., 2012). Functional characterization of RBM9 has lead to the classification of this protein as a FOX family splicing factor and the re-naming of this protein as FOX2 (Yeo et al., 2009; Zhang et al., 2008).

Our focus on somitic expression of Notch-pathway components, lead us to identify aberrant transcripts of the *dlc* and *dld* in *rbm24a*MO and *rbm24b*MO embryos. These aberrant transcripts resulted from the joining of distant truncated exons and skipping of several exons including those encoding domains required for Notch Delta ligand-receptor binding. The sequences flanking all possible break points for truncated exons did not reveal any cryptic splice sites, suggesting an alternate means of splice site recognition in the absence of normal levels of Rbm24a an Rbm24b. Our data suggest Rbm24a and Rbm24b normally act to impact proper processing of *dlc* and *dld* transcripts. This is supported by the reports that the product of SUP-12, the RBM24 homolog in *C. elegans*, acts as a splicing factor in muscle (Anyanful et al., 2004;

Kuroyanagi et al., 2007; Ohno et al., 2012). Our data implicates Rbm24a and Rbm24b in *dlc* and *dld* post-transcriptional processing. It is also likely that other transcripts, not necessarily associated with Notch signaling, are yet to be discovered. While we cannot be sure of a direct interaction relationship, all of our findings implicate both Rbm24a and Rbm24b in the modulation of the Notch-signaling pathway. This, however, does not exclude the possibility that Rbm24a and Rbm24b play additional roles in modulating other signaling pathways that contribute to cardiovascular, skeletal muscle and craniofacial development.

5.5 Final Remarks

Our data add to a growing body of literature highlighting the functional significance of RBM genes and the value of continuing to their continued study. This work provides substantial evidence that Rbm24a and Rbm24b are essential for normal cardiovascular development, somite biogenesis and craniofacial development. We further provide evidence to support a model in which Rbm24a and Rbm24b play roles impacting the Notch-signaling pathway. Specifically in the somites, Rbm24a and Rbm24b may play roles in post-transcriptional processing of Notch-ligand transcripts, *dlc* and *dld,* in turn providing a potential but as yet incomplete mechanistic explanation of the observed somite phenotypes. We acknowledge that although consistent with this model, it remains possible that depletion of Rbm24a and Rbm24b in the embryo causes primary/secondary effects on other developmentally critical pathways that may also contribute to these phenotypes.

The critical role for *rbm24* in cardiogenesis raises the question whether mutations at the homologous human locus may contribute to cardiac disorders. Interestingly, Wessels *et al.* recently identified a novel cardiac syndrome with noncompaction cardiomyopathy, bradycardia, pulmonary stenosis, atrial septal defects, and heterotaxy with genetic linkage to human chromosome 6p (Wessels et al., 2008). Genome-wide linkage analysis localized the implicated interval to chromosome 6p24.3-21.2, a region encompassing the human *RBM24* homolog (6p22.3), making it an ideal candidate for variation underlying this phenotype. However, sequencing of all *RBM24* coding exons, intron/exon boundaries and the upstream promoter region in two affecteds, revealed only known polymorphisms (rs10456798 and rs35860841) that were also observed in a heterozygous state in an unaffected family member. While we can exclude a role for *RBM24* coding mutations, additional sequencing of putative regulatory sequences will be necessary to determine if *RBM24* may play a role in this syndrome.

The studies described in this work have utilized translation blocking MO technology in zebrafish as a powerful tool to begin functional characterization of Rbm24a and Rbm24b. We are cognizant that such MOs provide a surrogate for but not precise equivalent of an *in vivo* genetic model. Translation blocking MOs can inhibit both maternal and zygotic transcripts (Bill et al., 2009). Hence, in future we are interested in characterizing the zygotic phenotype achieved through the generation of targeted mutant models. We will continue elucidate the role and mechanisms of *rbm24* function and that of other RBM proteins in embryonic development.

References

Adam, S. A., Nakagawa, T., Swanson, M. S., Woodruff, T. K., Dreyfuss, G., 1986. mRNA polyadenylate-binding protein: gene isolation and sequencing and identification of a ribonucleoprotein consensus sequence. Mol Cell Biol. 6**,** 2932-43.

Albers, C. A., Paul, D. S., Schulze, H., Freson, K., Stephens, J. C., Smethurst, P. A., Jolley, J. D., Cvejic, A., Kostadima, M., Bertone, P., Breuning, M. H., Debili, N., Deloukas, P., Favier, R., Fiedler, J., Hobbs, C. M., Huang, N., Hurles, M. E., Kiddle, G., Krapels, I., Nurden, P., Ruivenkamp, C. A., Sambrook, J. G., Smith, K., Stemple, D. L., Strauss, G., Thys, C., van Geet, C., Newbury-Ecob, R., Ouwehand, W. H., Ghevaert, C., 2012. Compound inheritance of a low-frequency regulatory SNP and a rare null mutation in exon-junction complex subunit RBM8A causes TAR syndrome. Nat Genet. 44**,** 435-9, S1-2.

Anyanful, A., Ono, K., Johnsen, R. C., Ly, H., Jensen, V., Baillie, D. L., Ono, S., 2004. The RNA-binding protein SUP-12 controls muscle-specific splicing of the ADF/cofilin pre-mRNA in C. elegans. J Cell Biol. 167**,** 639-47.

Auweter, S. D., Oberstrass, F. C., Allain, F. H., 2006. Sequence-specific binding of single-stranded RNA: is there a code for recognition? Nucleic Acids Res. 34**,** 4943-59.

Bahary, N., Goishi, K., Stuckenholz, C., Weber, G., Leblanc, J., Schafer, C. A., Berman, S. S., Klagsbrun, M., Zon, L. I., 2007. Duplicate VegfA genes and orthologues of the KDR receptor tyrosine kinase family mediate vascular development in the zebrafish. Blood. 110**,** 3627-36.

Baker, K., Warren, K. S., Yellen, G., Fishman, M. C., 1997. Defective "pacemaker" current (Ih) in a zebrafish mutant with a slow heart rate. Proc Natl Acad Sci U S A. 94**,** 4554-9.

Bakkers, J., 2011. Zebrafish as a model to study cardiac development and human cardiac disease. Cardiovasc Res. 91**,** 279-88.

Bandziulis, R. J., Swanson, M. S., Dreyfuss, G., 1989. RNA-binding proteins as developmental regulators. Genes Dev. 3**,** 431-7.

Berdougo, E., Coleman, H., Lee, D. H., Stainier, D. Y., Yelon, D., 2003. Mutation of weak atrium/atrial myosin heavy chain disrupts atrial function and influences ventricular morphogenesis in zebrafish. Development. 130**,** 6121-9.

Beres, B. J., George, R., Lougher, E. J., Barton, M., Verrelli, B. C., McGlade, C. J., Rawls, J. A., Wilson-Rawls, J., 2011. Numb regulates Notch1, but not Notch3, during myogenesis. Mech Dev. 128**,** 247-57.

Bigas, A., Robert-Moreno, A., Espinosa, L., 2010. The Notch pathway in the developing hematopoietic system. Int J Dev Biol. 54**,** 1175-88.

Bill, B. R., Petzold, A. M., Clark, K. J., Schimmenti, L. A., Ekker, S. C., 2009. A primer for morpholino use in zebrafish. Zebrafish. 6**,** 69-77.

Birney, E., Kumar, S., Krainer, A. R., 1993. Analysis of the RNA-recognition motif and RS and RGG domains: conservation in metazoan pre-mRNA splicing factors. Nucleic Acids Res. 21**,** 5803-16.

Blum, Y., Belting, H. G., Ellertsdottir, E., Herwig, L., Luders, F., Affolter, M., 2008. Complex cell rearrangements during intersegmental vessel sprouting and vessel fusion in the zebrafish embryo. Dev Biol. 316**,** 312-22.

Bray, S. J., 2006. Notch signalling: a simple pathway becomes complex. Nat Rev Mol Cell Biol. 7**,** 678-89.

Bruneau, B. G., 2008. The developmental genetics of congenital heart disease. Nature. 451**,** 943-8.

Bryson-Richardson, R. J., Currie, P. D., 2008. The genetics of vertebrate myogenesis. Nat Rev Genet. 9**,** 632-46.

Chen, Y., Varani, G., 2005. Protein families and RNA recognition. FEBS J. 272**,** 2088-97.

Chen, Y., Varani, G., 2013. Engineering RNA-binding proteins for biology. FEBS J. 280**,** 3734-54.

Choorapoikayil, S., Willems, B., Strohle, P., Gajewski, M., 2012. Analysis of her1 and her7 mutants reveals a spatio temporal separation of the somite clock module. PLoS One. 7**,** e39073.

Cinquin, O., 2007. Understanding the somitogenesis clock: what's missing? Mech Dev. 124**,** 501-17.

Coutelle, O., Blagden, C. S., Hampson, R., Halai, C., Rigby, P. W., Hughes, S. M., 2001. Hedgehog signalling is required for maintenance of myf5 and myoD expression and timely terminal differentiation in zebrafish adaxial myogenesis. Dev Biol. 236**,** 136-50.

Cross, L. M., Cook, M. A., Lin, S., Chen, J. N., Rubinstein, A. L., 2003. Rapid analysis of angiogenesis drugs in a live fluorescent zebrafish assay. Arterioscler Thromb Vasc Biol. 23**,** 911-2.

de Pater, E., Clijsters, L., Marques, S. R., Lin, Y. F., Garavito-Aguilar, Z. V., Yelon, D., Bakkers, J., 2009. Distinct phases of cardiomyocyte differentiation regulate growth of the zebrafish heart. Development. 136**,** 1633-41.

Drake, C. J., Brandt, S. J., Trusk, T. C., Little, C. D., 1997. TAL1/SCL is expressed in endothelial progenitor cells/angioblasts and defines a dorsal-to-ventral gradient of vasculogenesis. Dev Biol. 192**,** 17-30.

Dreyfuss, G., Swanson, M. S., Pinol-Roma, S., 1988. Heterogeneous nuclear ribonucleoprotein particles and the pathway of mRNA formation. Trends Biochem Sci. 13**,** 86-91.

Ekker, M., Wegner, J., Akimenko, M. A., Westerfield, M., 1992. Coordinate embryonic expression of three zebrafish engrailed genes. Development. 116**,** 1001-10.

Ellertsdottir, E., Lenard, A., Blum, Y., Krudewig, A., Herwig, L., Affolter, M., Belting, H. G., 2010. Vascular morphogenesis in the zebrafish embryo. Dev Biol. 341**,** 56-65.

Evans, S. M., Yelon, D., Conlon, F. L., Kirby, M. L., 2010. Myocardial lineage development. Circ Res. 107**,** 1428-44.

Finn, R. D., Mistry, J., Schuster-Bockler, B., Griffiths-Jones, S., Hollich, V., Lassmann, T., Moxon, S., Marshall, M., Khanna, A., Durbin, R., Eddy, S. R., Sonnhammer, E. L., Bateman, A., 2006. Pfam: clans, web tools and services. Nucleic Acids Res. 34**,** D247-51.

Gao, G., Xie, A., Huang, S. C., Zhou, A., Zhang, J., Herman, A. M., Ghassemzadeh, S., Jeong, E. M., Kasturirangan, S., Raicu, M., Sobieski, M. A., 2nd, Bhat, G., Tatooles, A., Benz, E. J., Jr., Kamp, T. J., Dudley, S. C., Jr., 2011. Role of RBM25/LUC7L3 in abnormal cardiac sodium channel splicing regulation in human heart failure. Circulation. 124**,** 1124-31.

Garg, V., Muth, A. N., Ransom, J. F., Schluterman, M. K., Barnes, R., King, I. N., Grossfeld, P. D., Srivastava, D., 2005. Mutations in NOTCH1 cause aortic valve disease. Nature. 437**,** 270-4.

Giudicelli, F., Ozbudak, E. M., Wright, G. J., Lewis, J., 2007. Setting the tempo in development: an investigation of the zebrafish somite clock mechanism. PLoS Biol. 5**,** e150.

Glickman, N. S., Kimmel, C. B., Jones, M. A., Adams, R. J., 2003. Shaping the zebrafish notochord. Development. 130**,** 873-87.

Goodrich, A. D., Ersek, A., Varain, N. M., Groza, D., Cenariu, M., Thain, D. S., Almeida-Porada, G., Porada, C. D., Zanjani, E. D., 2010. In vivo generation of beta-cell-like cells from CD34(+) cells differentiated from human embryonic stem cells. Exp Hematol. 38**,** 516-525 e4.

Gridley, T., 2006. The long and short of it: somite formation in mice. Dev Dyn. 235**,** 2330-6.

Guo, W., Schafer, S., Greaser, M. L., Radke, M. H., Liss, M., Govindarajan, T., Maatz, H., Schulz, H., Li, S., Parrish, A. M., Dauksaite, V., Vakeel, P., Klaassen, S., Gerull, B., Thierfelder, L., Regitz-Zagrosek, V., Hacker, T. A., Saupe, K. W., Dec, G. W., Ellinor, P. T., MacRae, C. A., Spallek, B., Fischer, R., Perrot, A., Ozcelik, C., Saar, K., Hubner, N., Gotthardt, M., 2012. RBM20, a gene for hereditary cardiomyopathy, regulates titin splicing. Nat Med. 18**,** 766-73.

Hamlett, K. W., Pellegrini, D. S., Katz, K. S., 1992. Childhood chronic illness as a family stressor. J Pediatr Psychol. 17**,** 33-47.

High, F. A., Epstein, J. A., 2008. The multifaceted role of Notch in cardiac development and disease. Nat Rev Genet. 9**,** 49-61.

Hogan, B. M., Herpers, R., Witte, M., Helotera, H., Alitalo, K., Duckers, H. J., Schulte-Merker, S., 2009. Vegfc/Flt4 signalling is suppressed by Dll4 in developing zebrafish intersegmental arteries. Development. 136**,** 4001-9.

Holley, S. A., Geisler, R., Nusslein-Volhard, C., 2000. Control of her1 expression during zebrafish somitogenesis by a delta-dependent oscillator and an independent wave-front activity. Genes Dev. 14**,** 1678-90.

Isogai, S., Horiguchi, M., Weinstein, B. M., 2001. The vascular anatomy of the developing zebrafish: an atlas of embryonic and early larval development. Dev Biol. 230**,** 278-301.

Jayasena, C. S., Bronner, M. E., 2012. Rbms3 functions in craniofacial development by posttranscriptionally modulating TGF-beta signaling. J Cell Biol. 199**,** 453-66.

Jiang, Y. J., Aerne, B. L., Smithers, L., Haddon, C., Ish-Horowicz, D., Lewis, J., 2000. Notch signalling and the synchronization of the somite segmentation clock. Nature. 408**,** 475-9.

Jin, D., Hidaka, K., Shirai, M., Morisaki, T., 2010. RNA-binding motif protein 24 regulates myogenin expression and promotes myogenic differentiation. Genes Cells. 15**,** 1158-67.

Jin, W., Niu, Z., Xu, D., Li, X., 2012. RBM5 promotes exon 4 skipping of AID pre-mRNA by competing with the binding of U2AF65 to the polypyrimidine tract. FEBS Lett. 586**,** 3852-7.

Johnston, J. J., Teer, J. K., Cherukuri, P. F., Hansen, N. F., Loftus, S. K., Chong, K., Mullikin, J. C., Biesecker, L. G., 2010. Massively parallel sequencing of exons on the X chromosome identifies RBM10 as the gene that causes a syndromic form of cleft palate. Am J Hum Genet. 86**,** 743-8.

Julich, D., Hwee Lim, C., Round, J., Nicolaije, C., Schroeder, J., Davies, A., Geisler, R., Lewis, J., Jiang, Y. J., Holley, S. A., 2005. beamter/deltaC and the role of Notch ligands in the zebrafish somite segmentation, hindbrain neurogenesis and hypochord differentiation. Dev Biol. 286**,** 391-404.

Kar, A., Havlioglu, N., Tarn, W. Y., Wu, J. Y., 2006. RBM4 interacts with an intronic element and stimulates tau exon 10 inclusion. J Biol Chem. 281**,** 24479-88.

Kasahara, M., Naruse, K., Sasaki, S., Nakatani, Y., Qu, W., Ahsan, B., Yamada, T., Nagayasu, Y., Doi, K., Kasai, Y., Jindo, T., Kobayashi, D., Shimada, A., Toyoda, A., Kuroki, Y., Fujiyama, A., Sasaki, T., Shimizu, A., Asakawa, S., Shimizu, N., Hashimoto, S., Yang, J., Lee, Y., Matsushima, K., Sugano, S., Sakaizumi, M., Narita, T., Ohishi, K., Haga, S., Ohta, F., Nomoto, H., Nogata, K., Morishita, T., Endo, T., Shin, I. T., Takeda, H., Morishita, S., Kohara, Y., 2007. The medaka draft genome and insights into vertebrate genome evolution. Nature. 447**,** 714-9.

Kenan, D. J., Query, C. C., Keene, J. D., 1991. RNA recognition: towards identifying determinants of specificity. Trends Biochem Sci. 16**,** 214-20.

Kimelman, D., 2006. Mesoderm induction: from caps to chips. Nat Rev Genet. 7**,** 360-72.

Kimmel, C. B., Ballard, W. W., Kimmel, S. R., Ullmann, B., Schilling, T. F., 1995. Stages of embryonic development of the zebrafish. Dev Dyn. 203**,** 253-310.

Kleinjan, D. A., Bancewicz, R. M., Gautier, P., Dahm, R., Schonthaler, H. B., Damante, G., Seawright, A., Hever, A. M., Yeyati, P. L., van Heyningen, V., Coutinho, P., 2008. Subfunctionalization of duplicated zebrafish pax6 genes by cis-regulatory divergence. PLoS Genet. 4**,** e29.

Kuroyanagi, H., Ohno, G., Mitani, S., Hagiwara, M., 2007. The Fox-1 family and SUP-12 coordinately regulate tissue-specific alternative splicing in vivo. Mol Cell Biol. 27**,** 8612-21.

Langheinrich, U., Hennen, E., Stott, G., Vacun, G., 2002. Zebrafish as a model organism for the identification and characterization of drugs and genes affecting p53 signaling. Curr Biol. 12**,** 2023-8.

Laux, D. W., Febbo, J. A., Roman, B. L., 2011. Dynamic analysis of BMP-responsive smad activity in live zebrafish embryos. Dev Dyn. 240**,** 682-94.

Li, H. Y., Bourdelas, A., Carron, C., Shi, D. L., 2010. The RNA-binding protein Seb4/RBM24 is a direct target of MyoD and is required for myogenesis during Xenopus early development. Mech Dev. 127**,** 281-91.

Li, L., Krantz, I. D., Deng, Y., Genin, A., Banta, A. B., Collins, C. C., Qi, M., Trask, B. J., Kuo, W. L., Cochran, J., Costa, T., Pierpont, M. E., Rand, E. B., Piccoli, D. A., Hood, L., Spinner, N. B., 1997. Alagille syndrome is caused by mutations in human Jagged1, which encodes a ligand for Notch1. Nat Genet. 16**,** 243-51.

Li, S., Guo, W., Dewey, C. N., Greaser, M. L., 2013. Rbm20 regulates titin alternative splicing as a splicing repressor. Nucleic Acids Res. 41**,** 2659-72.
Lin, J. C., Tarn, W. Y., 2011. RBM4 down-regulates PTB and antagonizes its activity in muscle cell-specific alternative splicing. J Cell Biol. 193**,** 509-20.
Lin, J. C., Tarn, W. Y., 2012. Multiple roles of RBM4 in muscle cell differentiation. Front Biosci (Schol Ed). 4**,** 181-9.
Lin, J. C., Yan, Y. T., Hsieh, W. K., Peng, P. J., Su, C. H., Tarn, W. Y., 2013. RBM4 promotes pancreas cell differentiation and insulin expression. Mol Cell Biol. 33**,** 319-27.
Lints, T. J., Parsons, L. M., Hartley, L., Lyons, I., Harvey, R. P., 1993. Nkx-2.5: a novel murine homeobox gene expressed in early heart progenitor cells and their myogenic descendants. Development. 119**,** 969.
Maragh, S., Miller, R. A., Bessling, S. L., McGaughey, D. M., Wessels, M. W., de Graaf, B., Stone, E. A., Bertoli-Avella, A. M., Gearhart, J. D., Fisher, S., McCallion, A. S., 2011. Identification of RNA binding motif proteins essential for cardiovascular development. BMC Dev Biol. 11**,** 62.
Marcelle, C., Stark, M. R., Bronner-Fraser, M., 1997. Coordinate actions of BMPs, Wnts, Shh and noggin mediate patterning of the dorsal somite. Development. 124**,** 3955-63.
Maris, C., Dominguez, C., Allain, F. H., 2005. The RNA recognition motif, a plastic RNA-binding platform to regulate post-transcriptional gene expression. FEBS J. 272**,** 2118-31.
Markus, M. A., Morris, B. J., 2006. Lark is the splicing factor RBM4 and exhibits unique subnuclear localization properties. DNA Cell Biol. 25**,** 457-64.
Maroto, M., Bone, R. A., Dale, J. K., 2012. Somitogenesis. Development. 139**,** 2453-6.
McBride, K. L., Riley, M. F., Zender, G. A., Fitzgerald-Butt, S. M., Towbin, J. A., Belmont, J. W., Cole, S. E., 2008. NOTCH1 mutations in individuals with left ventricular outflow tract malformations reduce ligand-induced signaling. Hum Mol Genet. 17**,** 2886-93.
McCright, B., Lozier, J., Gridley, T., 2002. A mouse model of Alagille syndrome: Notch2 as a genetic modifier of Jag1 haploinsufficiency. Development. 129**,** 1075-82.
Miller-Bertoglio, V. E., Fisher, S., Sanchez, A., Mullins, M. C., Halpern, M. E., 1997. Differential regulation of chordin expression domains in mutant zebrafish. Dev Biol. 192**,** 537-50.
Miller, R. A., Christoforou, N., Pevsner, J., McCallion, A. S., Gearhart, J. D., 2008. Efficient array-based identification of novel cardiac genes through differentiation of mouse ESCs. PLoS One. 3**,** e2176.
Mitchell, I. C., Brown, T. S., Terada, L. S., Amatruda, J. F., Nwariaku, F. E., 2010. Effect of vascular cadherin knockdown on zebrafish vasculature during development. PLoS One. 5**,** e8807.
Miyamoto, S., Hidaka, K., Jin, D., Morisaki, T., 2009. RNA-binding proteins Rbm38 and Rbm24 regulate myogenic differentiation via p21-dependent and -independent regulatory pathways. Genes Cells. 14**,** 1241-52.
Mount, S. M., 1982. A catalogue of splice junction sequences. Nucleic Acids Res. 10**,** 459-72.

Nakano, H., Mori, S., Maeshima, E., Ito, T., Sotobata, I., 1992. [Analysis of circulatory responses to orthostatic stress in the elderly]. Nihon Ronen Igakkai Zasshi. 29**,** 113-8.

Nasevicius, A., Ekker, S. C., 2000. Effective targeted gene 'knockdown' in zebrafish. Nat Genet. 26**,** 216-20.

Niwa, Y., Shimojo, H., Isomura, A., Gonzalez, A., Miyachi, H., Kageyama, R., 2011. Different types of oscillations in Notch and Fgf signaling regulate the spatiotemporal periodicity of somitogenesis. Genes Dev. 25**,** 1115-20.

Nousbeck, J., Spiegel, R., Ishida-Yamamoto, A., Indelman, M., Shani-Adir, A., Adir, N., Lipkin, E., Bercovici, S., Geiger, D., van Steensel, M. A., Steijlen, P. M., Bergman, R., Bindereif, A., Choder, M., Shalev, S., Sprecher, E., 2008. Alopecia, neurological defects, and endocrinopathy syndrome caused by decreased expression of RBM28, a nucleolar protein associated with ribosome biogenesis. Am J Hum Genet. 82**,** 1114-21.

Oates, A. C., Ho, R. K., 2002. Hairy/E(spl)-related (Her) genes are central components of the segmentation oscillator and display redundancy with the Delta/Notch signaling pathway in the formation of anterior segmental boundaries in the zebrafish. Development. 129**,** 2929-46.

Oates, A. C., Mueller, C., Ho, R. K., 2005. Cooperative function of deltaC and her7 in anterior segment formation. Dev Biol. 280**,** 133-49.

Oda, T., Elkahloun, A. G., Pike, B. L., Okajima, K., Krantz, I. D., Genin, A., Piccoli, D. A., Meltzer, P. S., Spinner, N. B., Collins, F. S., Chandrasekharappa, S. C., 1997. Mutations in the human Jagged1 gene are responsible for Alagille syndrome. Nat Genet. 16**,** 235-42.

Ohno, G., Ono, K., Togo, M., Watanabe, Y., Ono, S., Hagiwara, M., Kuroyanagi, H., 2012. Muscle-specific splicing factors ASD-2 and SUP-12 cooperatively switch alternative pre-mRNA processing patterns of the ADF/cofilin gene in Caenorhabditis elegans. PLoS Genet. 8**,** e1002991.

Osborn, D. P., Li, K., Hinits, Y., Hughes, S. M., 2011. Cdkn1c drives muscle differentiation through a positive feedback loop with Myod. Dev Biol. 350**,** 464-75.

Oubridge, C., Ito, N., Evans, P. R., Teo, C. H., Nagai, K., 1994. Crystal structure at 1.92 A resolution of the RNA-binding domain of the U1A spliceosomal protein complexed with an RNA hairpin. Nature. 372**,** 432-8.

Parsons, M. J., Campos, I., Hirst, E. M., Stemple, D. L., 2002. Removal of dystroglycan causes severe muscular dystrophy in zebrafish embryos. Development. 129**,** 3505-12.

Parsons, M. J., Pisharath, H., Yusuff, S., Moore, J. C., Siekmann, A. F., Lawson, N., Leach, S. D., 2009. Notch-responsive cells initiate the secondary transition in larval zebrafish pancreas. Mech Dev. 126**,** 898-912.

Pedrotti, S., Busa, R., Compagnucci, C., Sette, C., 2012. The RNA recognition motif protein RBM11 is a novel tissue-specific splicing regulator. Nucleic Acids Res. 40**,** 1021-32.

Penton, A. L., Leonard, L. D., Spinner, N. B., 2012. Notch signaling in human development and disease. Semin Cell Dev Biol. 23**,** 450-7.

Pickart, M. A., Klee, E. W., 2014. Zebrafish approaches enhance the translational research tackle box. Transl Res. 163**,** 65-78.
Poon, K. L., Liebling, M., Kondrychyn, I., Garcia-Lecea, M., Korzh, V., 2010. Zebrafish cardiac enhancer trap lines: new tools for in vivo studies of cardiovascular development and disease. Dev Dyn. 239**,** 914-26.
Pourquie, O., 2011. Vertebrate segmentation: from cyclic gene networks to scoliosis. Cell. 145**,** 650-63.
Raya, A., Koth, C. M., Buscher, D., Kawakami, Y., Itoh, T., Raya, R. M., Sternik, G., Tsai, H. J., Rodriguez-Esteban, C., Izpisua-Belmonte, J. C., 2003. Activation of Notch signaling pathway precedes heart regeneration in zebrafish. Proc Natl Acad Sci U S A. 100 Suppl 1**,** 11889-95.
Robu, M. E., Larson, J. D., Nasevicius, A., Beiraghi, S., Brenner, C., Farber, S. A., Ekker, S. C., 2007. p53 activation by knockdown technologies. PLoS Genet. 3**,** e78.
Sawada, A., Shinya, M., Jiang, Y. J., Kawakami, A., Kuroiwa, A., Takeda, H., 2001. Fgf/MAPK signalling is a crucial positional cue in somite boundary formation. Development. 128**,** 4873-80.
Scehnet, J. S., Jiang, W., Kumar, S. R., Krasnoperov, V., Trindade, A., Benedito, R., Djokovic, D., Borges, C., Ley, E. J., Duarte, A., Gill, P. S., 2007. Inhibition of Dll4-mediated signaling induces proliferation of immature vessels and results in poor tissue perfusion. Blood. 109**,** 4753-60.
Schroter, C., Ares, S., Morelli, L. G., Isakova, A., Hens, K., Soroldoni, D., Gajewski, M., Julicher, F., Maerkl, S. J., Deplancke, B., Oates, A. C., 2012. Topology and dynamics of the zebrafish segmentation clock core circuit. PLoS Biol. 10**,** e1001364.
Shapiro, M. B., Senapathy, P., 1987. RNA splice junctions of different classes of eukaryotes: sequence statistics and functional implications in gene expression. Nucleic Acids Res. 15**,** 7155-74.
Shifley, E. T., Cole, S. E., 2007. The vertebrate segmentation clock and its role in skeletal birth defects. Birth Defects Res C Embryo Today. 81**,** 121-33.
Sieger, D., Tautz, D., Gajewski, M., 2003. The role of Suppressor of Hairless in Notch mediated signalling during zebrafish somitogenesis. Mech Dev. 120**,** 1083-94.
Spinner, N. B., Colliton, R. P., Crosnier, C., Krantz, I. D., Hadchouel, M., Meunier-Rotival, M., 2001. Jagged1 mutations in alagille syndrome. Hum Mutat. 17**,** 18-33.
Stainier, D. Y., 2001. Zebrafish genetics and vertebrate heart formation. Nat Rev Genet. 2**,** 39-48.
Stainier, D. Y., Fouquet, B., Chen, J. N., Warren, K. S., Weinstein, B. M., Meiler, S. E., Mohideen, M. A., Neuhauss, S. C., Solnica-Krezel, L., Schier, A. F., Zwartkruis, F., Stemple, D. L., Malicki, J., Driever, W., Fishman, M. C., 1996. Mutations affecting the formation and function of the cardiovascular system in the zebrafish embryo. Development. 123**,** 285-92.
Stickney, H. L., Barresi, M. J., Devoto, S. H., 2000. Somite development in zebrafish. Dev Dyn. 219**,** 287-303.

Suvorova, E. S., Croken, M., Kratzer, S., Ting, L. M., de Felipe, M. C., Balu, B., Markillie, M. L., Weiss, L. M., Kim, K., White, M. W., 2013. Discovery of a splicing regulator required for cell cycle progression. PLoS Genet. 9**,** e1003305.

Swanson, M. S., Nakagawa, T. Y., LeVan, K., Dreyfuss, G., 1987. Primary structure of human nuclear ribonucleoprotein particle C proteins: conservation of sequence and domain structures in heterogeneous nuclear RNA, mRNA, and pre-rRNA-binding proteins. Mol Cell Biol. 7**,** 1731-9.

Szeto, D. P., Kimelman, D., 2006. The regulation of mesodermal progenitor cell commitment to somitogenesis subdivides the zebrafish body musculature into distinct domains. Genes Dev. 20**,** 1923-32.

Taber, L. A., 2006. Biophysical mechanisms of cardiac looping. Int J Dev Biol. 50**,** 323-32.

Targoff, K. L., Schell, T., Yelon, D., 2008. Nkx genes regulate heart tube extension and exert differential effects on ventricular and atrial cell number. Dev Biol. 322**,** 314-21.

Thisse, C., Thisse, B., 2008. High-resolution in situ hybridization to whole-mount zebrafish embryos. Nat Protoc. 3**,** 59-69.

Thomas, N. A., Koudijs, M., van Eeden, F. J., Joyner, A. L., Yelon, D., 2008. Hedgehog signaling plays a cell-autonomous role in maximizing cardiac developmental potential. Development. 135**,** 3789-99.

Tiedemann, H. B., Schneltzer, E., Zeiser, S., Hoesel, B., Beckers, J., Przemeck, G. K., de Angelis, M. H., 2012. From dynamic expression patterns to boundary formation in the presomitic mesoderm. PLoS Comput Biol. 8**,** e1002586.

Trofka, A., Schwendinger-Schreck, J., Brend, T., Pontius, W., Emonet, T., Holley, S. A., 2012. The Her7 node modulates the network topology of the zebrafish segmentation clock via sequestration of the Hes6 hub. Development. 139**,** 940-7.

Vacaru, A. M., Unlu, G., Spitzner, M., Mione, M., Knapik, E. W., Sadler, K. C., 2014. In vivo cell biology in zebrafish - providing insights into vertebrate development and disease. J Cell Sci. 127**,** 485-95.

van Eeden, F. J., Granato, M., Schach, U., Brand, M., Furutani-Seiki, M., Haffter, P., Hammerschmidt, M., Heisenberg, C. P., Jiang, Y. J., Kane, D. A., Kelsh, R. N., Mullins, M. C., Odenthal, J., Warga, R. M., Allende, M. L., Weinberg, E. S., Nusslein-Volhard, C., 1996. Mutations affecting somite formation and patterning in the zebrafish, Danio rerio. Development. 123**,** 153-64.

Walker, M. B., Kimmel, C. B., 2007. A two-color acid-free cartilage and bone stain for zebrafish larvae. Biotech Histochem. 82**,** 23-8.

Wessels, M. W., De Graaf, B. M., Cohen-Overbeek, T. E., Spitaels, S. E., de Groot-de Laat, L. E., Ten Cate, F. J., Frohn-Mulder, I. F., de Krijger, R., Bartelings, M. M., Essed, N., Wladimiroff, J. W., Niermeijer, M. F., Heutink, P., Oostra, B. A., Dooijes, D., Bertoli-Avella, A. M., Willems, P. J., 2008. A new syndrome with noncompaction cardiomyopathy, bradycardia, pulmonary stenosis, atrial septal defect and heterotaxy with suggestive linkage to chromosome 6p. Hum Genet. 122**,** 595-603.

Westerfield, M., 1995. The Zebrafish Book. A Guide for the Laboratory Use of Zebrafish (Danio
rerio). University of Oregon Press, Eugene, OR.

Whittock, N. V., Ellard, S., Duncan, J., de Die-Smulders, C. E., Vles, J. S., Turnpenny, P. D., 2004. Pseudodominant inheritance of spondylocostal dysostosis type 1 caused by two familial delta-like 3 mutations. Clin Genet. 66**,** 67-72.

Yeo, G. W., Coufal, N. G., Liang, T. Y., Peng, G. E., Fu, X. D., Gage, F. H., 2009. An RNA code for the FOX2 splicing regulator revealed by mapping RNA-protein interactions in stem cells. Nat Struct Mol Biol. 16**,** 130-7.

Yin, C., Solnica-Krezel, L., 2007. Convergence and extension movements affect dynamic notochord-somite interactions essential for zebrafish slow muscle morphogenesis. Dev Dyn. 236**,** 2742-56.

Zhang, C., Zhang, Z., Castle, J., Sun, S., Johnson, J., Krainer, A. R., Zhang, M. Q., 2008. Defining the regulatory network of the tissue-specific splicing factors Fox-1 and Fox-2. Genes Dev. 22**,** 2550-63.

Zhou, A., Ou, A. C., Cho, A., Benz, E. J., Jr., Huang, S. C., 2008. Novel splicing factor RBM25 modulates Bcl-x pre-mRNA 5' splice site selection. Mol Cell Biol. 28**,** 5924-36.

APPENDIX 1

Primer Sequences For Riboprobe, RT-PCR & qRT-PCR

Riboprobe	Forward 5' - 3'	Reverse 5' - 3'
rbm24a	CCAGGGGTTATGGATTTGTG	TGCAGTTGTTGGGGTTGATA
rbm24b	CGGAGGTCTTCCCTATCACA	CCAAACGCACACAAGAGCTA
myf5	CAATCACGCCTTTGAGGCAC	GGGAATCACTTCCGGTTGGA
myod	ACCCTTGCTTCAACACCAAC	GCCCATAAAATCCATCATGC
myog	GGATCGAAGAAAGGCCGCTA	GCCTCTGTTCCCGTTATGC
myf6	ACCTGTTTGAGACCAACGCT	TCTGAAGACTCCAACACGGC
fgf8a	AGCTTTACAGCCGAACCAGT	AGTAGCGGGTGCGTTTAGTC
tbx16	TCACCAAACCTGGCAGAAGG	AGAGCTTCACACGATGACGG
ntla	AGACGAATGTTTCCCGTGCT	GGTCTGGGACTTCCTTGTGG
dlc	GTGCACCTACGGCACCGGAA	CACTTGCACTCACCGGGGGC
dld	ATTCCTTTCGCGTTTGGGTTCACATGGCCA	TCCGTCTTGGCAAGTGCCGCC
notch1a	ACCCGTGTCTGAACCAGGGCT	TCCCGGCAAACACACGCAGG
notch3	AGCACCAAGGTATTCAGCAGC	TGGCGGCTCTTCAATAACAGC
her7	CATATCCTCATTGATATCAAC	AGAGATTACACAAGGCCCATCA
dla	TGGAAACCCCTGCCGCAACG	GACTACTGCGCACGCCACGA
dlb	ATCTCCGCAGAGCCCCCGTG	AAAGTCGGTGGGCATCGGCA
dll4	CAACTTTGGGTGGCCGGGGT	CTGGCCAGTGAAGCCCGCTC

Splice PCR	Forward 5' - 3'	Reverse 5' - 3'
dlc	TCGGACTACTCTCACAGTCTGCT	TGTGGTCAGGCCCACTGGTGT
dld	TGCCTGGCCCGTGGAAGTTT	CCGAGCCAGTATGGCCCAACG
her1	TCGTCTTCTTCCGATTTTCAGCC	ACAACGCTGGTTATTCTCATGCT
her7	CGATGAAAGACCTCCACCTGC	GGGGGAGAAGAAATCTGCGT

RT-PCR	Forward 5' - 3'	Reverse 5' - 3'
elfalpha	TCTGTTACCTGGCAAAGGGG	GGAGTCGACGTGGCCAATAA
dlc	TCGTGTCGTGTGCGATGAAT	ACAGCCAGACAAGCAGATGG
dld	GTCTTCCGGGGTGTGATGAA	GGCACGGTTTGTGATGTGTG
myod	CTGCCCAAAGTGGAGATTCTG	TTCTCGTCTGACACGTTGGG
dld short 1	GAGCATTACTACGGCGAGGG	AGCTACAGCTCTGTTGTGCAG
dld short 2	TGGCTAGCGCAGATCCATTT	TGGCGTTACACCTCGGTTG

APPENDIX 2

Zebrafish *dlc* RT-PCR short_1 alignment to NM_ 130944

Primers used for RT-PCR are highlighted in yellow

```
dlc wt  1     GGGTTTTGAAGAAACGTAACTGAAGGGTCCAAAGTCCCCTGGAGCTAGAA  50
dlc wt  51    ATCTGTTTTTATTTGCTTTGTAGGCTCCAAACACATGCGACATTGAGATA  100
dlc wt  101   CATTTTTATAAGAAATGTTCATTCGTTTAACTTTTTAACTTTACGCATTT  150
dlc wt  151   TTACAACTACTTTTTCCCTTTAAATTGTGGATAATACTTCAAACATTCAT  200
short_1                                                       T

dlc wt  201   ATCGGACTACTCTCACAGTCTGCTATCGTTCAGTAGCAGACAAGAAGGCA  250
short_1       ATCGGACTACTCTCACAGTCTGCTATCGTTCAGTAGCAGACAAGAAGGCA

dlc wt  251   AAGATGGCTCGTGTTTTATTAACGTGCTTTTTTATTTTGATATCATCGCA  300
short_1       AAGATGGCTCGTGTTTTATTAACGTGCTTTTTTATTTTGATAT-------

dlc wt  301   TCTGGGGAAATCATCCGGTGTGTTTGAGTTGAAAGTTCTGTCTTTCACAA  350
short_1       --------------------------------------------------

dlc wt  351   GCACGAGCAGTGTGTGTAAAGGGTCCAGCGACTGCCAGATCTTTTTCCGT  400
short_1       --------------------------------------------------

dlc wt  401   GTTTGCCTGAAGCACTCGCAAGCACTCATATTACCTGAGCCGCCGTGCAC  450
short_1       --------------------------------------------------

dlc wt  451   CTACGGCACCGGAATGTCAGAAATACTGAGCGCGGACTCCATCTCCAGCA  500
short_1       --------------------------------------------------

dlc wt  501   GTGCGTATATAAGCGTGCCTTTTAATTTCAAGTGGCCGGGAATCGTCTCT  550
short_1       --------------------------------------------------

dlc wt  551   TTGATAATCGAAACCTGGAACGCAGAAACCTCTGACCAGTCAACAGAGAA  600
short_1       --------------------------------------------------

dlc wt  601   TAACAACAACATGATAAGCCGTTTGGCCACCAAAAGAAGACTCGCTATCA  650
short_1       --------------------------------------------------

dlc wt  651   GTGAGGACTGGTCTCAGGACGTGCATCTCGGTCGACAAAGCCAACTGCGC  700
short_1       --------------------------------------------------

dlc wt  701   TTTTCTTATCGTGTCGTGTGCGATGAATTCTACCACGGCGAGGAATGCTC  750
short_1       --------------------------------------------------

dlc wt  751   GGATTTCTGCCGCCCACGGAATGATACCTTCGGCCACTTCAACTGTGACG  800
short_1       --------------------------------------------------

dlc wt  801   CCGCTGGCAACAGAATTTGCCTTCCTGGATGGAAAGGCGATTATTGCACC  850
short_1       --------------------------------------------------

dlc wt  851   GAACCCATCTGCTTGTCTGGCTGTAGTGAGGAGAACGGTTATTGTGAGGC  900
short_1       --------------------------------------------------

dlc wt  901   CCCCGGTGAGTGCAAGTGCCGGATTGGATGGGAAGGCCCCCTCTGTGATG  950
```

```
short_1       ------------------------------------------------

dlc wt  951   AGTGCACGCGGCACCCGGGGTGCTTGCATGGCACCTGCAACCAGCCTTTT  1000
short_1       ------------------------------------------------

dlc wt  1001  CAGTGCACTTGCAAAGAAGGTTGGGGCGGTCTGTTTTGCAATGAGGATCT  1050
short_1       ------------------------------------------------

dlc wt  1051  GAACTTTTGCACTAATCACAAGCCCTGTAGAAATGACGCCACGTGTACCA  1100
short_1       ------------------------------------------------

dlc wt  1101  ACACCGGCCAGGGCAGCTACACCTGCATTTGCAAGCCTGGCTTCAGTGGC  1150
short_1       ------------------------------------------------

dlc wt  1151  AAAAACTGTGAGATCGAAACCAATGAGTGTGACAGCAACCCCTGCAAGAA  1200
short_1       ------------------------------------------------

dlc wt  1201  TGGAGGCAGTTGCAATGACCAGGAGAATGATTACACTTGTACATGCCCGC  1250
short_1       ------------------------------------------------

dlc wt  1251  AAGGCTTCTATGGCAAGAACTGCGAGGTCAGCGCCATGACCTGTGCCGAT  1300
short_1       ------------------------------------------------

dlc wt  1301  GGACCCTGCTTCAATGGTGGAACCTGCATGGAGAAGGGATCCGGTAGCTA  1350
short_1       ------------------------------------------------

dlc wt  1351  TTCCTGCCGCTGCCCTCCTGGATACATGGGCTCCAACTGTGAGAAGAAAA  1400
short_1       --------------------------------------------------

dlc wt  1401  TCGACCGGTGCAGCAGTGACCCCTGTGCTAACGGTGGCCAGTGTCTCGAT  1450
short_1       ------------------------------------------------

dlc wt  1451  TTGGGCAACAAAGCGACGTGCCGTTGCCGGCCCGGGTTCACAGGCTCACG  1500
short_1       ------------------------------------------------

dlc wt  1501  TTGTGAAACAAACATTGACGACTGCTCAAGCAACCCCTGTCAAAATGCAG  1550
short_1       ------------------------------------------------

dlc wt  1551  GCACCTGCGTGGATGGTATCAACGGGTACACCTGCACATGCACGCTTGGT  1600
short_1       ------------------------------------------------

dlc wt  1601  TTCTCAGGCAAGGACTGTAGGGTTCGCTCTGACGCCTGCAGTTTCATGCC  1650
short_1       ------------------------------------------------

dlc wt  1651  CTGCCAGAACGGAGGAACCTGCTACACTCACTTCTCTGGGCCTGTCTGCC  1700
short_1       ------------------------------------------------

dlc wt  1701  AGTGCCCGGCAGGCTTCATGGGCACACAGTGCGAGTACAAACAGAAGCCC  1750
short_1       ------------------------------------------------

dlc wt  1751  ACGCCTGTGAACAGCCCTGCTCTTCCAGCAGCCTTAATAGTCTCATTTAC  1800
short_1       ------------------------------------------------

dlc wt  1801  TCTAGGCCTCATTACTCTGACCTTAGTGATCTGTGCTGCCATTGTGGTCC  1850
short_1       ------------------------------------------------
```

```
dlc wt  1851  TGCGACAGATGCGTCAGAACCACAAAGCCAGCTCAACCACAGTTCGAAAC  1900
short_1       --------------------------------------------------

dlc wt  1901  AACCTGGATTCTGTCAATAATCGCATTTCTTTGAGCCCAACCTCACCTTT  1950
short_1       ------------------AATCGCATTTCTTTGAGCCCAACCTCACCTTT

dlc wt  1951  AGGTAGAGAGAAGGAGGCCTTCCTTATTCCTGGTGGCCCATTTAAGGTGT  2000
short_1       AGGTAGAGAGAAGGAGGCCTTCCTTATTCCTGGTGGCCCATTTAAGGTGT

dlc wt  2001  CCAATAAAGATATGGCGCTCAGATCCACCTCTGTAGACACACATTCCAGT  2050
short_1       CCAATAAAGATATGGCGCTCAGATCCACCTCTGTAGACACACATTCCAGT

dlc wt  2051  GACAAATCAAACTATAAGCAGAAGATGGTGGACTACAATCTGAGCATTGA  2100
short_1       GACAAATCAAACTATAAGCAGAAGATGGTGGACTACAATCTGAGCATTGA

dlc wt  2101  TGAAAAGCACACAAACAACAAACTAGAGAAAAACTCTGAATCAACATTGC  2150
short_1       TGAAAAGCACACAAACAACAAACTAGAGAAAAACTCTGAATCAACATTGC

dlc wt  2151  TGGTTCCACCTTTAAACTATCCAAAAGAGGGAGTGTATCATCCTGTGTAC  2200
short_1       TGGTTCCACCTTTAAACTATCCAAAAGAGGGAGTGTATCATCCTGTGTAC

dlc wt  2201  ATCATTCCCGAACACATAGAACAACGTGTGTTTGCTACTGAGGTATAGCA  2250
short_1       ATCATTCCCGAACACATAGAACAACGTGTGTTTGCTACTGAGGTATAGCA

dlc wt  2251  GAATTCTTCAATCTGGAGCACCTCAAACACCAGTGGGCCTGACCACAAAA  2300
short_1       GAATTCTTCAATCTGGAGCACCTCAAACACCAGTGGGCCTGACCACA

dlc wt  2301  ATGTTTACAGTCTCTAAGGACAAAAGGAAGACGTGAAGAGAGTATATATC  2350
dlc wt  2351  ACATGCATTATATTATTTATTTATTCATGCTGCTCACTAAATGGACTACT  2400
dlc wt  2401  TCTTGATATGGATAATGAATTTGTGAAGACAAGCAAGAGACTTGAAGACC  2450
dlc wt  2451  CGAGGAACAACTTGCATTATTTGCACTATTTCCTTTCCCTTTTTTAATGA  2500
dlc wt  2501  CCCAAACAGAATTTTTATATATTTGTCATCATATTTAAATTGTACATAGA  2550
dlc wt  2551  CACAAGAACTCTCTGGAAGAGCTGAAGAATCAAGGATTTGATAATCACAG  2600
dlc wt  2601  AAGCCTTGAAAAGGAAGAAAATAGGCATCCTGAAGTTCATCTAACTCTGT  2650
dlc wt  2651  GAATCACATGAAGCCCAAACAATCAGCCTTATGGGTGGAGGAGGTGCAAC  2700
dlc wt  2701  TGAAGGATCTGGAACTGTGACTGTGGAGTATTTGCCTTTTATTTTTATTT  2750
dlc wt  2751  TTTCGATATGGTTCGAAATGCTATTTATAAATGGAACTGTGATGAGAAGC  2800
dlc wt  2801  AATCAAACTGAACAAAACAAGTTGTTCTGGCTGTGAACAATGTGAACAAC  2850
dlc wt  2851  TGTCTTGGAAATGTACAGTTTTATGCGGCAGTGATTTTACTTAGTGCCTA  2900
dlc wt  2901  CAATGGATCTGACTATCAGTGACATTTTCTCAAACCAAACCCAATCTCAA  2950
dlc wt  2951  TTAAGTGCCTCATTCTTTAATGTGCTACAGCTCAGTTACAAAGGTACTCC  3000
dlc wt  3001  TTAGAAACACTGAAAAGAGCCTTTTTTTAAACACTATAGGAGTATGCTTT  3050
dlc wt  3051  TCGACAGTAGATGTTTGGGTTGATTTGAGTACAGTTGTTTAAACAGCGAT  3100
dlc wt  3101  GGATGATGGATGCTGTTGTGTACAGCGGCCATCCTGTCAACATTCACTGG  3150
dlc wt  3151  TGGTAACTATTTCCGACATTCCCAAGGCTTGAAAGGACCCTTGGTCCAAA  3200
dlc wt  3201  CTGATAGCCTCAACATTGTCAAGATTTCCTGGGTTTGTAATCCTCTGCAA  3250
dlc wt  3251  TCAGAGTGTTTTTCAAAATTCACAACAACATAGATTGTTCTATGTCTTTT  3300
dlc wt  3301  CCTTTCCTATTTTATTTTTTATTTTTTAGTATGTGGCATTTGTTCCGTCA  3350
dlc wt  3351  TTTTCATTTTTTAAAACCCTTTAAACCCAAAGAGGTGGAACCTTTAATAT  3400
dlc wt  3401  TTTAAACCGTTTTCCTTAATTTACCAATGCCATAAGGGCCAAATTTTTGG  3450
dlc wt  3451  ATAATCCCCTATTTAATTGGGCCGTAAAAATTTTGGATTTATGAGAGGAT  3500
dlc wt  3501  GAATGGATATAAGGTTAAGGATTTTGCAAATATATATATATATTTTTTCA  3550
dlc wt  3551  AATAAATAAACCCCCGGAATAATTTAAAAAAAAAAAAAAAAAAAAAAAA  3600
dlc wt  3601  AAAAAAAAAA                                        3610
```

APPENDIX 3

Zebrafish *dld* RT-PCR short_1 & short_2 alignment to NM_ 130955

Primers used for RT-PCR are highlighted in yellow

```
dld wt  1     AGTCAGTCTCTCACATGGAAACAAGAGTACGGGATGAAAGTTTGGATCAG  50
dld wt  51    TAGTTTGGATCATCTCCACATGAACTTTTGAAACGGAAAATAAGCGCATA  100
dld wt  101   AATAACCCTGTGCTTGGGGTTTTGTCATTTTTCCGGCTTCCTAAACTACC  150
dld wt  151   CGAAAGTGGACTGCTAACTTTTTTTGACAACTTGGAGTACTCGACTTGTG  200
dld wt  201   AGGGATTTCCCAATCGTCTCCCTTTTGCGCATCGGGGTTTCCTCCTTCTA  250
dld wt  251   CATTCGTATTTGGGATTTAATTGCTGATTTATTTTCCAAGGGGGGACTTT  300
dld wt  301   GATGGGCTTGCATGAGCAGATAAACTGAACACAACAGAGCATCAACCCGA  350
dld wt  351   GCTGCCTCCCACTGAGCGGAGAACGACGAGTCTCAATGATTTATTGAGAC  400
dld wt  401   ACGGTCTCACACAATTGCCTGGCCCGTGGAAGTTTCACAACAGTTCAGAT  450
short_1                   TGCCTGGCCCGTGGAAGTTTCACAACAGTTCAGAT
short_2                   TGCCTGGCCCGTGGAAGTTTCACAACAGTTCAGAT

dld wt  451   CCTCTCCGCCATGGGACGACTAATGATAGCTGTTTTGCTTTGTGTCATGA  500
short_1       CCTCTCCGCCATGGGACGACTAATGATAGCTGTTTTGCTTTGTGTCATGA
short_2       CCTCTCCGCCATGGGACGACTAATGATAGCTGTTTTGCTTTGTGTCA---

dld wt  501   TAAGCCAGGGGTTTTGTTCAGGGGTTTTTGAGCTAAAGTTGCAAGAGTTT  550
short_1       TAAGCCAGGGGTTTTGTTCAGGGGTTTTTGAGCTAAAGTTGCAAGAGTTT
short_2       ---------------------------------------------------

dld wt  551   CTGAACAAGAAAGGAGTGACAGGCAACGCAAACTGCTGCAAGGGATCCGC  600
short_1       CTGAACAAGAAAGGAGTGACAGGCAACGCAAACTGCTGCAAGGGATCCGC
short_2       ---------------------------------------------------

dld wt  601   GGCAGAGGGTCTTCAGTGTGAATGCAAAACTTTTTTTAGGATTTGCCTGA  650
short_1       GGCAGAGGGTCTTCAGTGTGAATGCAAAACTTTTTTTAGGATTTGCCTGA
short_2       ---------------------------------------------------

dld wt  651   AACATTACCAAGCCAACGTATCTCCAGATCCTCCGTGCACCTACGGTGGC  700
short_1       AACATTACCAAGCCAACGTATCTCCAGATCCTCCGTGCACCTACGGTGGC
short_2       ---------------------------------------------------

dld wt  701   GCAGTTACCCCGGTGCTCGGATCAAACTCCTTCCAAGTTCCCGAAAGCTT  750
short_1       GCAGTTACCCCGGTGCTCGGATCAAACTCCTTCCAAGTTCCCGAAAGCTT
short_2       ---------------------------------------------------

dld wt  751   CCCTGACAGCTCGTTCACCAACCCCATTCCTTTCGCGTTTGGGTTCACAT  800
short_1       CCCTGACAGCTCGTTCACCAACCCCATTCCTTTCGCGTTTGGGTTCACAT
short_2       ---------------------------------------------------

dld wt  801   GGCCAGGAACATTTTCGCTGATTATTGAAGCGCTGCACACCGACTCCACT  850
short_1       GGCCAGGAACATTTTCGCTGATTATTGAAGCGCTGCACACCGACTCCACT
short_2       ---------------------------------------------------

dld wt  851   GATGACCTGTCTACAGAAAACCCAGACCGTCTGATCAGTCGCATGACCAC  900
short_1       GATGACCTGTCTACAGAAAACCCAGACCGTCTGATCAGTCGCATGACCAC
short_2       ---------------------------------------------------
```

```
dld wt  901   CCAGAGGCATCTAACAGTAGGCGAGGAATGGTCCCAAGATCTACAGGTTG  950
short_1       CCAGAGGCATCTAACAGTAGGCGAGGAATGGTCCCAAGATCTACAGGTTG
short_2       -------------------------------------------------

dld wt  951   GTGGGAGGACAGAGCTGAAGTACTCATACAGATTCGTTTGTGATGAGCAT  1000
short_1       GTGGGAGGACAGAGCTGAAGTACTCATACAGATTCGTTTGTGATGAGCAT
short_2       -------------------------------------------------

dld wt  1001  TACTACGGCGAGGGCTGCTCGGTCTTCTGCCGTCCGCGCGATGATACTTT  1050
short_1       TACTACGGCGAGGGCTGCTCGGTCTTCTGCCGTCCGCGCGATGATACTTT
short_2       -------------------------------------------------

dld wt  1051  CGGCCACTTCACCTGCGGAGAGCGCGGAGAAATTATCTGCAACTCCGGAT  1100
short_1       CGGCCACTTCACCTGCGGAGAGCGCGGAGAAATTATCTGCAACTCCGGAT
short_2       -------------------------------------------------

dld wt  1101  GGAAAGGACAGTACTGCACAGAACCAATCTGTCTTCCGGGGTGTGATGAA  1150
short_1       GGAAAGGACAGTACTGCACA----------------------------
short_2       -------------------------------------------------

dld wt  1151  GACCATGGCTTTTGCGACAAACCCGGTGAATGCAAATGCAGAGTAGGATT  1200
short_1       -------------------------------------------------
short_2       -------------------------------------------------

dld wt  1201  TAGTGGAAAGTACTGTGACGACTGCATTCGCTACCCAGGCTGCTTGCATG  1250
short_1       -------------------------------------------------
short_2       -------------------------------------------------

dld wt  1251  GCACCTGCCAACAGCCCTGGCAATGCAACTGCCAAGAGGGTTGGGGAGGT  1300
short_1       -------------------------------------------------
short_2       -------------------------------------------------

dld wt  1301  CTCTTCTGTAACCAAGATCTCAATTACTGCACACATCACAAACCGTGCCA  1350
short_1       -------------------------------------------------
short_2       -------------------------------------------------

dld wt  1351  GAATGGAGCCACTTGCACCAACACAGGCCAGGGAAGCTACACCTGCTCAT  1400
short_1       -------------------------------------------------
short_2       -------------------------------------------------

dld wt  1401  GCAGACCTGGCTTCACCGGGGACAGCTGTGAGATTGAGGTCAACGAATGC  1450
short_1       -------------------------------------------------
short_2       -------------------------------------------------

dld wt  1451  TCCGGCAGCCCGTGCAGAAATGGAGGAAGTTGCACTGATCTTGAAAACAC  1500
short_1       -------------------------------------------------
short_2       -------------------------------------------------

dld wt  1501  CTACAGCTGCACTTGTCCTCCTGGTTTCTACGGAAGAAACTGCGAGCTGA  1550
short_1       -------------------------------------------------
short_2       -------------------------------------------------

dld wt  1551  GTGCCATGACTTGTGCCGACGGCCCCTGCTTCAATGGTGGACAGTGTGCT  1600
short_1       -------------------------------------------------
short_2       -------------------------------------------------
```

```
dld wt  1601  GACAACCCAGAGGGAGGATATTTCTGCCAGTGCCCGATGGGTTATGCTGG  1650
short_1       --------------------------------------------------
short_2       --------------------------------------------------

dld wt  1651  ATTCAACTGTGAGAAGAAGATCGATCACTGCAGCTCCAACCCTTGCTCGA  1700
short_1       --------------------------------------------------
short_2       --------------------------------------------------

dld wt  1701  ATGATGCTCAGTGTCTCGATCTTGTGGACTCCTATCTTTGCCAGTGTCCT  1750
short_1       --------------------------------------------------
short_2       --------------------------------------------------

dld wt  1751  GAGGGATTCACAGGAACGCACTGCGAAGACAACATCGACGAGTGTGCCAC  1800
short_1       --------------------------------------------------
short_2       --------------------------------------------------

dld wt  1801  CTATCCCTGCCAGAATGGCGGCACTTGCCAAGACGGACTCAGCGACTACA  1850
short_1       --------------------------------------------------
short_2       --------------------------------------------------

dld wt  1851  CCTGCACCTGCCCGCCTGGATACACCGGCAAGAACTGCACCTCTGCGGTC  1900
short_1       --------------------------------------------------
short_2       --------------------------------------------------

dld wt  1901  AACAAGTGCCTCCACAACCCTTGCCACAACGGTGCCACTTGTCATGAAAT  1950
short_1       --------------------------------------------------
short_2       --------------------------------------------------

dld wt  1951  GGACGGTCGATATGTGTGCGCTTGCATCCCAGGTTATGGAGGACGCAACT  2000
short_1       --------------------------------------------------
short_2       --------------------------------------------------

dld wt  2001  GTCAGTTCTTACTCCCTGAAAACCCACAAGGACAAGCCATCGTTGAGGGA  2050
short_1       --------------------------------------------------
short_2       --------------------------------------------------

dld wt  2051  GCCGACAAGAGATACTCTTACGAAGAAGACGACGGTGGTTTTCCATGGAC  2100
short_1       --------------------------------------------------
short_2       --------------------------------------------------

dld wt  2101  GGCGGTTTGCGCTGGGATTATTTTAGTGCTTTTAGTGCTGATCGGCGGCT  2150
short_1       --------------------------------------------------
short_2       --------------------------------------------------

dld wt  2151  CCGTCTTTGTCATTTACATCCGTCTCAAGCTGCAGCAGAGGAGCCAGCAA  2200
short_1       --------------------------------------------------
short_2       --------------------------------------------------

dld wt  2201  ATCGATAGCCATAGTGAAATCGAGACCATGAACAACCTGACCAACAACCG  2250
short_1       --------------------------------------------------
short_2       --------------------------------------------------

dld wt  2251  CAGCCGAGAGAAGGACTTGTCCGTAAGCATCATCGGAGCCACGCAAGTGA  2300
short_1       --------------------------------------------------
short_2       --------------------------------------------------
```

```
dld wt  2301  AAAACATCAACAAGAAAGTGGACTTTCAGAGCGACGGCGACAAAAACGGA  2350
short_1       --------------------------------------------------
short_2       --------------------------------------------------

dld wt  2351  TTCAAATCGCGATACTCGCTAGTGGATTACAATCTTGTTCATGAGCTGAA  2400
short_1       --------------------------------------------------
short_2       --------------------------------------------------

dld wt  2401  GCAGGAGGACTTGGGGAAAGAGGATTCTGAGAGGAGCGAAGCCACAAAAT  2450
short_1       --------------------------------------------------
short_2       --------------------------------------------------

dld wt  2451  GCGAGCCTCTCGATTCCGACTCAGAGGAGAAGCACAGAAATCATTTAAAA  2500
short_1       --------------------------------------------------
short_2       -------------------------GAGAAGCACAGAAATCATTTAAAA

dld wt  2501  AG------------------------------------------------  2502
short_1       --------------------------------------------------
short_2       AGgtaaatgagtgtgaattttggctagcgcagatccatttgtcgatgtaa

dld wt  2503  --------------------------------TGACTCCTCAGAGAGGAA  2520
short_1       --------------------------------------------------
short_2       gcagtactaaagttgcctcttttcgttttcagTGACTCCTCAGAGAGGAA

dld wt  2521  ACGAACAGAATCTTTGTGCAAGGACACAAAGTACCAGTCAGTCTTTGTTT  2570
short_1       --------------------------------------------------
short_2       ACGAACAGAATCTTTGTGCAAGGACACAAAGTACCAGTCAGTCTTTGTTT

dld wt  2571  TATCAGAGGAGAAAGATGAATGTATTATTGCAACCGAGGTGTAACGCCAC  2620
short_1       --------------------------------------------------
short_2       TATCAGAGGAGAAAGATGAATGTATTATTGCAACCGAGGTGTAACGCCAC

dld wt  2621  AACAGAGCTGTAGCTCATCTTGTTCTACAGGAGGTTTTACTCCAGTAATG  2670
short_1       -ACAGAGCTGTAGCTCATCTTGTTCTACAGGAGGTTTTACTCCAGTAATG
short_2       AACAGAGCTGTAGCTCATCTTGTTCTACAGGAGGTTTTACTCCAGTAATG

dld wt  2671  CTGCTCAAACCAGAGGGAAGGTTCCCTTCACGTGACTGCTGCTGTGAAAC  2720
short_1       CTGCTCAAACCAGAGGGAAGGTTCCCTTCACGTGACTGCTGCTGTGAAAC
short_2       CTGCTCAAACCAGAGGGAAGGTTCCCTTCACGTGACTGCTGCTGTGAAAC

dld wt  2721  TAATGTTGAAGGTGATATTCAGAATGAGCTGGTTCTCAACTGAAGTAAAC  2770
short_1       TAATGTTGAAGGTGATATTCAGAATGAGCTGGTTCTCAACTGAAGTAAAC
short_2       TAATGTTGAAGGTGATATTCAGAATGAGCTGGTTCTCAACTGAAGTAAAC

dld wt  2771  ACAGTGACTGCAGGAAAGGACGTTGGGCCATACTGGCTCGGACTCTCAAA  2820
short_1       ACAGTGACTGCAGGAAAGGACGTTGGGCCATACTGGCTCGG
short_2       ACAGTGACTGCAGGAAAGGACGTTGGGCCATACTGGCTCGG

dld wt  2821  GTTTGTTTCCCAGGAACGTGCCAAATGGACTTGCTTGCACTTCCTGTAGG  2870
dld wt  2871  GACGTTTTTTTTTTACCTCATTGCACTATGATGGGTTGTATTTTTATTGT  2920
dld wt  2921  ATTTAACACACAATTGAATCGAATACTGTGTATGCATATGCACTGACTGC  2970
dld wt  2971  AGTGTGCATCTGGAAGTTCTCGGATCCTTGGATCGCGAGAGGAAGAACAC  3020
dld wt  3021  TGCCATCAATGATGTTTGTAACTGATTCGTTGTTTTATTTTCGGAAAGCT  3070
dld wt  3071  TGTGTTTTCTTTATTTAAATGTTATTTGTGATCGACGTGTTTGTGGTTTA  3120
dld wt  3121  CTTTGTGTGTGTGTGTGTGAAGTTTGATATAATTTAAAATCTTTTTTT  3170
dld wt  3171  CATTTCGCAGATATGTCTATTGTAAATAAGGCACTTCGGGTCGACGTGAC  3220
```

dld wt 3221 TGTTCTCTGTAAATGTATTTAAACGTGCTGGTAAAACTTACAGGAGTTGT 3270
dld wt 3271 TTTTATGACTGTTGTCCAATGAAAAAAAAATCACCTTAATATTTTTCCAA 3320
dld wt 3321 ATAAATCCTGTATGAAACTTCAAAAAAAAAAAAAAAAAAAAAAAAAAAA 3370
dld wt 3371 AAAAAAA 3377

APPENDIX 4

Maragh et al. BMC Developmental Biology 2011, 11:62
http://www.biomedcentral.com/1471-213X/11/62

BMC Developmental Biology

RESEARCH ARTICLE Open Access

Identification of RNA binding motif proteins essential for cardiovascular development

Samantha Maragh[1,2], Ronald A Miller[2], Seneca L Bessling[2], David M McGaughey[2], Marja W Wessels[3], Bianca de Graaf[3], Eric A Stone[4], Aida M Bertoli-Avella[3], John D Gearhart[5], Shannon Fisher[6] and Andrew S McCallion[1,7*]

Abstract

Background: We recently identified *Rbm24* as a novel gene expressed during mouse cardiac development. Due to its tightly restricted and persistent expression from formation of the cardiac crescent onwards and later in forming vasculature we posited it to be a key player in cardiogenesis with additional roles in vasculogenesis and angiogenesis.

Results: To determine the role of this gene in cardiac development, we have identified its zebrafish orthologs (*rbm24a* and *rbm24b*), and functionally evaluated them during zebrafish embryogenesis. Consistent with our underlying hypothesis, reduction in expression of either ortholog through injection of morpholino antisense oligonucleotides results in cardiogenic defects including cardiac looping and reduced circulation, leading to increasing pericardial edema over time. Additionally, morphant embryos for either ortholog display incompletely overlapping defects in the forming vasculature of the dorsal aorta (DA), posterior caudal vein (PCV) and caudal vein (CV) which are the first blood vessels to form in the embryo. Vasculogenesis and early angiogenesis in the trunk were similarly compromised in *rbm24* morphant embryos at 48 hours post fertilization (hpf). Subsequent vascular maintenance was impaired in both *rbm24* morphants with substantial vessel degradation noted at 72 hpf.

Conclusion: Taken collectively, our functional data support the hypothesis that *rbm24a and rbm24b* are key developmental cardiac genes with unequal roles in cardiovascular formation.

Background

During vertebrate embryogenesis the heart is the first organ to develop and achieve functionality. Model organism studies have uncovered a number of genes such as Nkx2.5, which have important functions in early vertebrate myocardial development and differentiation [1,2]. Despite an increasing body of data illuminating the roles played by several key genes during cardiac development, there is still much to learn about what other factors may be critical. The general stages of cardiac development are invariable throughout vertebrate model organisms where heart development has been examined, with zebrafish progressing through these stages at a particularly rapid rate [3]. During zebrafish cardiogenesis the heart cone is the first structure to form between 19-20 hpf, followed by the formation of a short cardiac tube lacking discrete chambers by 24 hpf. Subsequently the cardiac tube lengthens and distinct ventricle and atrium chambers are discernable by 30 hpf with heart tube looping occurring around 36 hpf. A functional two chambered zebrafish heart is visible by 48 hpf [4].

In a recent transcriptional profiling study, we compared the signatures of mouse embryonic stem cells as they were differentiated towards cardiac cell fates in an effort to uncover novel critical cardiac genes. In this initial study we described the cardiac developmental expression of 31 identified candidate genes with previously unknown roles in cardiogenesis. Furthermore, nine of these transcripts were expressed in the forming cardiac crescent of the mouse embryo [5], consistent with roles in the earliest stages of heart development. Based on the early cardiac expression of these genes we

* Correspondence: amccall2@jhmi.edu
[1]Biochemical Science Division, National Institute of Standards and Technology, Gaithersburg, MD 20899, USA
Full list of author information is available at the end of the article

predicted they likely play significant roles in heart development.

In this paper we report functional evaluation of one of these genes, *Rbm24*, through the identification, characterization and knockdown of its zebrafish (*Danio rerio*) orthologs. *Rbm24* is a member of the RNA binding protein family, based upon the identification of a RNA recognition motif (RRM) in amino acid residues 12-84. RRMs are the most common and best characterized RNA binding modules with many functioning in most post-transcriptional processes [6]. The RRM is composed of four-stranded anti-parallel β-sheets with two helices packed against it such that the domain has the split αβ (βαββαβ) topology [7]. Often, RRMs function in concert to increase binding specificity possibly because the number of nucleotides recognized by a single RRM is generally too small to define a unique binding sequence [8]. RRMs are found in a variety of RNA binding proteins, including several hnRNP proteins, proteins implicated in regulation of alternative splicing, and protein components of snRNPs indicating a diverse role of these motifs in cellular development and function.

As we have shown previously, the mouse *Rbm24* transcript is upregulated in the cardiac progenitor population and is expressed from the earliest stages of cardiac specification, in the cardiac crescent, and subsequently within the heart tube and looping heart [5]. Based upon these observations we hypothesized that *Rbm24* plays a crucial role in cardiogenesis. In this study we investigated the putative role of Rbm24 in cardiac development. We have identified two *rbm24* zebrafish orthologs (termed *rbm24a* and *rbm24b*), and demonstrate that their spatial expression is consistent with our observations in mice. We use *rbm24a* and *rbm24b* translation blocking morpholino antisense oligonucleotides (MO) in the early embryo and demonstrate that each zebrafish *rbm24* ortholog has a key but unequal role to play in cardiac development. Additionally, we demonstrate a role for *rbm24a* and *rbm24b* in normal vascular development. Vascular development consists of vasculogenesis which is the *de novo* formation of the first vascular vessels and subsequently angiogenesis which is the formation of additional vasculature as extensions of existing vasculature. Zebrafish vasculogenesis results in the formation of the main trunk vessels with the DA first to form (24 - 26 hpf) followed by the CV and PCV (28 - 30 hpf) and several heart vessels generating the first single circulation loop. Angiogenesis can be observed in the trunk by 24 hpf as intersegmetal vessels (Se) begin to form as paired dorsally extending branches off the DA and subsequently off the PCV (~32 hpf). As the Se reach the dorsal line of the embryo the ends of the vessels form connections resulting in two dorsal longitudinal anastomotic vessels (DLAVs) running along the anterior-posterior (A-P) axis of the embryo at the dorsal line. By 48 hpf these trunk vessels are fully formed with circulation [9,10]. Our findings show the requirement for *rbm24a* and *rbm24b* in cardiac development and vasculogenesis with a more pronounced role for *rbm24a*, and an additional putative role for *rbm24a* in angiogenesis.

Results

Phylogenetic comparative analysis establishes two *rbm24* orthologs in zebrafish

We recently reported the identification of *Rbm24* as one of a number of novel transcripts discretely expressed in the earliest stages of cardiac development in the mouse embryo [5]. To facilitate determination of the biological requirement for this gene during vertebrate embryonic development, we first set out to identify the orthologous gene/s in zebrafish. In the transition between assembly Zv8 and Zv9 of the zebrafish genome, first one and then a second putative *rbm24* ortholog was identified. The current assembly (Zv9) identifies a protein coding gene as *rbm24a* residing on chromosome 19 and also a novel annotation of a putative *rbm24b* protein coding gene residing on chromosome 16. To confirm the validity of these most recent changes to the genome annotation we compared these findings to our own comparative genomic analyses.

The first annotated *rbm24a* gene encodes a protein that displays strong similarity to the mouse Rbm24 (E-value = 3e-90; 188/237 (79%) amino acids). Using the mouse Rbm24 as a blastp query to search the NCBI RefSeq database of *D. rerio* proteins we detected strong similarity (E-value = 5e-61; 103/116 (88%)) to a hypothetical protein LOC562236 encoded by a gene (*zgc:136803*) on chromosome 16 (Zv8). This protein is now termed *rbm24b* in Zv9. The identification of these genes as *rbm24* orthologs is further supported by the identification of a pair of annotated *rbm24* paralogs in both the medaka (*Oryzias latipes*; chr. 11, 16) and pufferfish (*Tetraodon nigroviridis;* chr. 21 and 8) genomes. Zebrafish chromosome 19, where *rbm24a* resides, shares a common evolutionary origin with *O. latipes* chromosome 11 and *T. nigroviridis* chromosome 21 [11]. Similarly, chromosomes 16 and 8 in *O. latipes* and *T. nigroviridis*, respectively, map to the *rbm24b* region of chromosome 16 in *D. rerio*.

rbm24a and *rbm24b* display cardiovascular expression during embryogenesis

The spatial and temporal expression of both *rbm24* orthologs was determined using RNA *in situ* hybridization (ISH) (Figure 1). Both *rbm24* orthologs show cardiac expression early in development. At 15.5 hpf we detected *rbm24a* but not *rbm24b* expression in myocardial precursor cells (Figure 1B and 1C). By 24 hpf both

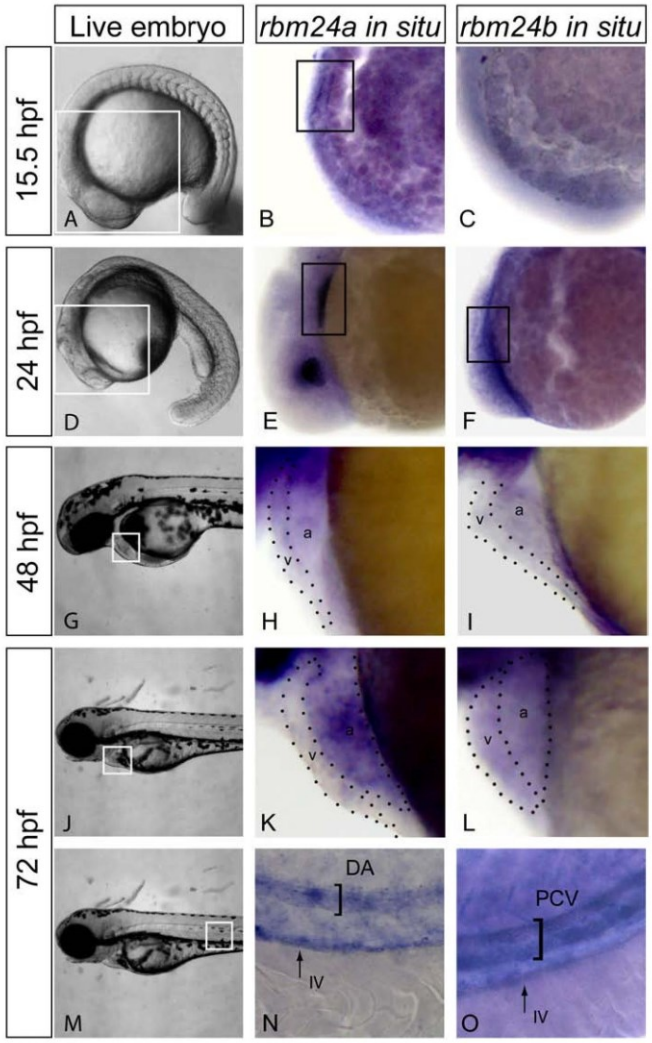

Figure 1 *rbm24a* and *rbm24b* display cardiovascular expression during embryogenesis. Expression of *rbm24* transcripts was evaluated in uninjected embryos fixed at 15.5, 24, 48 and 72 hpf. Live embryos 15.5 hpf with area of interest for rbm24 *in situ* boxed in white (A). Lateral heart views of *rbm24a* and *rbm24b in situs* on uninjected 15.5 hpf embryos showed expression linearly organized myocardial precursor cells for *rbm24a* (black box, B) but not *rbm24b* (C). Live embryos 24 hpf with area of interest for rbm24 *in situ* boxed in white (D). Lateral heart views of *rbm24a* and *rbm24b in situs* showed expression in the developing heart tube at 24 hpf (black box, E, F) with lens expression for *rbm24a* alone. 48 hpf live embryo showing the heart boxed in white (G). Lateral zoom of the heart showed *rbm24a* and *rbm24b* were expressed in the ventricle (v) and atrium (a) of the looped heart at 48 hpf (H, I). Live 72 hpf embryos with the heart boxed in white (J). Expression of both *rbm24* transcripts was detected in the heart at 72 hpf (K, L). Live image of a 72 hpf embryo with the area of interest for vascular expression boxed in white (M). Expression of both *rbm24* transcripts was detected in the trunk vasculature with differing expression patterns. *rbm24a* shows arterial expression in the DA (N) while *rbm24b* shows venous expression in the PCV (O) with both being expressed in the IV. DA, dorsal aorta; PCV, posterior caudal vein; IV, intestinal vasculature.

rbm24a and *rbm24b* expression was detected in the forming heart (Figure 1E and 1F). Expression of *rbm24a* was also detected in the lens of the eye. By 48 hpf, and continuing through 72 hpf, *rbm24a* and *rbm24b* exhibit broad expression throughout the heart, although expression of *rbm24a* was higher in the atrium than the ventricle. By contrast expression of *rbm24b* appeared uniformly expressed in both heart chambers (Figure 1I and 1L). These data are consistent with cardiac expression of the mouse *Rbm24* ortholog, and suggest incompletely overlapping requirements for *rbm24a* and *rbm24b* during zebrafish cardiac development.

By 72 hpf both *rbm24a* and *rbm24b* show incompletely overlapping vascular expression in addition to cardiac expression. *rbm24a* is expressed in the DA and intestinal vasculature (IV) while *rbm24b* is expressed in the PCV as well as the IV (Figure 1N and 1O). The early expression of both *rbm24a* and *rbm24b* in both the heart and vasculature suggests potentially important roles in cardiogenesis and vasculogenesis.

rbm24a and *rbm24b* are required for normal cardiac development

To determine the functional role of the *rbm24* orthologs in cardiac and vascular development, translation blocking morpholino antisense oligonucleotides (MO) were designed against the 5' UTR of each transcript. The effects of gene knockdown was assessed for each ortholog individually post microinjection of either MO into zebrafish embryos at the 1-2 cell stage. Titration experiments were conducted to determine MO quantities sufficient to induce a consistent phenotype in a majority of embryos injected (Additional File 1). Injection of 5 ng of *rbm24a* MO or 8 ng *rbm24b* MO resulted in a robust cardiac phenotype for a significant number of injected embryos at 48 hpf (64/67 and 59/62 respectively) (Table 1), compared to uninjected embryos (Figure 2A, B and 2D). During cardiogenesis the heart tubes of all affected morphant embryos failed to correctly loop, remaining linear but with distinct ventricular and atrial chambers (Figure 2). Affected embryos also exhibited reduced blood circulation, which led to cardiac edema in all cases by 48 hpf and continually worsened as development progressed (Additional File 2, 3, 4, 5, 6, 7, 8, 9, 10). A subset of *rbm24a* MO treated embryos (6/64) displayed an even more severe phenotype, lacking a distinct heart tube and exhibiting a beating focus of periodically contracting cells. This poorly organized cardiac structure was located ventral to the embryo between the embryo and the yolk suggesting a defect in the migration and organization of the cardiac fated cells. Similarly reduction of *rbm24a* or *rbm24b* expression using splice blocking morpholinos, designed against the second intron/exon boundary, also resulted in cardiac looping defects and cardiac edema in a majority of embryos (92.7% and 54.4% respectively) (Additional File 11). Knockdown efficiency was evaluated by RT-PCR for embryos displaying cardiac looping defects and cardiac edema after injection with splice blocking morpholino. Both rbm24a and rbm24b transcript levels were significantly reduced to 42.80% +/- 3.35, $P < 6.5 \times 10^{-4}$ and 40.27% +/- 3.19, $P < 4.4 \times 10^{-5}$ of transcript levels in respective uninjected controls (Additional File 12). We used translation blocking MO in all subsequent MO-based experiments due to their greater efficacy.

To confirm the phenotype observed in the *rbm24* morphants was not due to non-specific morpholino toxicity, embryos were co-injected with *p53* morpholino and *rbm24a* MO or *rbm24b* MO (Methods). The cardiac phenotypes remained unchanged in the presence of the *p53* morpholino (Additional File 13). We then performed phenotype rescue for both *rbm24* morphants to determine the sequence specificity of the observed morphant phenotypes. We generated full length capped poly-A RNA transcripts for each ortholog and co-injected each along with the respective *rbm24* MO, directed against the 5'UTR not present in the *in vitro* transcribed RNA. Rescue for *rbm24a* MO was achieved with 800 pg of RNA (36/45) while 50 pg of RNA was sufficient for *rbm24b* MO rescue (35/47). For both orthologs rescue resulted in properly looped hearts, normal systemic circulation and an absence of cardiac edema and by 72 hpf and continuing to 96 hpf (Figure 2F, H, J, K, M and 2P). Taken collectively, these data suggest the phenotype seen with each *rbm24* MO is a specific result of reduction in gene expression and support the inference from ISH expression data that both *rbm24* orthologs are required for normal cardiac development.

Depletion of *rbm24a* and *rbm24b* compromise cardiac myocardium development

To better evaluate the impact to the heart of reducing *rbm24a* or *rbm24b* we assayed the expression of several

Table 1 Number of embryos with cardiac defects in *rbm24* morphant and rescue conditions

Morpholino	Dosage	Embryos Studied	Looping Defects	Cardiac Edema	No Cardiac Organization
rbm24a MO	5 ng	67	58 (86.6%)	64 (95.5%)	6 (9%)
rbm24a rescue	+ 800 pg RNA	45	9 (20%)	9 (20%)	0
rbm24b MO	8 ng	62	59 (95.2%)	59 (95.2%)	0
rbm24b rescue	+ 50 pg RNA	47	12 (25.5%)	12 (25.5%)	0

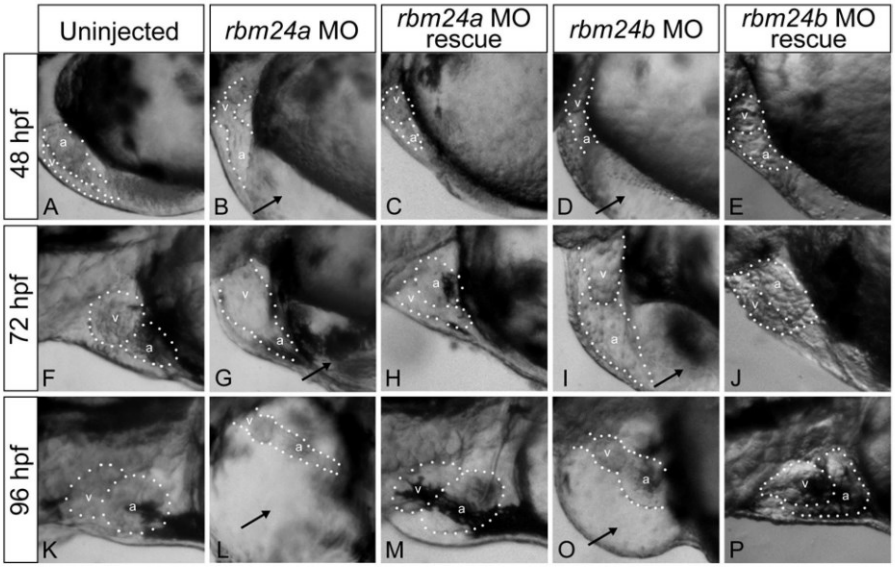

Figure 2 *rbm24a* and *rbm24b* are required for normal cardiac development. Translation blocking morpholinos complementary to *rbm24a* (5 ng) *or rbm24b* (8 ng) were injected into 1-2 cell stage zebrafish embryos and the resulting phenotypes were evaluated compared to uninjected controls at 48 hpf (A, B, D), 72 hpf (F,G,I), and 96 hpf (K, L, O). Lateral heart views are shown with a dotted outline around the heart chambers. Both morphant embryo conditions exhibited cardiac looping defects and edema at all stages. Heart chambers are shown with a dotted outline with chambers denoted: v, ventricle; a, atrium; black arrows, cardiac edema. Phenotype rescue was achieved for each *rbm24* via co-injection of each respective full length capped poly-A RNA transcript (*rbm24a* 800 pg, *rbm24b* 50 pg) along with the respective complementary translation blocking morpholino into 1-2 cell stage embryos where 800 pg *rbm24a* (C, H, M) or 50 pg *rbm24b* (E, J, P) achieved rescue. Rescued embryos posses looped hearts absent of edema.

key myocardial transcripts by ISH, including myosin light polypeptide 7, *myl7* (heart), myosin heavy polypeptide 6, *myh6* (atrium) and ventricular myosin heavy chain, *vmhc* (ventricle). Expression of each marker was evaluated in control (uninjected), *rbm24a* MO and *rbm24b* MO injected embryos fixed at 72 hpf at which point the zebrafish heart is normally, looped, fully developed and functioning, allowing us to comment in greater detail on the structural deficits contributing to the gross morphological morphant phenotypes. When examining the entire heart, both *rbm24a* and *rbm24b* morphant embryos exhibit strong *myl7* expression levels comparable to that of controls albeit within an unlooped heart tube. The hearts of controls by contrast are appropriately looped (Figure 3A - F). Additionally in *rbm24a* morphants defects of the presumptive atrium of the forming heart tube appear more severe than in the ventricular portion (Figure 3C and 3D). By contrast organization of the developing ventricle and atrium in *rbm24b* MO embryos appears equally compromised (Figure 3E and 3F). Expression of the atrial marker *myh6* for both *rbm24* morphants appears qualitatively similar to levels in uninjected controls. Presumptive atria of *rbm24a* morphant heart tubes appear linear and truncated, while to *rbm24b* morphants also have linear longer heart tubes, both contrasting with the looped atrium observed in uninjected controls (Figure 3G - L). These data are consistent with the observations that *rbm24a* expression was higher in the atrium than the ventricle by 72 hpf, contrasting with the more uniform expression observed for *rbm24b* across both heart chambers (Figure 1).

Both *rbm24* morphant conditions exhibited a near abrogation of the levels of the ventricular marker *vmhc* compared to strong expression in uninjected controls (Figure 3M - 3R). In *rbm24a* MO morphants expression of *vmhc* was faint but with expression clearly bounded to the heart tube with a clear ventricular portion; however, the expression uncharacteristically extended

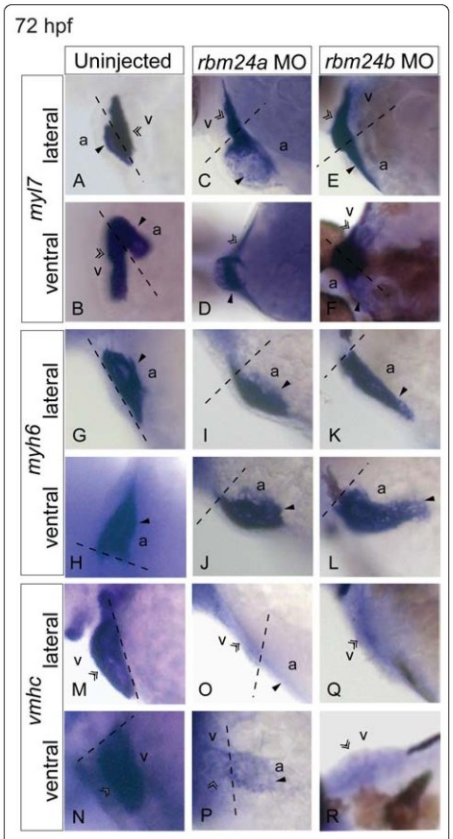

Figure 3 Depletion of *rbm24a* and *rbm24b* compromise cardiac myocardial development. The expression patterns of cardiac markers were analyzed in *rbm24* morphants and uninjected controls at 72 hpf. Ventral and lateral images of the heart are shown with a dotted line marking the boundary between heart chambers. By *myl7* expression of the entire heart, uninjected controls possess looped hearts with defined ventricle and atrium chambers (A, B) in contrast to unlooped hearts for both *rbm24* morphants. *rbm24a* morphants displayed linear presumptive ventricle and an incompletely formed presumptive atrium (C, D). *rbm24b* morphants displayed a linear presumptive atria and ventricle (E, F). *myh6* marking the atrium displayed a looped atrium in controls (G, H) with linear atrium in *rbm24a* (I, J), and *rbm24b* morphants (K, L). *vmhc* expression demarks looped ventricles in controls (M, N). *rbm24a* morphants displayed little expression bound to an unlooped heart tube where expression extends to the presumptive atrium (O, P). Almost no *vmhc* expression is detectable in *rbm24b* morphants (Q, R). v, ventricle region; double arrow, ventricular expression a, atrium region; solid black arrow, atrial expression.

beyond the ventricular portion into the presumptive atrium of the heart tube (Figure 3O and 3P). For *rbm24b* morphants *vmhc* expression was very diffuse and failed to clearly mark a ventricular boundary. These findings for *vmhc* expression were unexpected; both in the reduction of total expression seen for both *rbm24* morphants and the apparent stronger severity of the ventricular phenotype compared to the atrial phenotype for both *rbm24* morphants. Taken together the expression of these markers highlight the differential spatial impact of each *rbm24* ortholog in heart structure development of the myocardium, and is consistent with our previous gross morphological observations. These data indicate an incompletely overlapping role for *rbm24a* and *rbm24b* in heart tube formation and subsequent heart looping.

Edema in morphant embryos may have multiple origins

The observed cardiac edema may result from reduced circulation as a consequence of defects in heart structure, heart rate, aberrant vasculature or combinations of these factors. Given the observed structural defects, we additionally assayed heart rate as a potential contributor to cardiac edema in the *rbm24a* MO and *rbm24b* MO injected embryos [12]. Heart rate counts were determined for uninjected, *rbm24a* MO and *rbm24b* MO injected embryos (n = 50) at 48, 72 and 96 hpf. At 48 hpf both *rbm24a* and *rbm24b* morphants displayed significantly lower heart rate compared to uninjected controls ($P < 0.0002$) (Figure 4). Heart rates in *rbm24a* MO injected embryos remain significantly lower than uninjected controls at 72 hpf and 96 hpf. By contrast the heart rate of *rbm24b* MO injected embryos recovered such that it did not differ significantly from uninjected controls at 72 hpf and 96 hpf ($P > 0.12$) despite their continued structural anomalies. These data demonstrate cardiac edema is not ameliorated in *rbm24b* morphants despite heart rates increasing to normal levels, suggesting the role of other factors must be considered as contributing to compromised circulation. Although defects in structure and rates of contraction may contribute to compromised circulatory function, we posit that vascular disruption likely also plays a role in the resulting edema.

rbm24a and *rbm24b* are required for normal vasculogenesis with a potential role in early angiogenesis

To determine the functional role of *rbm24a* and *rbm24b* in vascular development we also undertook MO-based analyses of each ortholog in the TG(*kdrl*:G-RCFP) transgenic zebrafish reporter line which fluorescently marks all endothelial cells highlighting the forming cardiovascular structures [13]. Embryos were examined for vascular expression, after injection of *rbm24a* MO or *rbm24b* MO as described above, after heart formation and

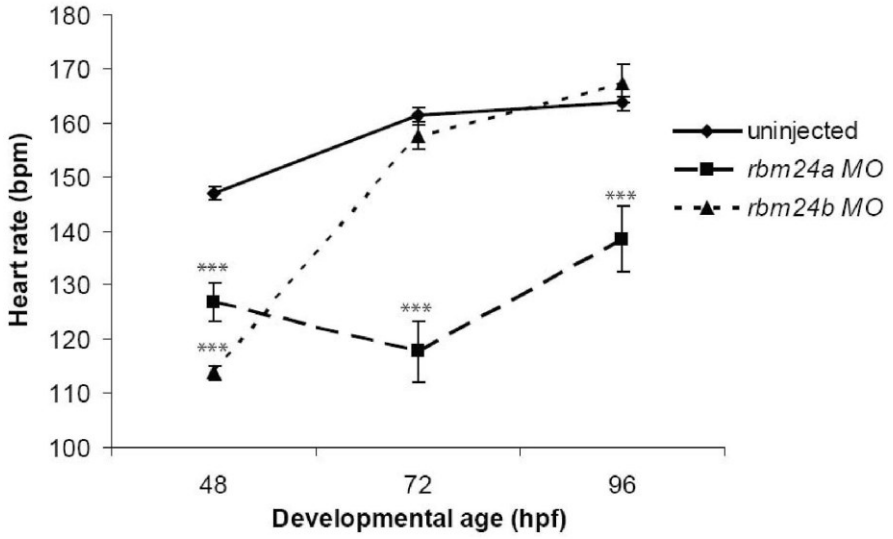

Figure 4 Slow heart rate may contribute to cardiac edema in *rbm24* morphants. Heart rates were determined for uninjected control, *rbm24a* and *rbm24b* morphant embryos at 48, 72 & 96 hpf and significance was ascribed from a t-test statistic. 50 embryos were examined for each condition at each time point. At all time-points the heart rate of *rbm24a* morphants was significantly lower than controls where $P < 2 \times 10^{-5}$. At 48 hpf *rbm24b* morphants had significantly lower heart rates than controls ($P = 1 \times 10^{-32}$). The heart rates for *rbm24b* morphants then rose to rates not different from controls by 72 hpf and 96 hpf ($P > 0.12$) while maintaining the features of the morphant phenotype. Error bars here are standard error. *** $P < 0.001$.

completion of vasculogenesis at 48 and 72 hpf (Figure 5). As per our earlier experiments, morphant embryos for both genes exhibit endocardial cardiac edema and a lack of heart looping displaying little to no circulation with 30/31 and 45/50 embryos displaying cardiac defects for *rbm24a* and *rbm24b* morphants respectively (Figure 5D - F and 5M - O). Additionally, all *rbm24a* and *rbm24b* morphant embryos display a reduction in total trunk vasculature and vascular organization in 100% of the embryos (Figure 5G - I and 5P - R); however vasculogenic and angiogenic vessels are disrupted to differing degrees. At 48 hpf *rbm24a* morphants posses a clearly present PCV appearing thicker than normal with no detectable DA or CV (Figure 5H). Angiogenesis is severely disrupted in these embryos with unpaired stunted dysmorphic Se also appearing thicker extending only to the midline of the embryo and thus a complete lack of DLAVs. By contrast the *rbm24b* morphant at 48 hpf shows little to no disruption of the DA, a visible but malformed CV and no detectable PCV (Figure 5 I). Unlike *rbm24a* morphants, *rbm24b* morphants have less disruption of angiogenesis. Se in *rbm24b* morphants display pairing at the posterior end of the embryo and extend dorsally the length of the embryo forming one DLAV; however, all these vessels are structurally dysmorphic. Both *rbm24a* and *rbm24b* vascular morphant phenotypes become progressively more severe between 48 hpf and 72 hpf. Vessels are less well organized and the number of vessels present is reduced, with no evidence of IV (Figure 5J - L and 5P - R). Of the morphant embryos displaying cardiac defects *rbm24a* and *rbm24b* morphants segregated into different classes of vascular defects, with 31/31 *rbm24a* morphants analyzed possessing disorganized trunk vasculature where Se do not extend the entire dorsal length of the embryo and the DA and CV are undetectable; and 50/50 *rbm24b* morphants had disorganized trunk vasculature where the Se formed DLAV and yet the PV was undetectable (Figure 5S and 5T). These data correlate with respective primary vascular expression locations of *rbm24a* of DA and *rbm24b* of PCV and both displaying expression in the IV (Figure 1G and 1H). When expression of *rbm24a* or *rbm24b* is compromised formation of the vessels required for the initial circulation loop is similarly

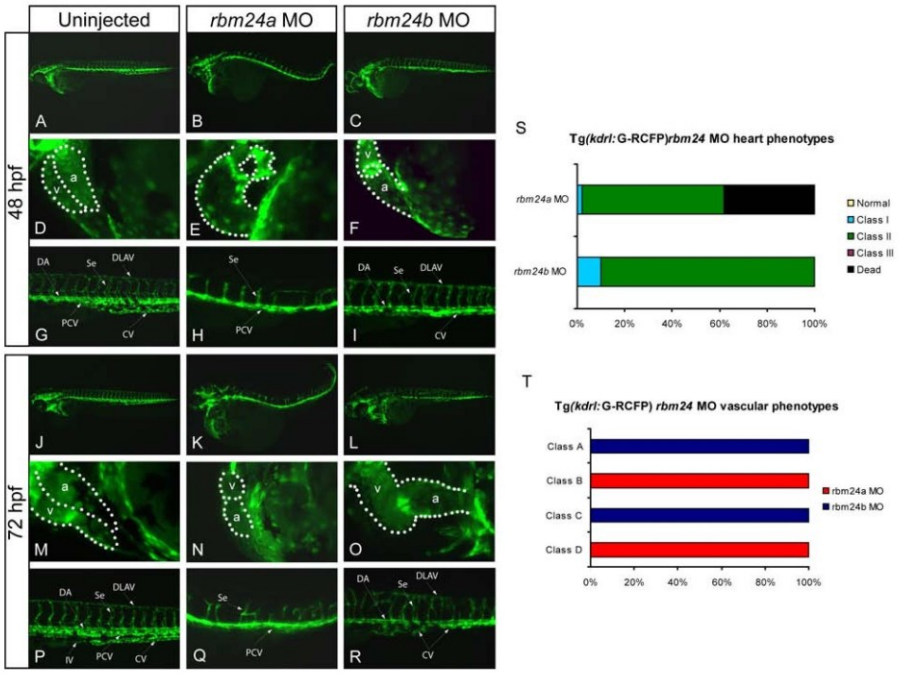

Figure 5 Reduction of *rbm24a* or *rbm24b* results in aberrant vasculature and a lack of vascular maintenance. TG(*kdrl*:G-RCFP) zebrafish line was used to asses the impact of *rbm24* depletion on vasculature at 48 hpf and 72 hpf. Lateral views are shown for whole embryo, heart and trunk with a dotted outline indicating heart chamber boundaries. Uninjected controls at all time-points display looped hearts and properly developed vasculature. (A, D, G, J, M, P). 48 hpf *rbm24a* morphants possess unlooped hearts but display only the PCV and stunted disorganized Se (B, E, H). 48 hpf *rbm24b* morphants possess unlooped hearts, and only the DA and CV are visible with disorganized Se (C, F, I). By 72 hpf there was increased vascular disorganization and degeneration and a lack of heart looping and in both *rbm24* morphants (K, N, L, O, Q, R). Cardiac morphant phenotypes are displayed quantitatively as percentages; Normal, looped beating heart with no cardiac edema; Class I, looped beating heart with cardiac edema. Class II, unlooped beating heart tube with cardiac edema, Class III, beating heart cell mass with cardiac edema; Dead, extreme cell death and degradation of embryo (S). Morphant vascular phenotype classes; Class A, disorganized trunk vasculature with formed DLAV; Class B, disorganized trunk vasculature with truncated Se and no DLAV; Class C, no discernable PCV; Class D, no discernable DA or CV (T). v, ventricle; a, atrium; DA, dorsal aorta; CV, caudal vein; PCV, posterior caudal vein; Se, intersegmental vessels, DLAV, dorsal longitudinal anastomotic vessels; IV, intestinal vasculature.

compromised, likely contributing significantly to the observed cardiac edema in morphant embryos. These findings indicate the endocardium is also compromised as a result of *rbm24* knockdown and also suggests that both *rbm24a* and *rbm24b* are independently necessary for normal early vascular development and support a putative role for *rbm24a* in angiogenesis.

rbm24a and *rbm24b* exhibit incompletely overlapping functions in zebrafish development

To determine whether *rbm24a* and *rbm24b* interact genetically in the developing zebrafish embryo, we injected low doses of both *rbm24a* and *rbm24b* MOs into the same embryo. Although each MO dosage amount was too low (2.5 ng and 4 ng respectively) to elicit a strong consistent phenotype alone as evidenced by titration experiments (Additional File 1), a much more severe phenotype resulted in the morphants receiving both MOs in concert (Figure 6). The double morphants displayed greater cardiac edema at 24 hpf than either morphant alone (Figure 6A - D). By 48 hpf, the double morphants also displayed very little cardiac organization, with most (73/93) failing to form any heart tube structure. No double morphants displayed

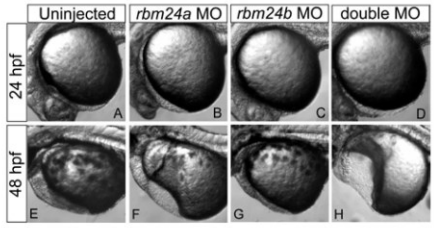

Figure 6 Double *rbm24a* and *rbm24b* morphants display more severe cardiac defects. Morpholinos directed to each *rbm24* ortholog were injected individually and in tandem into zebrafish embryos and assessed at 24 hpf and 48 hpf compared to uninjected embryo hearts (A and E). Individual morpholino injections were titrated to a low dose for both *rbm24a*, 2.5 ng (B and F) and *rbm24b*, 4ng (C and G). Embryos receiving low doses of both *rbm24a* and *rbm24b* morpholinos resulted in more severe phenotype than either low dose MO alone, exhibiting severe cardiac defects and increased edema (D and H).

any circulation (Figure 6E- H). This severe and distinctive phenotype exceeds that observed for either MO when assayed independently, even at the higher concentrations that yield consistent cardiac defects (5 ng of *rbm24a* MO or 8 ng *rbm24b* MO). These data support the possibility that roles for *rbm24* orthologs may overlap during cardiovascular development.

Discussion

Rbm24 is a novel cardiac gene candidate identified through transcript profiling of differentiating mESCs [5]. It was initially selected for functional analysis due to its early cardiac expression during mouse development, first detected by *in situ* hybridization in the cardiac crescent of mice, and subsequently in the heart tube and looping heart.

We integrated syntenic and sequence-based comparative genomic analyses to identify two *rbm24* orthologs in zebrafish, establishing that their expression was concordant with our earlier observations in mice. In the zebrafish embryo, a reduction of either *rbm24* ortholog expression by injection of morpholinos results in cardiac looping defects and reduced circulation. These embryos later exhibit cardiac edema and distention as early as 48 hpf, but this is likely a secondary effect of reduced *rbm24* expression, due instead to reduced circulation [14]. Our data suggests that reduced circulation is likely due to a reduction in critical vasculature and not simply reduced heart rate. Additionally, reduction of either *rbm24a* or *rbm24b* independently yielded vascular defects of both myocardium and endocardium. We exclude general toxicity or off target effects as the cause of the observed morphant phenotype by confirming they remain without amelioration in the presence of *p53* MO. We also confirmed the morphant phenotypes are sequence-specific by successfully achieving RNA-based phenotype rescue.

Investigation of molecular markers for myocardial development further illuminated the impact of reducing *rbm24* expression. Both *rbm24* orthologs are detected in the developing heart by *in situ* hybridization by 24 hpf and sustain expression at least through 72 hpf. In all cases a reduction of *rbm24a* or *rbm24b* was sufficient to prevent heart looping noted at 48 hpf and beyond, where normal heart looping occurs at approximately 36 hpf. Expression of *rbm24a* is unequal between the ventricle and atrium with stronger expression in the atrium while *rbm24b* shows equivalent expression in both chambers. This skewed expression of *rbm24a* at higher levels in the atrium is illustrated by truncated and abnormal atrium formation of the developing heart in *rbm24a* MO injected embryos demonstrating its requirement for cardiogenesis, including atrial specification, at this early stage. A reduction in either *rbm24* ortholog severely disrupts the expression level and localization of ventricular marker *vmhc* yielding little to no expression visible in either *rbm24* morphant condition. Reduced ventricular myocardial count disproportionate to the atrium has also been reported with deficient *nkx* and hedgehog signaling [15,16]. Although reduction of each *rbm24* results in incompletely overlapping atrial and ventricular phenotypes, reduction of either is sufficient to compromise the looping of the heart tube. The looping of the heart tube is a result of both genetic and biophysical mechanisms, and perturbation of the mechanical force generated by the contraction of the heart chambers can affect proper heart formation [17]. Zebrafish *wea* mutants (*myh6*), display distortions in cardiac looping, but still maintain a functional circulatory system due to the adaptation of the ventricle [18]. This suggests that reduction in *rbm24a* expression impacts both the ventricle and atrium, likely in the organization or structure of the muscle filaments, in addition to cardiomyocyte count, in turn affecting the ability of the heart to circulate blood.

Although both *rbm24a* MO and *rbm24b* MO injected embryos display an additional phenotype of aberrant vascular morphology, with defects in vasculogenesis and angiogenesis the defect in *rbm24a* morphants appears more severe. The observed phenotypes, however, are also consistent with the exhibited localization of each *rbm24* ortholog, wherein *rbm24a* is expressed in the DA and *rbm24b* is expressed in the PCV by 72 hpf. The expression difference likely reflects the acquisition of independent roles since duplication of the ancestral gene [19,20], resulting in incompletely overlapping functions for these orthologs in vasculogenesis. Angiogenesis

is impaired when expression of either *rbm24* ortholog is reduced. The integrity of these first vessesls of angiogenesis (Se and two DLAVs) deteriorates over time. In *rbm24a* morphants Se are more severely affected not reaching the dorsal line to form DLAVs at 48 hpf and continue to deteriorate by 72 hpf. This may result form the lack of any discernable DA. *rbm24b* morphants still possessed a visible DA but no PCV, Se and one DLAV were present and only displayed mild morphology alterations at 48 hpf with subsequent severe deterioration by 72 hpf. In the case of all *rbm24* morphants there is an inability to maintain the new vessels formed during angiogenesis and a wasting of any vessels resulting from vasculogenesis. It is unclear the molecular basis of this blood vessel deterioration. Normal *rbm24* expression may be playing a direct role in the vascular maintenance or the angiogenesis pathway. Also to be considered is that a lack of sufficient concentrations of growth factors and mitogens due to insufficient circulation may be preventing maintenance of initiated vasculature, since it has been shown Se sprouting and extension involves several rounds of cell division [21] and *vegfA* is required for vascular maintenance [22].

The incompletely overlapping role of *rbm24a* and *rbm24b* in the developing heart and vasculature is underscored by the extreme phenotype observed in the double morpholino injections. *rbm24a* and *rbm24b* appear to act in parallel in cardiac development, converging on a common phenotype for which they are both overtly required. By contrast in vasculogenesis, *rbm24a* and *rbm24b* appear to function in parallel but differentially in artery and vein formation, resulting in different vascular phenotypes which are individually sufficient to disrupt formation of the initial embryonic circulation loop. Further analyses will be required to determine the mechanistic role played by *rbm24a/b* and whether their roles involve one or all of the above-discussed mechanisms.

The critical role for *rbm24* in cardiogenesis raises the question whether mutations at the orthologous human locus may contribute to cardiac disorders. Interestingly, Wessels *et al.* recently identified a novel cardiac syndrome with noncompaction cardiomyopathy, bradycardia, pulmonary stenosis, atrial septal defects, and heterotaxy with genetic linkage to human chromosome 6p [23]. Genome-wide linkage analysis localized the implicated interval to chromosome 6p24.3-21.2, a region encompassing the human *RBM24* ortholog (6p22.3), making it an ideal candidate for variation underlying this phenotype. However, sequencing of all *RBM24* coding exons, intron/exon boundaries and the upstream promoter region in two affecteds, revealed only known polymorphisms (rs10456798 and rs35860841) that were also observed in a heterozygous state in an unaffected family member. While we can exclude a role for *RBM24* coding mutations, additional sequencing of putative regulatory sequences will be necessary to determine if *RBM24* may play a role in this syndrome.

Conclusion

Our data provide significant insight into the role of *rbm24* in formation of cardiac and vascular systems, however much remains to be learned about the exact mechanism by which it functions and the role *RBM24* may play in human disease. Other RRM containing proteins have also been shown to serve important roles in embryonic development [24,25] and post-transcriptional regulation is a frequent theme. With this in mind, we hypothesize that the protein plays a role in the post-transcriptional regulation of gene expression important for cardiac and vascular development. In the case of *rbm24a and rbm24b* depletion for instance, we found that expression of the ventricular marker *vmhc* is nearly abolished in the heart at 72 hpf, suggesting they both may contribute to specific regulation of *vmhc* mRNA. We will continue elucidate the role and mechanisms of *rbm24* function in embryonic development. Furthermore, this study demonstrates the power of the screen that uncovered *Rbm24* as a candidate cardiac gene, adding significant value to the original data set for which this work represents just the first of many such analyses awaiting completion.

Methods

Zebrafish maintenance

Adult AB zebrafish were maintained in system water according to standard methods [26]. Embryos were obtained from natural mating of adult fish. All experiments were in accordance with ethical permits by Johns Hopkins Animal Care and Use Committee under protocol number FI10M369.

Bioinformatic identification of zebrafish rbm24 orthologs

We used the amino acid sequence of the protein encoded by the mouse *Rbm24* gene to perform a blastp query searching the NCBI RefSeq database of *D. rerio* proteins from the Zv8 2008 genome assembly. Two genes were identified (*rbm24* and *zgc:136803*) which encode proteins displaying strong similarity to the mouse Rbm24 protein (E-value = 5e-61; 103/116 (88%) and E-value = 3e-90; 188/237 (79%), respectively). As of the Zv9 2010 *D. rerio* genome assembly NCBI RefSeq now annotates the two genes we previously identified as two *rbm24* paralogs with protein coding transcripts: *rbm24a* on chromosome 19 (RefSeq ID: NM_212865) and *rbm24b* on chromosome 16 (RefSeq ID: NM_001039925).

Nucleic Acid in situ hybridization

Total RNA was isolated from whole zebrafish embryos at 24 hpf using **TRIzol** Reagent and total cDNA was

generated with oligo-dT using the SuperScript III First-Strand Synthesis Kit (Invitrogen). Riboprobes for *rbm24a*, *rbm24b*, *myl7*, *myh6*, and *vmhc* were generated by PCR amplification of embryo cDNA. PCR fragments were TOPO cloned into PCRII vector (TA Cloning Kit Dual Promoter with pCRII vector, Invitrogen) and transformed into TOP 10 Cells (Invitrogen). Colonies were mini cultured and plasmid DNA was harvested using the QIAprep Spin Miniprep Kit (Qiagen) Digoxygenin-labeled riboprobes were synthesized from 1 μg plasmid DNA using Sp6 and T7 RNA Polymerase (DIG RNA Labeling Kit SP6/T7, Roche), and purified (SigmaSpin Colums, Sigma). Embryos for *in situ* hybridization at 48 hpf and older were treated with 0.003% 1-phenyl-2-thiourea (PTU) beginning at 48 hpf to reduce pigmentation. Embryos were fixed in 4% paraformaldehyde in PBS overnight at 4°C at 15.5 hpf, 24 hpf, 48 hpf, and 72 hpf; and *in situ* hybridization was performed as previously described [27].

Morpholino design and injection

Antisense morpholinos for *rbm24a* and *rbm24b* were designed and provided by Gene Tools, LLC. The *rbm24a* translation blocking morpholino (5'-TGCATCCTCACGAAACGCTCAAGTG-3') and the *rbm24b* translation blocking morpholino (5'-AAATAAACTCCTTGCTCCTTGAAGG-3') were designed to hybridize to the 5' UTR immediately upstream of the translational start site. Morpholinos were diluted with dH_2O to 20 ng/nL and titration experiments were conducted at 1, 2, 5 and 10 ng *rbm24a* MO and 1, 2.5, 5, 7 and 9 ng *rbm24b* MO to determine an effective dose (n = 100 embryos per concentration). Experimental concentrations of 5 ng *rbm24a* or 8 ng *rbm24b* MO were selected and injected into the yolks of 1-2 cell fertilized embryos (n = 75). Double knockdown experiments were conducted with co-injection of 2.5 ng *rbm24a* and 4 ng *rbm24b* translation blocking MO into embryos and compared to embryos injected with these amounts of either MO alone. The *rbm24a* splice blocking MO (5' CGTTATTTGAGATGCCTGACTGTT 3') and the *rbm24b* splice blocking MO (5' TATTTTGACGTTATTTACCTGGCTG 3') were designed to hybridize to the boundary of the second exon and second intron of the transcript and injected at 7.5 ng and 9 ng respectively. Antisense *p53* MO (5'-GCGCCATTGCTTTGCAAGAATTG-3') previously published [28] was purchased from Gene Tools, LLC and 1 ng was injected into 1-2 cell stage fertilized embryos both with and without each *rbm24* translation blocking MO (n = 50) [29]. Embryos were analyzed for cardiac and vascular phenotypes at 48, 72 and 96 hpf.

RT-PCR to determine transcript knock down efficiency

Total RNA was isolated using **TRIzol** Reagent (Invitrogen) from whole morphant zebrafish embryos at 24 hpf after injection of either 7.5 ng *rbm24a* or 9 ng *rbm24b* splice blocking MO. Total cDNA was generated with oligo-dT using SuperScript III First-Strand Synthesis (Invitrogen). RT-PCR was carried out via the standard curve method on a Bio-Rad DNA Engine Opticon 2 Real-Time Detection System with primers specific to the correctly spliced transcripts at 100 ng input cDNA. Uninjected 24 hpf embryo cDNA was used to generate a standard curve and cDNA from uninjected experimental control embryos was assayed at 100 ng cDNA as the standard for 100% expression. All reactions were run in triplicate at 25 μL volumes using Power Sybr Green PCR Master Mix (1x final) (Applied Biosystems), primers at final concentration 0.08 μM each. Significance of expression reduction was determined using the students t-test statistic comparing transcript levels of *rbm24a* or *rbm24b* in uninjected controls to that measured cDNA from their respective morphants.

rbm24 MO phenotype rescue

Total RNA was isolated from whole zebrafish embryos 24 hpf using **TRIzol** Reagent (Invitrogen) and total cDNA was generated with oligo-dT using SuperScript III First-Strand Synthesis (Invitrogen). Full length *rbm24a* and *rbm24b* cDNA were PCR amplified and cloned into the pCR8 gateway vector (pCR8GW/TOPO TA Cloning Kit, Invitrogen) before being cloned into the pCSDEST destination vector (kindly provided by the lab of Nathan Lawson, UMass Med School). Full length sense capped Poly-A RNA was generated for *rbm24a* and *rbm24b* with the **mMESSAGE** mMACHINE kit (Ambion) and quantified with a NanoDrop 1000. Full length RNA was co-injected into 1-2 cell embryos with *rbm24a* MO or *rbm24b* MO at titrating levels and evaluated for phenotype rescue at 48, 72 and 96 hpf. Rescue was confirmed with 800 pg *rbm24a* RNA and 50 pg *rbm24b* RNA.

Sequence analysis

Genomic DNA from two patients and an unaffected family member were included [23]. Direct sequencing of part of the promoter region (1031 bp), all exons plus exon-intron boundaries and a putative regulatory element in intron 3 (1164 bp) of the *RBM24* gene was undertaken. Primers were designed to cover all four exons representing the "canonical" sequence (ENST00000379052, transcript length 2,458 bp and 236 aa, http://www.ensembl.org). PCR primers were designed by Primer3 software http://frodo.wi.mit.edu/cgi-bin/primer3/primer3.cgi and are available on request. Amplified PCR products were purified and sequenced using BigDye Terminator chemistry v3.1 on an ABI Prism 3130*xl* genetic analyzer (Applied Biosystems). Biomedical research involving human subjects

has been performed according to the principles of the Helsinki's Declaration. Written informed consents were obtained from the patients and relatives involved in the research. Genomic DNA was taken from patients as per standard care and therefore ethical approval was not required.

Heart Rate counts

Heart rates (beats per minute) were counted for uninjected, *rbm24a* MO and *rbm24b* MO injected embryos displaying the morphant phenotype at 48, 72 and 96 hpf. 50 embryos were analyzed per condition per time point. Average heart rates with standard error were plotted and significant heart rate deviation of morphants compared to uninjected controls was determined using the students t-test.

Fluorescent vascular imaging

The transgenic zebrafish line TG(*kdrl*:G-RCFP) generated by Cross and colleagues [13] was used for vascular expression. Adult fish and embryos were maintained as described [26]. Embryos were injected with either 5 ng *rbm24a* MO or 8 ng *rbm24b* MO at the 1-2 cell stage and analyzed at 48 and 72 hpf for G-RCFP expression via fluorescence microscopy.

Additional material

Additional file 1: Translation Blocking MO titrations. Quantitative representation of percentage of embryos displaying cardiac phenotypes achieved from MO titrations. *rbm24a* MO 1, 2, 5 and 10 ng injected (A). *rbm24b* MO 1, 2.5, 5, 7 and 9 ng (B). Normal, looped beating heart with no cardiac edema; Class I, looped beating heart with cardiac edema; Class II, unlooped beating heart tube with cardiac edema; Class III, beating heart cell mass with cardiac edema; Dead, extreme cell death and degradation of embryo. n = 100 embryos per concentration.

Additional file 2: Uninjected zebrafish heart 48 hpf. Digital video (time-lapse) captured of an uninjected control embryo (lateral) at 48 hpf. Movie demonstrates the looped structure and regular rhythm of the normal heart.

Additional file 3: *rbm24a* MO injected zebrafish heart 48 hpf. Digital video (time-lapse) captured of an *rbm24a* MO injected embryo (lateral) at 48 hpf. Movie highlights the unlooped (linear) structure of the *rbm24a* morphant heart displaying edema at this stage in development. Atrial and ventricular chambers are still evident despite structural anomaly; however contraction is slow.

Additional file 4: *rbm24b* MO injected zebrafish heart 48 hpf. Digital video (time-lapse) captured of an *rbm24b* MO injected embryo (lateral) at 48 hpf. Movie highlights the unlooped (linear) structure of the *rbm24b* morphant heart displaying edema at this stage in development. Atrial and ventricular chambers are still evident despite structural anomaly.

Additional file 5: Uninjected zebrafish heart 72 hpf. Digital video (time-lapse) captured of an uninjected control embryo (lateral) at 72 hpf. Movie demonstrates the looped structure and regular rhythm of the normal heart, with circulation at this stage in development.

Additional file 6: *rbm24a* MO injected zebrafish heart 72 hpf. Digital video (time-lapse) captured of an *rbm24a* MO injected embryo (lateral) at 72 hpf. Movie highlights the unlooped (linear) structure of the *rbm24a* morphant heart at this stage in development with cardiac edema. Heart atrial and ventricular chambers are difficult to distinguish and contracting with marked irregularity, with no circulation is detectable.

Additional file 7: *rbm24b* MO injected zebrafish heart 72 hpf. Digital video (time-lapse) captured of an *rbm24b* MO injected embryo (lateral) at 72 hpf. Movie highlights the unlooped (linear) structure of the *rbm24b* morphant heart at this stage in development with additional cardiac edema. Atrial and ventricular chambers are still evident but highly distended, with no circulation is detectable.

Additional file 8: Uninjected zebrafish heart 96 hpf. Digital video (time-lapse) captured of an uninjected control embryo (lateral) at 96 hpf. Movie demonstrates the looped structure and regular rhythm of the normal heart, with circulation at this stage in development.

Additional file 9: *rbm24a* MO injected zebrafish heart 96 hpf. Digital video (time-lapse) captured of an *rbm24a* MO injected embryo (lateral) at 96 hpf. Movie highlights the unlooped (linear) structure of the *rbm24a* morphant heart at this stage in development with extreme cardiac edema. Heart atrial and ventricular chambers are difficult to distinguish and contracting with marked irregularity, with no circulation is detectable.

Additional file 10: *rbm24b* MO injected zebrafish heart 96 hpf. Digital video (time-lapse) captured of severe example of one *rbm24b* MO injected embryo (lateral) at 96 hpf. Movie highlights the phenotype of the unlooped (linear) highly distended heart of *rbm24b* morphants at this stage in development, with no detectable circulation. The heart with distinct atrial and ventricular chambers is highly distended and contracting with marked irregularity, with no circulation is detectable.

Additional file 11: *rbm24a* and *rbm24b* splice blocked morphants display cardiac defects. Injection of 7.5 ng of *rbm24a* splice blocking morpholino results in a substantial reduction of full-length transcript (A). Injection of 9 ng of *rbm24b* splice blocking morpholino results in aberrant splicing of the transcript. There is a reduction of full-length transcript 250 bp fragment and appearance of trace amounts of the shortened frameshift fragment 164 bp and shortened in-frame transcript 109 bp (B). RT-PCR measurement of transcript levels show both *rbm24a* (42.80% +/- 3.35, $P < 6.5 \times 10^{-4}$) and *rbm24b* (40.27 +/- 3.19, $P < 4.4 \times 10^{-5}$) morphants have significant reduction of transcript levels compared to uninjected controls (C) Error bars are standard deviation, *** $P < 0.001$.

Additional file 12: Supplemental Table 1. Cardiac phenotypes displayed upon knockdown of *rbm24a* or *rbm24b* expression via splice blocking morpholino.

Additional file 13: *p53 MO* co-injection does not alter *rbm24a* and *rbm24* morphant phenotypes. Phenotypes were evaluated for embryos post injection *rbm24a* MO (5 ng) *or rbm24b* MO (8 ng) alone or in conjunction with *p53* MO (1 ng) phenotypes were compared at 48, 72 & 96 hpf. Lateral heart views are shown with a dotted outline around embryo heart chambers. No cardiac phenotype is detected for *p53* MO embryos compared to uninjected controls at any time point (A-B, G, H, M, N). At all time points *rbm24a* morphants maintain unlooped hearts and display cardiac edema in the presence of *p53* MO (C, D, I, J, O, P). Morphant phenotype was also maintained between *rbm24b* morphants in the presence of *p53* MO (E, F, K, L, Q, R). v, ventricle; a, atrium; black arrows, cardiac edema.

Abbreviations

DA: dorsal aorta; PCV: posterior caudal vein; CV: caudal vein; hpf: hours post fertilization; RRM: RNA recognition motif; MO: morpholino antisense oligonucleotide; ISH: in situ hybridization; Se: intersegmetal vessels; DLAVs: dorsal longitudinal anastomotic vessels.

Acknowledgements

This study was supported by a grant from the MSCRF (2007-MSCRFE-0205) to ASM and the Johns Hopkins University Institute for Cell Engineering to JDG. SM is supported by funds from the National Institute of Standards and Technology. We thank Colin Huck and the Johns Hopkins FINZ Center for zebrafish husbandry and technical support.

Author details
[1]Biochemical Science Division, National Institute of Standards and Technology, Gaithersburg, MD 20899, USA. [2]McKusick-Nathans Institute of Genetic Medicine, Johns Hopkins University School of Medicine, Baltimore, MD, 21205, USA. [3]CBG Department of Clinical Genetics, Erasmus Medical Centre, 3016 AH Rotterdam, The Netherlands. [4]Department of Genetics and Bioinformatics Research Center, North Carolina State University, Raleigh, NC, 27695-7566, USA. [5]Institute for Regenerative Medicine, University of Pennsylvania, Philadelphia, PA 19104, USA. [6]Department of Cell and Developmental Biology, University of Pennsylvania, Philadelphia, PA 19104, USA. [7]Department of Molecular and Comparative Pathobiology, Johns Hopkins University School of Medicine, Baltimore MD, 21205, USA.

Authors' contributions
SM and RM carried out *in situ* hybridization, morpholino analysis, experimental design and drafted the manuscript, while RM also designed antisense morpholinos. SM additionally conducted heart rate experiments, vascular experiments and assembled the figures and manuscript draft. SB carried out microinjections. DM contributed to *in situ* hybridization experimental data. MW, BD and AB conducted human RBM24 sequencing experiments on patient samples. ES, JG and SF provided intellectual input and experimental expertise. AM edited the manuscript, provided continuous experimental design, intellectual input and experimental expertise. All authors read and approve the final manuscript.

Received: 8 May 2011 Accepted: 19 October 2011
Published: 19 October 2011

References

1. Lints TJ, Parsons LM, Hartley L, Lyons I, Harvey RP: **Nkx-2.5: a novel murine homeobox gene expressed in early heart progenitor cells and their myogenic descendants.** *Development* 1993, **119**:969.
2. Stainier DY, Fouquet B, Chen JN, Warren KS, Weinstein BM, Meiler SE, Mohideen MA, Neuhauss SC, Solnica-Krezel L, Schier AF, *et al*: **Mutations affecting the formation and function of the cardiovascular system in the zebrafish embryo.** *Development* 1996, **123**:285-92.
3. Evans SM, Yelon D, Conlon FL, Kirby ML: **Myocardial lineage development.** *Circ Res* 2010, **107**:1428-44.
4. Stainier DY: **Zebrafish genetics and vertebrate heart formation.** *Nat Rev Genet* 2001, **2**:39-48.
5. Miller RA, Christoforou N, Pevsner J, McCallion AS, Gearhart JD: **Efficient array-based identification of novel cardiac genes through differentiation of mouse ESCs.** *PLoS ONE* 2008, **3**:e2176.
6. Finn RD, Mistry J, Schuster-Bockler B, Griffiths-Jones S, Hollich V, Lassmann T, Moxon S, Marshall M, Khanna A, Durbin R, *et al*: **Pfam: clans, web tools and services.** *Nucleic Acids Res* 2006, **34**:D247-51.
7. Oubridge C, Ito N, Evans PR, Teo CH, Nagai K: **Crystal structure at 1.92 A resolution of the RNA-binding domain of the U1A spliceosomal protein complexed with an RNA hairpin.** *Nature* 1994, **372**:432-8.
8. Auweter SD, Oberstrass FC, Allain FH: **Sequence-specific binding of single-stranded RNA: is there a code for recognition?** *Nucleic Acids Res* 2006, **34**:4943-59.
9. Ellertsdottir E, Lenard A, Blum Y, Krudewig A, Herwig L, Affolter M, Belting HG: **Vascular morphogenesis in the zebrafish embryo.** *Dev Biol* 2010, **341**:56-65.
10. Isogai S, Horiguchi M, Weinstein BM: **The vascular anatomy of the developing zebrafish: an atlas of embryonic and early larval development.** *Dev Biol* 2001, **230**:278-301.
11. Kasahara M, Naruse K, Sasaki S, Nakatani Y, Qu W, Ahsan B, Yamada T, Nagayasu Y, Doi K, Kasai Y, *et al*: **The medaka draft genome and insights into vertebrate genome evolution.** *Nature* 2007, **447**:714-9.
12. Baker K, Warren KS, Yellen G, Fishman MC: **Defective "pacemaker" current (Ih) in a zebrafish mutant with a slow heart rate.** *Proc Natl Acad Sci USA* 1997, **94**:4554-9.
13. Cross LM, Cook MA, Lin S, Chen JN, Rubinstein AL: **Rapid analysis of angiogenesis drugs in a live fluorescent zebrafish assay.** *Arterioscler Thromb Vasc Biol* 2003, **23**:911-2.
14. Mitchell IC, Brown TS, Terada LS, Amatruda JF, Nwariaku FE: **Effect of vascular cadherin knockdown on zebrafish vasculature during development.** *PLoS One* 2010, **5**:e8807.
15. Targoff KL, Schell T, Yelon D: **Nkx genes regulate heart tube extension and exert differential effects on ventricular and atrial cell number.** *Dev Biol* 2008, **322**:314-21.
16. Thomas NA, Koudijs M, van Eeden FJ, Joyner AL, Yelon D: **Hedgehog signaling plays a cell-autonomous role in maximizing cardiac developmental potential.** *Development* 2008, **135**:3789-99.
17. Taber LA: **Biophysical mechanisms of cardiac looping.** *Int J Dev Biol* 2006, **50**:323-32.
18. Berdougo E, Coleman H, Lee DH, Stainier DY, Yelon D: **Mutation of weak atrium/atrial myosin heavy chain disrupts atrial function and influences ventricular morphogenesis in zebrafish.** *Development* 2003, **130**:6121-9.
19. Ekker M, Wegner J, Akimenko MA, Westerfield M: **Coordinate embryonic expression of three zebrafish engrailed genes.** *Development* 1992, **116**:1001-10.
20. Kleinjan DA, Bancewicz RM, Gautier P, Dahm R, Schonthaler HB, Damante G, Seawright A, Hever AM, Yeyati PL, van Heyningen V, *et al*: **Subfunctionalization of duplicated zebrafish pax6 genes by cis-regulatory divergence.** *PLoS Genet* 2008, **4**:e29.
21. Blum Y, Belting HG, Ellertsdottir E, Herwig L, Luders F, Affolter M: **Complex cell rearrangements during intersegmental vessel sprouting and vessel fusion in the zebrafish embryo.** *Dev Biol* 2008, **316**:312-22.
22. Bahary N, Goishi K, Stuckenholz C, Weber G, Leblanc J, Schafer CA, Berman SS, Klagsbrun M, Zon LI: **Duplicate VegfA genes and orthologues of the KDR receptor tyrosine kinase family mediate vascular development in the zebrafish.** *Blood* 2007, **110**:3627-36.
23. Wessels MW, De Graaf BM, Cohen-Overbeek TE, Spitaels SE, de Groot-de Laat LE, Ten Cate FJ, Frohn-Mulder IF, de Krijger R, Bartelings MM, Essed N, *et al*: **A new syndrome with noncompaction cardiomyopathy, bradycardia, pulmonary stenosis, atrial septal defect and heterotaxy with suggestive linkage to chromosome 6p.** *Hum Genet* 2008, **122**:595-603.
24. Anyanful A, Ono K, Johnsen RC, Ly H, Jensen V, Baillie DL, Ono S: **The RNA-binding protein SUP-12 controls muscle-specific splicing of the ADF/cofilin pre-mRNA in C. elegans.** *J Cell Biol* 2004, **167**:639-47.
25. Markus MA, Morris BJ: **Lark is the splicing factor RBM4 and exhibits unique subnuclear localization properties.** *DNA Cell Biol* 2006, **25**:457-64.
26. Westerfield M: **The Zebrafish Book. A Guide for the Laboratory Use of Zebrafish (Danio rerio).** Eugene, OR: University of Oregon Press;, 3 1995.
27. Miller-Bertoglio VE, Fisher S, Sanchez A, Mullins MC, Halpern ME: **Differential regulation of chordin expression domains in mutant zebrafish.** *Dev Biol* 1997, **192**:537-50.
28. Langheinrich U, Hennen E, Stott G, Vacun G: **Zebrafish as a model organism for the identification and characterization of drugs and genes affecting p53 signaling.** *Curr Biol* 2002, **12**:2023-8.
29. Robu ME, Larson JD, Nasevicius A, Beiraghi S, Brenner C, Farber SA, Ekker SC: **p53 activation by knockdown technologies.** *PLoS Genet* 2007, **3**:e78.

doi:10.1186/1471-213X-11-62
Cite this article as: Maragh *et al.*: Identification of RNA binding motif proteins essential for cardiovascular development. *BMC Developmental Biology* 2011 **11**:62.

Curriculum vitae

S A M A N T H A D E N I S E M A R A G H

smaragh@loyola.edu

8816 Bluebird Trace
Laurel, MD 20723

Mobile: 301.266.8396

EDUCATION

Johns Hopkins Medical Institutions Baltimore, MD Sept. 2008 – Present
McKusick-Nathans Institute of Genetic Medicine

- **Doctoral Candidate** : Human Genetics and Molecular Biology (expected completion May 2014)
- **Dissertation:** RBM24 is essential for normal early embryonic development

Johns Hopkins University Baltimore, MD May 2008

- **Master of Science**: Biotechnology, concentration Molecular Targets & Drug Discovery
  Summa Cum Laude GPA: 3.94

Loyola College Baltimore, MD May 2005

- **Bachelor of Science**: Biology, specialization in Cellular and Molecular Biology, Chemistry Minor
  Cum Laude; Overall GPA: 3.63 Biology GPA: 3.93

Dissertation related research experience

2008-present. John Hopkins University School of Medicine. Baltimore, MD.

- Thesis advisor: Dr. Andrew S. McCallion.
- The goal of my research was to functionally evaluate the role of the gene RBM24 in early cardiovascular and skeletal muscle development using a zebrafish model system.
- I confirmed the presence of two RBM24 homologs in zebrafish and determined these homologs to be expressed in the developing cardiovascular system and skeletal muscle precursors.
- I conducted functional studies on the zebrafish RBM24 homologs by morpholino knockdown experiments in zebrafish and found both homologs to be essential for normal cardiovascular, somite and craniofacial development using in vivo and in vitro imaging and staining techniques.
- I conducted an analysis of Notch-signaling pathway components required for normal skeletal muscle development and found evidence that both zebrafish RBM24 may be required for post-transcriptional processing of dlc and dld Notch lignand transcripts.

WORK EXPERIENCE

National Institute of Standards and Technology (NIST) – Scientist Gaithersburg, MD May 2006-Present
Biochemical Sciences Division; DNA Science Group; NCI/NIST Biomarker Reference Laboratory

- Part of the National Cancer Institute's Early Detection Research Network (NCI EDRN)
- Contract position held by SAIC was rolled over into a government position Scientist. See job description below.

SAIC San, Diego, CA Aug 2005 – April 2006
(Formerly employed by **GEO-CENTERS Inc.** Newton, MA merger acquisition by SAIC 10/7/05)

Life Scientist II -Working at NIST
Contract Assignment:
National Institute of Standards and Technology (NIST) Gaithersburg, MD
Biochemical Sciences Division
DNA Science Group
Part of the National Cancer Institute's Early Detection Research Network

NCI/NIST Biomarker Reference Laboratory (NCI EDRN)

General Statement of Duties
Responsible for molecular biological research involved in cancer biomarker validation for the Early Detection Research Network project; organizing and operation of assigned laboratory equipment and for collecting and summarizing experiment or test data and perform other duties as required following established methods and procedures.

Duties and Responsibilities
- Adapt protocols techniques and procedures as necessary as dictated by differences in samples, condition, or new technology.
- DNA , RNA and protein based assay development involving cancer biomarkers.
- Responsible for working from supplied samples to isolate DNA, RNA, and protein.
- Sequence and genotype DNA using high throughput technologies.
- Use high throughput instruments including array chips, genetic analyzers, and robotic stations to develop and complete validation projects.
- Conduct gene cloning and sequencing; DNA probe labeling and purification.
- Analyze data for trends and statistical value.
- Compile and organize raw and analyzed data into presentation form.
- Manuscript preparation of research from validation projects to be submitted to scientific journals.
- Collection, analysis and interpretation of study data; assistance in the preparation of protocols and laboratory reports, presentation of findings or results; maintaining and updating detailed laboratory notes or recordings.
- Attend and present research via talks and posters at scientific meetings, conferences and seminars.
- Develop a good working relationship with the research community and the private sector involved in these studies.

PRESENTATIONS

"rbm24a and rbm24b are required for normal somitogenesis and craniofacial development and are essential for Notch signaling" Annual ASHG Meeting: San Francisco, CA 11/6-11/10/12. Nov 10, 2012- poster

"Multiple strand displacement amplification of mitochondrial DNA from clinical samples" Annual AACR Meeting: San Diego, CA 4/11-4/16/08. Apr 15, 2008- poster.

"Mitochondrial genome deletion aids in the identification of false and true negative prostate needle core biopsies" EDRN 5th Scientific Meeting: Bethesda, MD 3/17-19/08. Mar 18, 2008- poster.

"Biomarker Research and Validation at NIST" NCI/EDRN 15th Annual Steering Committee Meeting: Ann Arbor, MI, 9/17-19/07. Sept.18, 2007- invited talk.

. PUBLICAITONS

Burzynski GM, Reed X, Maragh S, Matsui T, McCallion AS. **Integration of genomic and functional approaches reveals enhancers at LMX1A and LMX1B.** Mol Genet Genomics. 2013 Nov;288(11):579-89. doi: 10.1007/s00438-013-0771-7. Epub 2013 Aug 13.

Sosa MX, Sivakumar IK, Maragh S, Veeramachaneni V, Hariharan R, Parulekar M, Fredrikson KM, Harkins TT, Lin J, Feldman AB, Tata P, Ehret GB, Chakravarti A. **Next-generation sequencing of**

human mitochondrial reference genomes uncovers high heteroplasmy frequency. PLoS Comput Biol. 2012;8(10):e1002737. doi: 10.1371/journal.pcbi.1002737. Epub 2012 Oct 25.

Doyle AJ, Doyle JJ, Bessling SL, Maragh S, Lindsay ME, Schepers D, Gillis E, Mortier G, Homfray T, Sauls K, Norris RA, Huso ND, Leahy D, Mohr DW, Caulfield MJ, Scott AF, Destrée A, Hennekam RC, Arn PH, Curry CJ, Van Laer L, McCallion AS, Loeys BL, Dietz HC. **Mutations in the TGF-β repressor SKI cause Shprintzen-Goldberg syndrome with aortic aneurysm.** Nat Genet. 2012 Nov;44(11):1249-54. doi: 10.1038/ng.2421. Epub 2012 Sep 30.

Maragh S, Miller RA, Bessling SL, McGaughey DM, Wessels MW, de Graaf B, Stone EA, Bertoli-Avella AM, Gearhart JD, Fisher S, McCallion AS. **Identification of RNA binding motif proteins essential for cardiovascular development.** BMC Dev Biol. 2011 Oct 19;11:62. doi: 10.1186/1471-213X-11-62.

Taher L, McGaughey DM, Maragh S, Aneas I, Bessling SL, Miller W, Nobrega MA, McCallion AS, Ovcharenko I. **Genome-wide identification of conserved regulatory function in diverged sequences.** Genome Res. 2011 Jul;21(7):1139-49. doi: 10.1101/gr.119016.110. Epub 2011 May 31.

Xiao Y, Gao X, Maragh S, Telford WG, Tona A. **Cell lines as candidate reference materials for quality control of ERBB2 amplification and expression assays in breast cancer**. Clinical Chemistry, 2009 Jul 55(7):1307-15.

Jakupciak JP, Maragh S, Markowitz ME, Greenberg AK, Hoque MO, Maitra A, Barker PE, Wagner PD, Rom WN, Srivastava S, Sidransky D, O'Connell CD. **Performance of mitochondrial DNA mutations detecting early stage cancer.** BMC Cancer, Oct 2008 3;8:285.

John P. Jakupciak, Andrea Maggrah, Samantha Maragh, Jennifer Maki, Brian Reguly, Katrina Maki, Roy Wittock, Kerry Robinson, Paul D. Wagner, Robert E.Thayer, Ken Gehman, Teresa Gehman, Sudhir Srivastava, Alioune Ngom, Gabriel D. Dakubo, and Ryan L. Parr. **Facile whole mitochondrial genome resequencing from nipple aspirate fluid using MitoChip v2.0**.BMC Cancer, Apr 2008, 10;8(1):95

Samantha Maragh, John P Jakupciak, Paul D Wagner, William N Rom, David Sidransky, Sudhir Srivastava, and Catherine D O'Connell. **Multiple strand displacement amplification of mitochondrial DNA from clinical samples.** BMC Medical Genetics, Feb 2008, 9**:**7 doi:10.1186/1471-2350-9-7.

Jennifer Maki, HBSc, Kerry Robinson, MSc, Brian Reguly, BSc, Jude Alexander, MSc, Roy Wittock, MSc, Andrea Aguirre, MSc, Eleftherios P. Diamandis, MD, PhD, Nicholas Escott, MD, Anthony Skehan, MD, PhD, Owen Prowse, MD, Robert E. Thayer, MD, M. Kent Froberg, MD, Michael J. Wilson, MD, Samantha Maragh, John P. Jakupciak, PhD, Paul D. Wagner, PhD, Sudhir Srivastava, PhD, Gabriel D. Dakubo, MB, ChB, and Ryan L. Parr, PhD. **Mitochondrial genome deletion aids in the identification of both false and true negative prostate needle core biopsies**. American Journal of Clinical Pathology, 129(1):57-66, 2008

Lisa Kalman, Monique A. Johnson, Jeanne Beck, Elizabeth Berry-Kravis, Arlene Buller, Brett Casey, Gerald L. Feldman, James Handsfield, John P. Jakupciak, Samantha Maragh, Karla Matteson, Kasinathan Muralidharan, Kristy L. Richie, Elizabeth M. Rohlfs, Frederick Schaefer, Tina Sellers, Elaine Spector, C. Sue Richards. **Development of Genomic Reference Materials for Huntington Disease Genetic Testing**. Genetics in Medicine, 9(10):719-23, 2007

Jakupciak, J.P., Dakubo, G.D., Maragh, S., Parr, R.L. **Analysis of potential cancer biomarkers in mitochondrial DNA**. Curr Opin Mol Ther. 2006 Dec;8(6):500-6. Review.